THREE-DIMENSIONAL LAYERWISE MODELING OF LAYERED MEDIA WITH BOUNDARY INTEGRAL EQUATIONS

by

FILIS-TRIANTAPHYLLOS T. KOKKINOS

Dissertation submitted to the Faculty of the
Virginia Polytechnic Institute and State University
in partial fulfillment of the requirements for the degree of

DOCTOR OF PHILOSOPHY

in

ENGINEERING MECHANICS

Approved:

JN Reddy
Dr. J. N. Reddy, Chairman

O. H. Griffin Jr.
Dr. O. H. Griffin, Jr.

Scott L. Hendricks
Dr. S. L. Hendricks

Saad Ragab
Dr. S. A. Ragab

Y Renardy
Dr. Y. Renardy

Jean Thomas
Dr. J. T. Katsikadelis

December 1995
Blacksburg, Virginia

Keywords: layered media, layerwise theory, sandwich plates, laminated plates, thick plates, fundamental solutions, boundary integral equations, finite element models, boundary element models, BEM and FEM coupling.

THREE-DIMENSIONAL LAYERWISE MODELING OF LAYERED MEDIA WITH BOUNDARY INTEGRAL EQUATIONS

by

Filis-Triantaphyllos T. Kokkinos

Chairman of Advisory Committee: Dr. J. N. Reddy

ENGINEERING MECHANICS

ABSTRACT

A hybrid method is presented for the analysis of layers, plates, and multilayered systems consisting of isotropic and linear elastic materials. The problem is formulated for the general case of a multilayered system using a total potential energy formulation and employing the layerwise laminate theory of Reddy. A one-dimensional finite element model is used for the analysis of the multilayered system through its thickness, and integral Fourier transforms are used to obtain the exact solution for the in-plane problem. Explicit expressions are obtained for the fundamental solution of the typical infinite layer, which are applied in the two-dimensional boundary integral equation model to produce the integral representation of the solution. The boundary integral equation model is two-dimensional, displacement-based and assumes piecewise continuous distribution of the displacement components through the system's thickness. The developed model describes the three-dimensional displacement field, the stress field, the strains and the interlaminar stresses

over the entire domain of the problem as continuous functions of the position. This detailed three-dimensional analysis is achieved by incorporating only contour integrals.

The boundary integral equations are discretized using the boundary element method and a numerical model is developed for the single numerical layer (element). This model is extended to the case of a multilayered system by introducing appropriate continuity conditions at the interfaces between the layers (firmly bonded layers, or separation, slip and friction between the layers). Assembly of the element matrices yields the global system of equations, which can be solved via iterative techniques. In addition, numerical techniques are developed for the evaluation of the boundary and domain integrals involved in the construction of the element matrices. The singular boundary integrals are computed using a special coordinate transformation, along with a subdivision of the boundary element and a transformation of the Gauss points. The domain integrals (regular, singular or near-singular) are transformed to regular definite integrals along the boundary through a semi-analytical approach.

The proposed method provides a simple, efficient, and versatile model for a three-dimensional analysis of thick plates or multilayered systems. It can also be used to study plates resting on elastic foundations or plates with internal supports. The proposed method can be applied in an obvious manner to anisotropic materials and vibration problems.

ACKNOWLEDGMENTS

It is a special privilege, pleasure and chance to express through these pages my thanks and feelings towards some very special people that followed me in the journey which brings me to the successful completion of this work.

I will be forever indebted to Professor J. N. Reddy for his technical, professional and personal guidance, and the financial support that he provided during the past five years of study and research leading to my Ph.D. degree in Engineering Mechanics. It was a unique experience for me to work with, and be with, Prof. J. N. Reddy, who has influenced greatly my perspectives and my life itself. His expertise and fascinating teaching abilities helped me not only to develop a good understanding of mechanics and become a better scientist, but also to realize the dedication and love required for the functions of a professor, something that I will always use as a guide in my career. His encouragement, genuine concern, kindness, high confidence in me and above all his wisdom strengthened me, made me a better person and showed clearly to me the real values in life. Being impossible to express all the feelings that I have for Professor J. N. Reddy, I would just like to say that I consider an honor to have him advisor, teacher and friend, and to me he is "the man", whom the philosopher Diogenes was desperately seeking, by walking into the crowd and holding a torch in perfect daylight.

Special thanks are also given to the Professors Odis H. Griffin Jr., Scott L. Hendricks, Saad A. Ragab of the Engineering Science and Mechanics Department and Professor Yuriko Renardy of the Department of Mathematics

for serving on the Ph.D. dissertation and advisory committee, for their encouragement, for their exceptional teaching, and for their helpful comments and suggestions.

I am also grateful to Professor J. T. Katsikadelis of the Civil Engineering Department of the National Technical University of Athens for serving on the advisory committee, for his special interest in my work and for his invaluable recommendations, ideas and insights. His support, technical guidance, expert advise and wisdom have followed me not only through the course of the present research, but from the very beginning of my studies in Greece. I am indebted to him for helping me to build a strong background, without which the successful completion of my graduate studies and of this dissertation would have been impossible.

I would also like to thank the Department of Engineering Science and Mechanics for awarding me twice an Instructional Fee Scholarship that helped me financially during the first years of my studies.

A special debt of gratitude is owed to my wife Kalli, for her unselfish support, understanding, patience and courage during the years. Her precious love, constant encouragement and tireless efforts gave me the strength to overcome many difficulties and disappointments that I encountered in the course of my research and enhanced my motivation to succeed in this research and achieve my goals.

I will always be indebted to my parents Theodore and Klio Kokkinos for their unconditional love and support, and for their many sacrifices that have enabled me to pursue my goals. They have inspired and enriched my life with their love, tender care, wisdom, high morality and they have greatly contributed to the crystallization and development of my professional goals.

Finally, this dissertation is dedicated to the most wonderful people in my life, my parents Theodore and Klio, my wife Kalli, and my mentor Professor J. N. Reddy.

TABLE OF CONTENTS

LIST OF FIGURES

Chapter 1

INTRODUCTION

1.1 LITERATURE REVIEW

In recent years the boundary element method (BEM) has become an established method for analyzing structures, and it is widely used to solve elastostatic and elastodynamic problems (Banerjee and Butterfield, 1981; Brebbia *et al.*, 1984; Hartmann, 1989; Beskos (ed.), 1991). In many cases the method is more economical and accurate than the domain methods (*e.g.*, finite difference and finite element methods). The method is applied by obtaining first an integral representation of the solution (usually the displacement field for elasticity problems) which involves only integrals of the boundary displacements and tractions. The integrals are over a surface for two-dimensional problems or along a line for two-dimensional problems. The application of the method requires then discretization only on the boundaries of the domain and thus it reduces the spatial dimensions of the problem by one. The boundary displacement and traction vectors are calculated with the same degree of

accuracy, and once the solution on the boundary has been obtained, displacements and stresses can be computed at any point in the interior of the domain as accurately as the boundary quantities. Since, the solution is continuous in the domain of the problem and not discrete values at nodal points, the strains and stresses can also be expressed as continuous functions of the position. Any approximation is introduced in the final stage of the analysis, where a variation of the primary variables (the displacement components) has to be assumed in order to numerically evaluate the boundary integrals.

The formulation of boundary integral equations via the direct method requires a *fundamental solution*. This is generally characterized as the particular singular solution of a boundary value problem (elliptic for the linear elasticity) which corresponds to a "concentrated load." In general, however, the singular part of the fundamental solution is not uniquely determined by this specification. The determinacy is usually eliminated by requiring the solution to be well behaved in the infinite region exterior to the singular point and to have proper decay behavior at infinity (the so-called free-field condition). The dependence of BEM on fundamental solutions that satisfy the governing differential equations makes the formulation of this method more complicated compared to the domain methods, which use simple approximations of the solution in the domain, but more accurate and more economical since approximation of the variables is required only on the boundary in the numerical solution of the integral equations. These features are particularly advantageous for problems extending to infinity and for modeling accurately and efficiently regions with high stress gradients, making the BEM an appealing tool for solving boundary value problems of the mathematical physics.

In a number of papers, different boundary integral formulations have been shown to be useful for different classes of boundary value problems. The main difference among them is the fundamental solution, which is dependent on the geometry of the problem. Kelvin's (1848) fundamental solution of a concentrated load in an infinite medium has been widely used for two- and three-dimensional elastostatic problems (Rizzo, 1967; Cruse, 1973; Katsikadelis and Kokkinos, 1987). For problems involving a free-surface the solution presented by Melan (1932) for the stress distribution due to point loads applied within the isotropic half-plane or the one given by Mindlin (1936) for the half-space are of special interest (Telles and Brebbia, 1981). Mindlin constructed the solution for the infinite half-space by combining Lamé's strain potentials and Galerkin's vectors and utilizing the method of images (Westergaard, 1952). The same problem for concentrated normal force on the surface of the isotropic half-space was also studied by Boussinesq (1885) and the case of tangential force by Cerutti (see, Love, 1944). These fundamental solutions have been applied to BEM by many researchers and they find extensive application in soil mechanics, in problems of soil-structure interaction, and generally, in problems with a half-space. They have also been used to construct nonsingular boundary integral equations (Stern, 1985; Wu and Stern, 1991).

The problems of a single infinite layer or the multilayered half-space have received extensive attention because of their relevance to the theory of plates, foundations, geotechnical engineering, micro-mechanics, and composite materials. For these problems it is rather cumbersome to evaluate the exact state of stress and displacement, and most of the solutions that have been reported in the literature are not readily and efficiently applied to the analysis of multilayered systems and, especially, to the BEM for the case of finite plates or laminates.

Michell (1899a, 1899b) applied a stress formulation to the theory of plates and obtained two fourth order differential equations for the determination of two unknown functions in terms of which the normal displacement and the stretch of the median plane were expressed. He formulated the problem of the infinite plate subjected to unit loads and the transmission of stress across the interface between two plates in contact for the cases of complete bond or free slipping. Michell (1900a) also obtained some elementary stress distributions for the case of a force applied to an isotropic elastic solid, either at an internal point, or on a plane boundary, or at the vertex of a cone, making assumptions for the variation of the displacement and stress components. He used these distributions to solve problems of infinite cylinders and infinite thin plates under plane stress conditions (Michell, 1900b). The problem of a single elastic layer in equilibrium was considered thoroughly for the first time by Dougall (1904), who conducted an extensive study of a thick plate subjected to arbitrary surface or internal loading using potential functions. He proposed an approximate solution in series of Bessel functions and, using Betti's reciprocal theorem, he deduced the solution for finite circular plates and thin plates from the infinite layer solution. Green and Zerna (1960) used conformal transformation and complex potentials to study isotropic and some special cases of orthotropic plates under isolated forces. Luré (1964) constructed a solution by expressing the unknown displacement components in power series of the normal to the plate coordinate and employing a symbolic method of operators. The problem was reduced to the determination of stress functions. Kupradze (1979) studied elastic bodies bounded by either one or two parallel planes, and sought the solution in the form of Fourier type integrals involving Kelvin's fundamental matrix. In the area of soil mechanics, Shekhter and Prikhodchenko (1964), and Shekhter (1965) studied the

response of a three-dimensional layer on a rigid base under a horizontal force by using Kelvin's solution and an auxiliary Galerkin's vector.

Burmister (1945) extended the classic solution of Boussinesq (1885) to include the problems of normal static loads acting on the surface of a two- and three-layered half-space. Harding and Sneddon (1945) studied the elastic stresses produced by the indentation of the plane surface of a semi-infinite elastic solid by a rigid punch in cylindrical coordinates, and discussed the application of their solution to the case of a plate of finite thickness. Sneddon (1946) also studied thick plates under the application of pressure to their free surfaces. The same problem was later considered by Bufler (1971), who provided a suitable and systematic matrix formulation in Cartesian coordinates by means of two-dimensional integral transforms introduced by Sneddon. Bufler's paper contained a comprehensive elastostatic formulation of the multilayered system in the two-dimensional Fourier transform domain but did not provide any information regarding the distribution of stresses and displacements in the physical domain of a single layer or a multilayered system.

Bufler's work (1971) was completed by Benitez and Rosakis (1987), who considered the more general problem of a three-dimensional layer containing arbitrary internal loads. For the specific case of a concentrated unit load, analytical expressions for the stresses and displacements were obtained in terms of convergent integrals that involved Bessel functions. The solution was obtained by transforming the three-dimensional elasticity equations to the two-dimensional Fourier space and solving the ordinary matrix differential equations by means of the Caley-Hamilton theorem. They also showed how their formulation for the single layer can be applied to the case of a multilayered medium subjected to both surface and internal loads through the methods of transfer matrices and flexibility matrices that were presented in

Bufler's paper. This is the most complete solution reported in the literature, since it presents for the first time analytical expressions for the stress distribution and the displacement field in an infinite layer which is subjected to unit loads. However, this solution has two drawbacks. First, the expressions for the displacement and stress components are very complicated and involve infinite integrals with kernels that consist of Bessel functions, and second, the approach cannot be used efficiently to solve problems with multiple layers. Nevertheless, it is a powerful tool for detailed and accurate analysis of single infinite layers which are subjected to arbitrary loading and may include holes.

More recently, a similar approach was used by Chatterjee (1987) to study the three- and two-dimensional stress fields near delaminations in laminated composite plates, and by Madenci and Westmann (1993) to study the problem of delamination growth in layered systems under compressive load. In the latter, the authors solved the problem of an infinite layer with slightly imperfect circular delamination subjected to axisymmetric and uniaxial in-plane compressive loading. Pindera and Lane (1993) used Fourier transforms and expansions in Chebyshev polynomials to study the frictionless contact of layered half-planes in two dimensions.

1.2 MOTIVATION

The review of the pertinent research on the subject of unit load solutions and solutions for infinite layers and layered media reveals that, due to the inherent complexity of these problems, the mathematical and numerical approach greatly affects the form, efficiency, and applicability of the solution. These problems appear to have two phases. The first is the determination of the

displacement and stress distributions along the direction perpendicular to the faces of the system (x_3 direction), and the second phase is the derivation of the in-plane distributions (x_1 and x_2 directions) using the results of the first phase. Since the domain in the plane extends to infinity, it is convenient to transform the governing partial differential equations of the three-dimensional elasticity to the Fourier space where they become ordinary differential equations in one independent variable, x_3. The exact solution of these equations (first phase) can be obtained in a simple manner (Bufler, 1971; Benitez and Rosakis, 1987), but because it involves hyperbolic functions it produces complicated expressions in the Fourier domain, which become even more complicated and lengthy when they are transformed back to the physical space. Actually, in most of the solutions that can be found in the literature, the final expressions in the physical space are in the form of either infinite series or convergent infinite integrals involving Bessel functions.

In the present work, the author assumes *a priori* a specific variation of the dependent variables of the problem through the layer thickness, derives in a formal and systematic way new governing equations based on these approximations, and then applies the integral transforms. The advantage of this modeling is that the first phase of the problem is treated in the physical space using matrix formulation from the beginning, avoiding differential equations higher than the second order, and reducing the independent variables to two (*i.e.*, x_1 and x_2). Transformation of the new governing equations in the Fourier domain yields algebraic equations, instead of ordinary differential equations, that can be solved for the unknown transformed variables. The dependent variables may be the three displacement components for a displacement formulation, or the displacements and the stress components in the x_3 direction for a mixed formulation. These predefined distributions

can be chosen to be polynomials in x_3, and their degree will depend on the required accuracy of the solution, the type of loading, and the complexity of the geometry.

This approach of assumed variation of the displacement field through the thickness of laminates was first introduced by Reddy (1987), the so-called *layerwise laminate theory of Reddy*. This theory has been used to develop, displacement-based, finite element models for the study of laminated composite plates (Reddy *et al.*, 1989; Reddy, 1990; Barbero *et al.*, 1990; Robbins and Reddy, 1993). The resulting model is capable of computing interlaminar stresses and other localized effects with the same degree of accuracy as the conventional three-dimensional finite element models. In the present work, this concept of layerwise approximation of the displacement field is adopted as an alternative to the complicated exact displacement variation through the thickness.

1.3 THESIS OBJECTIVES AND OUTLINE

The overall goal of this research is to develop a hybrid methodology for the analysis of layers, plates, and multilayered systems consisting of isotropic or orthotropic linear elastic materials. The basic characteristic of this methodology is to produce a one-dimensional model for the analysis of the three-dimensional multilayered system which maintains all the advantages and salient features of a pure three-dimensional model. This methodology, which incorporates integral equations, provides a continuous and accurate representation of the solution over the domain of the system, along with detailed information about the stresses and strains in the domain of each layer or at the interface between two contiguous layers.

Objective of this work is to develop a suitable and systematic derivation of discrete governing equations in Cartesian coordinates, find the fundamental solution for a typical single layer, and formulate a hybrid model for the analysis of multilayered systems. From the beginning of the analysis in the physical space, the problem is decomposed in a one-dimensional problem through the thickness, and a two-dimensional problem in the plane. A one-dimensional finite element model is constructed for the analysis of the first problem and the method of integral Fourier transforms is used to obtain the exact solution of the second problem. The behavior of each layer is mainly described by the corresponding stiffness matrix or alternatively by the corresponding flexibility matrix. Continuity and boundary conditions yield an algebraic system of equations for the components of the displacement and stress vectors at the faces and interfaces of the multilayered system. The final expressions for the displacement and stress components can be directly applied to a boundary integral equation model for the analysis of thick plates or multilayered systems with finite dimensions. Here we restrict ourselves to a displacement formulation, to plane elastic and isotropic layers and Cartesian coordinates. The proposed method can be applied in an obvious manner to anisotropic materials. The problem of delaminations, thermal stresses, vibrations or stability is treatable in an analogous manner.

An outline of the steps taken in developing this methodology is presented below.

➢ ***I. Method for deriving fundamental solutions***

Develop a methodology for deriving semi-analytical fundamental solutions for problems related to single layers and multilayered systems. The method is general and can be applied to either isotropic or orthotropic materials. The solutions are based on an assumed variation

of the displacement field through the thickness of the system, and produce displacement or mixed models. These solutions are obtained through an energy formulation of the problem, development of a one-dimensional finite element model through the thickness of the structure, and use of integral Fourier transforms to solve the differential equations for the plane problem. From the displacement solution one can derive expressions for the tractions and stresses which correspond to the problem of the infinite single or multiple layer system subjected to unit point loads. In the present work explicit expressions for the fundamental solution, tractions and stresses of a single isotropic layer have been derived. Fundamental solutions for orthotropic materials can be derived in a similar way. The methodology is the same and only the material constants (coefficients in the constitutive relations) will be different. The following steps II and III will be the same whether the layers consist of material with isotropic or orthotropic properties.

➢ ***II.*** *Boundary integral equations for a single layer*

Develop the boundary integral equations for a single layer. Derive the integral representation of the solution for points in the domain of the problem, and from this derive the solution for points on the boundary. Using these solutions find explicit expressions in integral form for the stress and strain components at any point in the three-dimensional layer.

➢ ***III.*** *Boundary Element Modeling*

Discretize the boundary integral equations of a single layer and develop the boundary element model for the single layer. Extend the model to the case of multilayered systems through appropriate continuity conditions at the interfaces between the layers.

➢ ***IV.*** *Numerical Analysis and Implementation*

Obtain the matrix form of all the equations that describe each numerical layer and construct the element matrices. Assemble the local matrices for the numerical layers and apply the discretized continuity equations at the interfaces between the layers, to produce the global matrices (like a stiffness matrix) for the multilayered system. This is the global system of equations which, after incorporating the prescribed boundary conditions, will yield the solution to the problem. The element matrices are developed in such a way so that they can be introduced into an iterative solver.

➢ ***V.*** *Evaluation of boundary and domain integrals*

Develop a purely numerical technique for the evaluation of singular and near-singular boundary integrals. Introduce another technique for the evaluation of regular and singular domain integrals, which transforms the domain integrals to boundary integrals, and in addition removes any singularities.

Chapter 2

GOVERNING EQUATIONS

2.1 DESCRIPTION OF THE MULTILAYERED SYSTEM

Consider a thick multilayered plate of arbitrary shape and total thickness H occupying the domain V in the three-dimensional space and bounded by a surface S. Each layer of this plate is made of an isotropic and linear elastic material, and has elastic constants and thickness generally different from those of other layers. Each layer can also contain a finite number of inclusions and holes, which need not extend through the whole thickness of the plate (Figure 2.1).

The multilayered system can be subjected to body forces distributed over the entire volume or over a subregion, shared by some of the layers. It can be subjected to line loads and/or point loads either on the boundary or in the domain, and distributed boundary tractions. Regarding the support conditions of the system, its boundary may be free, clamped, or subjected to prescribed displacements along parts of it and/or at discrete points. It can also be

elastically supported over a part or at discrete points on the boundary, and simply supported in a prescribed direction at a point.

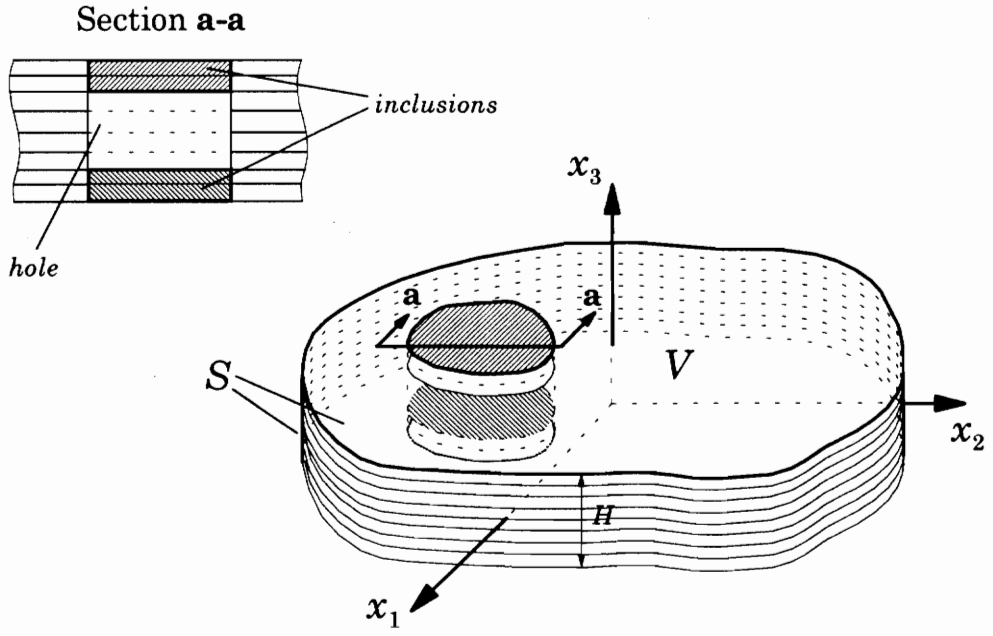

Figure 2.1 Components and geometry of the multilayered plate.

The total potential energy for the multilayered system or for any of its layers is given as

$$\Pi(u_i) = \int_V \tfrac{1}{2}\sigma_{ij}\,\varepsilon_{ij}\,dV - \int_V f_i\,u_i\,dV - \int_S \hat{t}_i\,u_i\,dS \tag{2.1}$$

where f_i denotes the applied body forces per unit volume and $\hat{t}_i$ the externally applied tractions on the boundary. In equation (2.1) and in the remaining part of this paper summation on repeated indices is implied, unless otherwise stated.

The strain-displacement relations for geometrically linear behavior are

$$\varepsilon_{ij} = \tfrac{1}{2}\left(\frac{\partial u_i}{\partial x_j} + \frac{\partial u_j}{\partial x_i}\right) \tag{2.2}$$

and the constitutive relations for isotropic materials are

$$\sigma_{ij} = \lambda \delta_{ij} \varepsilon_{kk} + 2\mu \varepsilon_{ij} = \lambda\, \delta_{ij} \frac{\partial u_k}{\partial x_k} + \mu \left(\frac{\partial u_i}{\partial x_j} + \frac{\partial u_j}{\partial x_i} \right) \quad (i, j, k = 1, 2, 3) \tag{2.3}$$

where λ and μ are the Lamé constants, which are given in terms of the modulus of elasticity E and Poisson's ratio ν as

$$\lambda = \frac{\nu E}{(1+\nu)(1-2\nu)} \quad \text{and} \quad \mu = \frac{E}{2(1+\nu)} \,. \tag{2.4}$$

Substitution of equations (2.2) and (2.3) into equation (2.1) for the total potential energy yields:

$$\Pi(u_i) = \int_V \tfrac{1}{2} \left[\lambda\, \delta_{ij} \frac{\partial u_k}{\partial x_k} + \mu \left(\frac{\partial u_i}{\partial x_j} + \frac{\partial u_j}{\partial x_i} \right) \right] \tfrac{1}{2} \left(\frac{\partial u_i}{\partial x_j} + \frac{\partial u_j}{\partial x_i} \right) dV$$

$$- \int_V f_i\, u_i\, dV - \int_S \hat{t}_i\, u_i\, dS \tag{2.5}$$

where the volume V and surface S in the above statement correspond to a single layer of the multilayered plate.

The total potential energy principle is used to derive the governing equations and boundary conditions of the problem. The principle states that $\delta\Pi = 0$ and using equation (2.5) it is written as

$$\delta\Pi = 0 = \int_V \left[\lambda \frac{\partial\, \delta u_k}{\partial x_k} \frac{\partial u_i}{\partial x_i} + \mu \frac{\partial\, \delta u_i}{\partial x_j} \left(\frac{\partial u_i}{\partial x_j} + \frac{\partial u_j}{\partial x_i} \right) \right] dV$$

$$- \int_V f_i\, \delta u_i\, dV - \int_S \hat{t}_i\, \delta u_i\, dS \,, \tag{2.6}$$

which is also called *weak form* of the differential equation of the problem (Reddy, 1984). Integrating by parts the terms in equation (2.6) that involve

partial derivatives of the virtual displacements δu_i, we obtain the following integral statement

$$0 = \int_V \left[-\lambda \frac{\partial^2 u_i}{\partial x_i \partial x_k} \delta u_k - \mu \left(\frac{\partial^2 u_i}{\partial x_j \partial x_j} + \frac{\partial^2 u_j}{\partial x_i \partial x_j} \right) \delta u_i \right] dV - \int_V f_i \, \delta u_i \, dV$$

$$- \int_S \hat{t}_i \, \delta u_i \, dS + \int_S \left[n_k \lambda \, \delta u_k \frac{\partial u_i}{\partial x_i} + n_j \mu \left(\frac{\partial u_i}{\partial x_j} + \frac{\partial u_j}{\partial x_i} \right) \delta u_i \right] dS \ . \qquad (2.7)$$

The Euler-Lagrange equations and boundary conditions associated with the functional are

$$(\lambda + \mu) \frac{\partial^2 u_j}{\partial x_i \partial x_j} + \mu \frac{\partial^2 u_i}{\partial x_j \partial x_j} + f_i \equiv \frac{\partial \sigma_{ji}}{\partial x_j} + f_i = 0 \qquad \text{in } V \qquad (2.8)$$

$$n_j \left[\lambda \, \delta_{ij} \frac{\partial u_k}{\partial x_k} + \mu \left(\frac{\partial u_i}{\partial x_j} + \frac{\partial u_j}{\partial x_i} \right) \right] - \hat{t}_i \equiv n_j \, \sigma_{ji} - \hat{t}_i = 0 \qquad \text{on } S \, . \qquad (2.9)$$

Equations (2.8) are the well known *Navier equations of equilibrium* for a three-dimensional elastic body.

2.2 INTEGRAL SOLUTION FOR TWO- AND THREE-DIMENSIONAL ELASTICITY

The differential equations (2.8) along with the boundary conditions (2.9) govern the general boundary value problem of the two- and three-dimensional elasticity. The problem can be solved using any of the popular numerical techniques, namely, the finite element method (FEM) and the boundary element method (BEM). The former utilizes a *domain discretization* into elements and assumes *a priori* a displacement approximation over each element, while the latter requires, first, a continuous representation of the solution in the form of *integral equations*, and then, a *boundary disretization* for the numerical evaluation of the boundary integrals. These are surface

integrals for the three-dimensional problems and line integrals for the two-dimensional problems.

The starting point for the FEM is the weak form (2.6), which is applied for every element in the mesh and in which, both the displacement components and their variations are represented by an assumed and approximate displacement field over each element. The starting point for the BEM is a variational statement obtained from the weak form through an integration by parts. The objective of this integration is to relieve the primary variables (displacement components) of any differentiation and the resulting expression for the total potential energy has the form

$$\delta\Pi = 0 = \int_V \left[-\lambda \frac{\partial^2 \delta u_k}{\partial x_i \, \partial x_k} - \mu \left(\frac{\partial^2 \delta u_i}{\partial x_j \partial x_j} + \frac{\partial^2 \delta u_j}{\partial x_j \partial x_i} \right) \right] u_i \, dV - \int_V f_i \, \delta u_i \, dV$$

$$- \int_S \hat{t}_i \, \delta u_i \, dS + \int_S n_j \left[\lambda \delta_{ij} \frac{\partial \delta u_k}{\partial x_k} + \mu \left(\frac{\partial \delta u_i}{\partial x_j} + \frac{\partial \delta u_j}{\partial x_i} \right) \right] u_i \, dS \, . \qquad (2.10)$$

The virtual displacements in the above equation are chosen in such a way that, the kernel in the first domain integral of (2.10) becomes equal to the Dirac delta function, *i.e.*,

$$-\lambda \frac{\partial^2 \delta u_k}{\partial x_i \, \partial x_k} - \mu \left(\frac{\partial^2 \delta u_i}{\partial x_k \partial x_k} + \frac{\partial^2 \delta u_k}{\partial x_k \partial x_i} \right) = P_i \, \delta\left(\vec{x} - \vec{\xi} \right), \qquad (2.11)$$

and also, the following boundary conditions are satisfied

$$\delta u_i \to 0 \quad \text{and} \quad \frac{\partial \delta u_i}{\partial x_k} \to 0, \quad \text{for } \vec{x} \to \infty \qquad (2.12)$$

where the subscripts i, k =1,2,3 for the three-dimensional problem. The concentrated load $\vec{\mathbf{P}}$ is a unit load applied along the x_j direction and is given in the form

$$\vec{\mathbf{P}} = \delta_{ij} \, \delta\left(\vec{x} - \vec{\xi} \right) \hat{e}_i \, . \qquad (2.13)$$

The boundary value problem defined by equations (2.11) and (2.12) corresponds to the problem of an infinity elastic medium subjected to a unit load at a point $\vec{\xi}$. The solution of this problem is the so-called *Kelvin's solution* (see Sir Thompson, W., 1848) or *fundamental solution* of the elasticity problem (2.8). This solution for the two-dimensional plane strain problem is

$$U_{ij}\left(\vec{x},\vec{\xi}\right) = -\frac{1}{8\pi\mu(1-\nu)}\left[(3-4\nu)\,\delta_{ij}\,\ln r - \frac{y_i\,y_j}{r^2}\right], \tag{2.14}$$

while, for the three-dimensional problem it is

$$U_{ij}\left(\vec{x},\vec{\xi}\right) = \frac{1}{16\pi\mu(1-\nu)}\frac{1}{r}\left[(3-4\nu)\,\delta_{ij} + \frac{y_i\,y_j}{r^2}\right], \tag{2.15}$$

where $y_i = x_i - \xi_i$ and $r^2 = y_i\,y_i$. $U_{ij}\left(\vec{x},\vec{\xi}\right)$ is a two-point tensor and represents the displacement field $\delta u_i(\vec{x})$ at point $\vec{x}$ due to a unit load applied in the x_j direction at point $\vec{\xi}$.

The fundamental solutions (2.14) and (2.15) can be substituted in the virtual statement of (2.10) to produce the integral representation of the displacement field, which is also called *Somigliana's identity*. The displacement field at any point in the domain is then expressed as

$$u_j\left(\vec{\xi}\right) = \int_V f_i(\vec{x})\,U_{ij}\left(\vec{x},\vec{\xi}\right)dV_x + \int_S \hat{t}_i\,U_{ij}\left(\vec{x},\vec{\xi}\right)dS_x - \int_S u_i\,T_{ij}\left(\vec{x},\vec{\xi}\right)dS_x \tag{2.16}$$

in which $\vec{x}$ is the integration point and $T_{ij}\left(\vec{x},\vec{\xi}\right)$ is a two-point tensor called *traction tensor* and it is built from the kernel of the last boundary integral of equation (2.10). The traction tensor is expressed in terms of the fundamental solution as

$$T_{ij}\left(\vec{x},\vec{\xi}\right) = n_m\left[\lambda\,\delta_{im}\frac{\partial U_{kj}}{\partial x_k} + \mu\left(\frac{\partial U_{ij}}{\partial x_m} + \frac{\partial U_{mj}}{\partial x_i}\right)\right]. \tag{2.17}$$

Equation (2.16) is the integral representation of the solution. It is a continuous function of the position vector $\vec{\xi}$, and it is the *exact solution* for the boundary value problem governed by equations (2.8) and (2.9). The application of this equation to problems with complicated geometry or inhomogeneities is almost impossible, and that is why it is required to discretize the boundary S into elements. This leads to discrete boundary equations and then the problem is rendered to the BEM (Katsikadelis and Kokkinos, 1987). This numerical method will provide an accurate solution (displacements and stresses) not only at the boundary nodal points, but also at any interior point (see equation 2.16).

In the case of a multilayered system, as the one described in section 2.1, it is very "expensive" to apply the general solution (2.16) along with the fundamental solution (2.15) for each layer of the system. The reason is that such an approach requires discretization not only of the side surface of each layer, but also of the bottom and top surfaces. The double integrals must be evaluated over the boundaries of all the layers and the complete model of the multilayered system is obtained by applying the appropriate displacement compatibility and traction equilibrium conditions at the interfaces between the layers.

The boundary integral model of (2.16) may become very efficient, simple, flexible and applicable to the case of layered plates, if instead of using the fundamental solution (2.15) for the unbounded three-dimensional space (Kelvin's solution), an *appropriate* fundamental solution for the *infinite layer* is employed. If the problem for the infinite domain is set up with the appropriate boundary conditions for a layer or system of layers, its fundamental solution will produce in (2.16) line integrals instead of surface integrals, although the domain of the problem at hand is three-dimensional.

2.3 LAYERWISE DISPLACEMENT APPROXIMATION AND FINITE ELEMENT MODEL

The governing differential equations of a multilayered system are the Navier equations (2.8) along with the boundary conditions (2.9). These equations must be applied for any individual layer, taking into account its material properties and its geometry in the x_1x_2-plane. The multilayered system must be divided through its thickness and in the plane into homogeneous and simply connected sub-systems. Since a discretization of the continuum multilayered system is inevitable, and the closed form solution for a single layer is very complex and not efficiently applicable to the case of multiple layers (see Benitez and Rosakis, 1987), the most suitable approach is to subdivide each layer of the plate into a number of layers through the thickness. These sublayers can be viewed as numerical layers with elastic constants and geometry in the x_1x_2-plane identical to those of the physical layer, but with different thickness. According to the *layerwise theory of Reddy* (1987, 1990), the displacements are expanded within each layer using the Lagrange family of interpolation functions. The nodal values through the thickness are functions of the in-plane coordinates (x_1, x_2), and the i-th displacement component of each numerical layer is expressed as,

$$u_i(x_1, x_2, x_3) = \sum_{n=1}^{N} v_i^n(x_1, x_2)\,\phi_n(x_3) \qquad (i = 1, 2, 3) \tag{2.18}$$

where N is the number of subdivisions through the thickness of the layer and $\phi_n(x_3)$ are known functions of the thickness coordinate, x_3. It is assumed that each numerical layer consists of N nodal points along the x_3 direction and its thickness is $2h$, as shown in Figure 2.2.

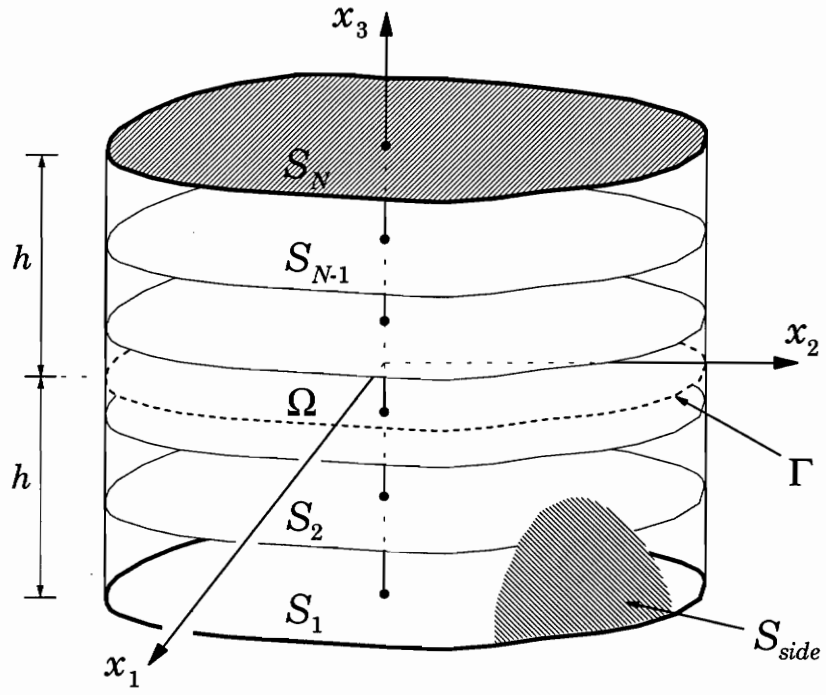

Figure 2.2 Definitions and geometry of a typical numerical layer with N nodes in the transverse direction.

Substituting the approximations (2.18) into the weak form (2.6) and separating the in-plane components u_I (I=1,2) from the component in the transverse direction, u_3, one arrives at the statement

$$\begin{aligned}\delta\Pi = \int_{\Omega}\int_{-h}^{h} \Bigg[& \lambda\left(\frac{\partial \delta v_J^p}{\partial x_J}\phi_p + \delta v_3^p \frac{d\phi_p}{dx_3}\right)\left(\frac{\partial v_I^n}{\partial x_I}\phi_n + v_3^n \frac{d\phi_n}{dx_3}\right) \\ & + \mu \frac{\partial \delta v_i^p}{\partial x_J}\phi_p \frac{\partial v_i^n}{\partial x_J}\phi_n + \mu\, \delta v_i^p \frac{d\phi_p}{dx_3} v_i^n \frac{d\phi_n}{dx_3} \\ & + \mu \frac{\partial \delta v_I^p}{\partial x_J}\phi_p \frac{\partial v_J^n}{\partial x_I}\phi_n + \mu\, \delta v_I^p \frac{d\phi_p}{dx_3}\frac{\partial v_3^n}{\partial x_I}\phi_n \\ & + \mu \frac{\partial \delta v_3^p}{\partial x_J}\phi_p v_J^n \frac{d\phi_n}{dx_3} + \mu\, \delta v_3^p \frac{d\phi_p}{dx_3} v_3^n \frac{d\phi_n}{dx_3} \Bigg] dx_3\, d\Omega \\ & - \int_{\Omega}\int_{-h}^{h} f_i\, \delta v_i^p\, \phi_p\, dx_3\, d\Omega - \int_S \hat{t}_i\, \delta v_i^p\, \phi_p\, dS \end{aligned} \tag{2.19}$$

where the superscripts n, p represent the element nodes, and they take the values n, p=1,2,..., N, the subscripts I, J=1,2 and i=1,2,3 denote the directions x_1, x_2 and x_3, and repeated indices imply summation convention. All quantities and interpolation functions in equation (2.19) are understood to be defined over a typical element; *i.e.*, all expressions and quantities should have the element label e, but these were omitted in the interest of brevity. In equation (2.19), Ω represents the area occupied by the element in the x_1x_2-plane and S is the boundary of the three-dimensional body. This boundary can be decomposed into three different parts, $S = S_{side} \cup S_1 \cup S_N$, where S_{side} represents the side area of the cylindrical surface and S_1, S_N are the areas of the horizontal planes that pass through the first and last nodal point of the element, respectively. According to this decomposition the surface integral which involves the tractions on the boundary can be written as

$$\begin{aligned}\int_S \hat{t}_i\, \delta v_i^p\, \phi_p\, dS = & \int_{S_1} \hat{t}_i(x_1, x_2, -h)\, \delta v_i^1\, dS + \int_{S_N} \hat{t}_i(x_1, x_2, h)\, \delta v_i^N\, dS \\ & + \int_{S_{side}} \hat{t}_i(x_1, x_2, x_3)\, \delta v_i^p\, dS \\ = & \int_\Omega \left[\hat{t}_i(x_1, x_2, -h)\, \delta v_i^1 + \hat{t}_i(x_1, x_2, h)\, \delta v_i^N\right] d\Omega \\ & + \oint_\Gamma \int_{-h}^{h} \hat{t}_i\, \delta v_i^p\, \phi_p\, dx_3\, d\Gamma \end{aligned} \tag{2.20}$$

where in the last integral Γ denotes the closed contour that encloses the domain Ω and which apparently is also the same for the domains S_1 and S_N.

In equation (2.19), integrals over the thickness of the typical numerical layer are applied only on the shape functions $\phi_n(x_3)$ and their derivatives, since these are the only continuous functions of x_3. Integrals of products

between the shape functions and their derivatives are the entries of the element matrices associated with the one-dimensional finite element model for the thickness problem. The matrices are defined in the following way:

$$K_{np} = \int_{-h}^{h} \frac{d\phi_n}{dx_3} \frac{d\phi_p}{dx_3}\, dx_3 \qquad \text{(symmetric)}\,, \tag{2.21}$$

$$M_{np} = \int_{-h}^{h} \phi_n\, \phi_p\, dx_3 \qquad \text{(symmetric)}\,, \tag{2.22}$$

$$C_{np} = \int_{-h}^{h} \phi_n \frac{d\phi_p}{dx_3}\, dx_3 \qquad \text{(non-symmetric)}, \tag{2.23}$$

$$D_{np} = C_{pn} = \int_{-h}^{h} \frac{d\phi_n}{dx_3}\, \phi_p\, dx_3 \qquad \text{(non-symmetric)}\,, \tag{2.24}$$

$$F_i^p = \int_{-h}^{h} f_i\, \phi_p\, dx_3\,, \tag{2.25}$$

$$\hat{Q}_i^p = \int_{-h}^{h} \hat{t}_i\, \phi_p\, dx_3\,. \tag{2.26}$$

Using the above definitions in equation (2.19) and collecting terms that contain the virtual displacements δv_i^p and multiply the displacements v_i, the following expression is obtained for the total potential energy

$$\begin{aligned}
\delta\Pi \;&= 0 = \\
&\int_{\Omega} \left[\lambda \left(M_{np} \frac{\partial \delta v_J^p}{\partial x_J} + C_{np}\, \delta v_3^p \right) \frac{\partial v_I^n}{\partial x_I} + \left(\lambda D_{np} \frac{\partial \delta v_J^p}{\partial x_J} + (\lambda + 2\mu) K_{np}\, \delta v_3^p \right) v_3^n \right. \\
&\quad + \mu\, M_{np} \left(\frac{\partial \delta v_J^p}{\partial x_I} + \frac{\partial \delta v_I^p}{\partial x_J} \right) \frac{\partial v_J^n}{\partial x_I} + \mu \left(M_{np} \frac{\partial \delta v_3^p}{\partial x_I} + C_{np}\, \delta v_I^p \right) \frac{\partial v_3^n}{\partial x_I} \\
&\quad \left. + \mu \left(K_{np}\, \delta v_I^p + D_{np} \frac{\partial \delta v_3^p}{\partial x_I} \right) v_I^n \right] d\Omega \;-\; \int_{\Omega} F_i^p\, \delta v_i^p\, d\Omega \\
&- \int_{\Omega} \left[\hat{t}_i(x_1, x_2, -h)\, \delta v_i^1 + \hat{t}_i(x_1, x_2, h)\, \delta v_i^N \right] d\Omega \;-\; \oint_{\Gamma} \hat{Q}_i^p\, \delta v_i^p\, d\Gamma
\end{aligned} \tag{2.27}$$

in which, i=1,2,3; I, J=1,2; n, p=1,2,...,N, and the surface integrals of the boundary tractions have been expressed according to the results of (2.20).

2.4 LAYERWISE GOVERNING DIFFERENTIAL EQUATIONS

Equation (2.27) may be used to derive the governing differential equations for a single layer, whose displacement field is described by equations (2.18). This is accomplished by integrating by parts equation (2.27) in such a way that δv_i^p are relieved of any differentiation, by using the properties of the coefficient (element) matrices (*i.e.*, $C_{np} = D_{pn}$, $M_{np} = M_{pn}$, $K_{np} = K_{pn}$), and applying the fundamental lemma of calculus of variations. The resulting differential equations (Euler-Lagrange equations) for the typical numerical layer are

$$\delta v_I^p: \quad -(\lambda+\mu)\, M_{pn} \frac{\partial^2 v_J^n}{\partial x_I \partial x_J} - \mu\, M_{pn} \frac{\partial^2 v_I^n}{\partial x_J \partial x_J} + (\mu\, D_{pn} - \lambda\, C_{pn}) \frac{\partial v_3^n}{\partial x_I}$$

$$+\mu\, K_{pn}\, v_I^n - \hat{F}_I^p = 0 \tag{2.28a}$$

$$\delta v_3^p: \quad -\mu\, M_{pn} \frac{\partial^2 v_3^n}{\partial x_I \partial x_I} + (\lambda\, D_{pn} - \mu\, C_{pn}) \frac{\partial v_I^n}{\partial x_I} + (\lambda+2\mu)\, K_{pn}\, v_3^n - \hat{F}_3^p = 0 \tag{2.28b}$$

and the associated boundary conditions are

$$\delta v_I^p: \quad n_I\, \lambda \left(M_{pn} \frac{\partial v_J^n}{\partial x_J} + C_{pn}\, v_3^n \right) + n_J\, \mu\, M_{pn} \left(\frac{\partial v_I^n}{\partial x_J} + \frac{\partial v_J^n}{\partial x_I} \right) - \hat{Q}_I^p = 0 \tag{2.29a}$$

$$\delta v_3^p: \quad n_J\, \mu \left(C_{pn}\, v_J^n + M_{pn} \frac{\partial v_3^n}{\partial x_J} \right) - \hat{Q}_3^p = 0 \tag{2.29b}$$

where, in equations (2.28), the body forces are

$$\hat{F}_i^1 = F_i^1 + \hat{t}_i(x_1, x_2, -h), \quad \hat{F}_i^N = F_i^N + \hat{t}_i(x_1, x_2, h),$$

and

$$\hat{F}_i^p = F_i^p \quad (p=2,3,\ldots, N-1).$$

2.5 LAYERWISE BOUNDARY INTEGRAL EQUATIONS

Equation (2.27) may also be used to develop the boundary integral equations (BIE) that govern the deformation of a single layer, with a displacement variation through its thickness in the form of (2.18). In this case, expression (2.27) for the total potential energy is integrated in such a way that all derivatives of v_i are transferred to the δv_i. The integral statement (variational statement), which yields the BIE model, is given as

$$
\begin{aligned}
0 = \int_{\Omega} \Bigg[& -\lambda \left(M_{np} \frac{\partial^2 \delta v_J^p}{\partial x_I \partial x_J} + C_{np} \frac{\partial \delta v_3^p}{\partial x_I} \right) v_I^n - \mu M_{np} \left(\frac{\partial^2 \delta v_I^p}{\partial x_J \partial x_J} + \frac{\partial^2 \delta v_J^p}{\partial x_J \partial x_I} \right) v_I^n \\
& + \mu \left(K_{np} \delta v_I^p + D_{np} \frac{\partial \delta v_3^p}{\partial x_I} \right) v_I^n + \left(\lambda D_{np} \frac{\partial \delta v_J^p}{\partial x_J} + (\lambda + 2\mu) K_{np} \delta v_3^p \right) v_3^n \\
& - \mu \left(C_{np} \frac{\delta v_I^p}{\partial x_I} + M_{np} \frac{\partial^2 \delta v_3^p}{\partial x_I \partial x_I} \right) v_3^n \Bigg] d\Omega - \int_{\Omega} F_i^p \, \delta v_i^p \, d\Omega \\
& - \int_{\Omega} \left[\hat{t}_i(x_1, x_2, -h) \, \delta v_i^1 + \hat{t}_i(x_1, x_2, h) \, \delta v_i^N \right] d\Omega - \oint_{\Gamma} \hat{Q}_i^p \, \delta v_i^p \, d\Gamma \\
& + \oint_{\Gamma} \Bigg[\lambda \, n_I \left(M_{np} \frac{\partial \delta v_J^p}{\partial x_J} + C_{np} \delta v_3^p \right) v_I^n + \mu \, M_{np} \, n_J \left(\frac{\partial \delta v_I^p}{\partial x_J} + \frac{\partial \delta v_J^p}{\partial x_I} \right) v_I^n \\
& + \mu \, n_I \left(C_{np} \delta v_I^p + M_{np} \frac{\partial \delta v_3^p}{\partial x_I} \right) v_3^n \Bigg] d\Gamma \, .
\end{aligned}
\tag{2.30}
$$

In the last contour integral of equation (2.30) the terms that multiply the v_I^n are the traction components δt_I^n, and the term that multiplies v_3^n is the traction component δt_3^n:

$$
\delta t_I^n = n_I \, \lambda \left(M_{np} \frac{\partial \delta v_J^p}{\partial x_J} + C_{np} \delta v_3^p \right) + n_J \, \mu \, M_{np} \left(\frac{\partial \delta v_I^p}{\partial x_J} + \frac{\partial \delta v_J^p}{\partial x_I} \right) \tag{2.31a}
$$

$$
\delta t_3^n = n_I \, \mu \left(C_{np} \delta v_I^p + M_{np} \frac{\partial \delta v_3^p}{\partial x_I} \right). \tag{2.31b}
$$

The following quantities are also defined,

$$\delta p_I^n = -(\lambda+\mu)\, M_{np} \frac{\partial^2 \delta v_M^p}{\partial x_I \partial x_M} - \mu\, M_{np} \frac{\partial^2 \delta v_I^p}{\partial x_M \partial x_M} + (\mu\, D_{np} - \lambda\, C_{np}) \frac{\partial \delta v_3^p}{\partial x_I} + \mu\, K_{np}\, \delta v_I^p \tag{2.32a}$$

$$\delta p_3^n = -\mu\, M_{np} \frac{\partial^2 \delta v_3^p}{\partial x_M \partial x_M} + (\lambda\, D_{np} - \mu\, C_{np}) \frac{\partial \delta v_M^p}{\partial x_M} + (\lambda+2\mu)\, K_{np}\, \delta v_3^p\,. \tag{2.32b}$$

which essentially represent concentrated unit loads applied at points in the domain of the numerical layer and, if they are equated to zero, they form the equations that must be satisfied by the fundamental solution of the problem.

Comparing equations (2.32a) and (2.32b) to the discretized governing equations (2.28a) and (2.28b), it becomes apparent that the differential operator which is applied on v_i^n and its adjoint which is applied on δv_i^p are identical, and thus the operator for the two-dimensional problem is self-adjoint. Substitution of the definitions (2.31) and (2.32) into statement (2.30), yields the following simplified integral equation for the typical numerical layer

$$\begin{aligned} 0 = & \int_\Omega \delta p_i^n\, v_i^n\, d\Omega - \int_\Omega F_i^p\, \delta v_i^p\, d\Omega \\ & - \int_\Omega \left[\hat{t}_i(x_1, x_2, -h)\, \delta v_i^1 + \hat{t}_i(x_1, x_2, h)\, \delta v_i^N \right] d\Omega \\ & - \oint_\Gamma \hat{Q}_i^p\, \delta v_i^p\, d\Gamma + \oint_\Gamma \delta t_i^n\, v_i^n\, d\Gamma\,. \end{aligned} \tag{2.33}$$

The above integral statement gives rise to the boundary integral equations for the single numerical layer, and forms the basis for the development of the BIE model in the analysis of the two-dimensional counterpart of the problem. However, in order to apply this method it is necessary to obtain the *fundamental solution* of this problem, *i.e.*, the unit load solution to the problem of a

layer which has thickness $2h$ and extends to infinity in the x_1 and x_2 directions.

The virtual statement for the multilayered system of Figure 2.1, can be expressed in a form similar to that of equation (2.33). The multilayered plate is divided into L numerical layers through the thickness. At the interface between adjacent numerical layers appropriate conditions hold to ensure the displacement continuity and traction equilibrium. Denoting by e the typical layer, these conditions are expressed as

$$(v_i^N)_e = (v_i^1)_{e+1} \ , \quad (\delta v_i^N)_e = (\delta v_i^1)_{e+1} \tag{2.34}$$

$$t_i^e(x_1, x_2, h_e) + t_i^{(e+1)}(x_1, x_2, -h_{e+1}) = \hat{t}_i^{(e+1)}(x_1, x_2) \tag{2.35}$$

$$(e = 1, 2, \ldots, L; \ \ n = 1, 2, \ldots, N; \ \ i = 1, 2, 3)$$

where $\hat{t}_i^{(e+1)}$ denotes the components of the externally applied loads at the interface between the e and $(e+1)$ numerical layers, and $t_i^e(x_1, x_2, h_e)$ are the components of the tractions that develop at the upper surface of the e-th numerical layer. Taking into account conditions (2.34) and (2.35), the virtual statement for a multilayered system is written as

$$\begin{aligned}
0 = \int_\Omega \Bigg\{ & \sum_{e=1}^{L} \sum_{n=2}^{N-1} (\delta p_i^n v_i^n)_e + (\delta p_i^1 v_i^1)_1 + \ldots + \left[(\delta p_i^N)_e + (\delta p_i^1)_{e+1} \right] (v_i^1)_{e+1} \\
& + \ldots + (\delta p_i^N v_i^N)_L \Bigg\} \, d\Omega \\
- \int_\Omega \Bigg\{ & \sum_{e=1}^{L} \sum_{n=2}^{N-1} (F_i^n \delta v_i^n)_e + (F_i^1 \delta v_i^1)_1 + \ldots + \left[(F_i^N)_e + (F_i^1)_{e+1} \right] (\delta v_i^1)_{e+1} \\
& + \ldots + (F_i^N \delta v_i^N)_L \Bigg\} \, d\Omega \\
- \int_\Omega & \left\{ \hat{t}_i^1 (\delta v_i^1)_1 + \ldots + \hat{t}_i^e (\delta v_i^1)_e + \hat{t}_i^{(e+1)} (\delta v_i^1)_{e+1} + \ldots + \hat{t}_i^{(L+1)} (\delta v_i^N)_L \right\} d\Omega
\end{aligned}$$

$$-\oint_{\Gamma}\Bigg\{\sum_{e=1}^{L}\sum_{n=2}^{N-1}(\hat{Q}_i^n\delta v_i^n)_e+(\hat{Q}_i^1\delta v_i^1)_1+\ldots+\Big[(\hat{Q}_i^N)_e+(\hat{Q}_i^1)_{e+1}\Big](\delta v_i^1)_{e+1}$$
$$+\ldots+(\hat{Q}_i^N\delta v_i^N)_L\Bigg\}\,d\Gamma$$
$$+\oint_{\Gamma}\Bigg\{\sum_{e=1}^{L}\sum_{n=2}^{N-1}(\delta t_i^n v_i^n)_e+(\delta t_i^1 v_i^1)_1+\ldots+\Big[(\delta t_i^N)_e+(\delta t_i^1)_{e+1}\Big](v_i^1)_{e+1}$$
$$+\ldots+(\delta t_i^N v_i^N)_L\Bigg\}\,d\Gamma \tag{2.36}$$

where the components δp_i^n of the virtual body forces are given in equations (2.32a) and (2.32b) in terms of the layer's elastic constants and the virtual displacements, and $(\hat{Q}_i^n)_e$ are the components of the nodal forces acting on the side surface of the e-th numerical layer and are given in terms of the externally applied tractions in equation (2.26). The differential equations that are satisfied by the fundamental solution of the multilayered system are deduced from the first domain integral of (2.36). Equation (2.36) is the BIE model of the multilayered system that has been divided into L numerical layers.

The boundary integral equations for the typical numerical layer in equation (2.33), and for the multilayered system in equation (2.36), are given at this stage of the analysis in the form of variational statements. They will produce, however, the corresponding boundary integral models, if appropriate fundamental solutions are derived and then utilized in these variational statements as an admissible set of virtual displacements. For this purpose, a methodology has been developed for deriving fundamental solutions of a single layer or multiple layers and it is presented thoroughly in the following chapter.

Chapter 3

FUNDAMENTAL SOLUTIONS FOR LAYERED MEDIA

3.1 GOVERNING EQUATIONS OF AN INFINITE LAYER

The governing equations for a typical infinite layer (unbounded numerical layer) which is subjected to concentrated loads and which has been discretized through the thickness into N nodal points, are given by equations (2.32). These equations can also be written in the following convenient form:

$$-(\lambda+\mu)\,M_{np}\,\frac{\partial^2 V_M^p}{\partial x_I\,\partial x_M}-\mu\,M_{np}\,\frac{\partial^2 V_I^p}{\partial x_M\,\partial x_M}+(\mu\,D_{np}-\lambda\,C_{np})\,\frac{\partial V_3^p}{\partial x_I}$$

$$+\mu\,K_{np}\,V_I^p=P_I^n \tag{3.1}$$

$$-\mu\,M_{np}\,\frac{\partial^2 V_3^p}{\partial x_M\,\partial x_M}+(\lambda\,D_{np}-\mu\,C_{np})\,\frac{\partial V_M^p}{\partial x_M}+(\lambda+2\mu)\,K_{np}\,V_3^p=P_3^n \tag{3.2}$$

in which the subscripts I, M take the values 1 and 2, while the indices n, p take the values 1,2,..., N. The virtual displacements δv_i^p (i=1,2,3) have been

replaced by V_i^p, and the virtual body forces δp_i^n have been replaced by the unit concentrated load P_i^n which is applied in the x_i direction at the n-th node associated with an arbitrary point $(\xi_1, \xi_2) \in \Omega$. These forces P_i^n are expressed as

$$P_i^n(x_1, x_2) = \delta(x_1 - \xi_1)\ \delta(x_2 - \xi_2) = \delta(x)\,\delta(y) \tag{3.3}$$

where $\delta(x_i - \xi_i)$ is the Dirac function, and $x = x_1 - \xi_1$, $y = x_2 - \xi_2$ is the distance between the two points in the x_1 and x_2 directions, respectively. It must be emphasized that, the load is applied only at node n in the x_i direction, which means that there are no loads applied in the other two directions at this node and at the other (N–1) nodes as it is depicted in Figure 3.1.

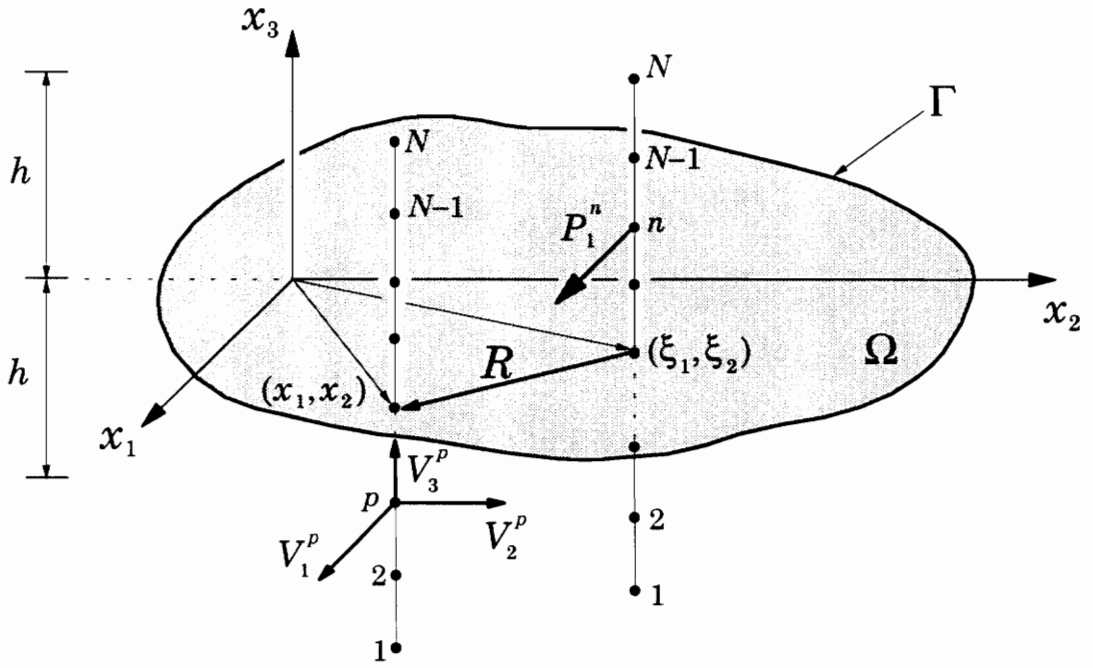

Figure 3.1 Displacement components $V_i^p(x_1, x_2)$ at node p of point (x_1, x_2) for a unit load applied in the x_1 direction at node n of point (ξ_1, ξ_2).

The domain of the problem at hand is considered to be discrete in the transverse direction and continuous over the entire middle plane Ω of the layer. Therefore, each point on this plane is associated with N nodal points through the thickness of the layer. Equations (3.1) and (3.2) along with the free-field boundary condition, that the solution should vanish at infinity, provide the displacement field as a continuous function of x_1 and x_2 at the N nodes associated with an arbitrary point $(x_1, x_2) \in \Omega$, for concentrated loads applied at the nodal points of another arbitrary point (ξ_1, ξ_2) of plane Ω (see Figure 3.1).

The fundamental solution in this case is a $3N \times 3N$ matrix whose entries are denoted by $U_{qs}(x_1, x_2; \xi_1, \xi_2)$, where the subscripts q and s are defined as

$$q = 3(p-1)+i \quad \text{and} \quad s = 3(n-1)+j\,, \tag{3.4}$$

with p, n=1,2,...,N, and i, j=1,2,3. $U_{qs}(x_1, x_2; \xi_1, \xi_2)$ represents the displacement along the x_i direction of node p at point (x_1, x_2), due to a unit concentrated load applied at the n-th node of (ξ_1, ξ_2) in the x_j direction, where the i, j, p and n are uniquely determined from the q and s using expressions (3.4). The unit load is given in equation (3.3) and all other point forces at the nodes through the thickness at point (ξ_1, ξ_2) are assumed to be zero (see Figure 3.1). The fundamental solution in its matrix form can also be viewed as the flexibility matrix of a typical element having N nodes along the transverse direction.

The stresses at any point (x_1, x_2, x_3) in the domain V, occupied by the typical element, can be expressed in terms of the displacements at the N nodes associated with point (x_1, x_2) of the middle plane Ω of the element, by introducing the displacement approximations (2.18) into the constitutive relations (2.3). The six stress components will be denoted by the stress vector $\tau_k(x_1, x_2, x_3)$ whose entries are defined as

$$\{\tau_1\ \tau_2\ \tau_3\ \tau_4\ \tau_5\ \tau_6\}^{\mathrm{T}} = \{\sigma_{11}\ \sigma_{22}\ \sigma_{33}\ \sigma_{12}\ \sigma_{23}\ \sigma_{31}\}^{\mathrm{T}}, \tag{3.5}$$

where the stress components can be expressed in terms of the displacement components V_i^p in the following way

$$\begin{Bmatrix} \sigma_{11} \\ \sigma_{22} \\ \sigma_{33} \\ \sigma_{12} \\ \sigma_{23} \\ \sigma_{31} \end{Bmatrix} = \sum_{p=1}^{N} \begin{bmatrix} (\lambda+2\mu)\phi_p \dfrac{\partial}{\partial x_1} & \lambda\phi_p \dfrac{\partial}{\partial x_2} & \lambda \dfrac{d\phi_p}{dx_3} \\ \lambda\phi_p \dfrac{\partial}{\partial x_1} & (\lambda+2\mu)\phi_p \dfrac{\partial}{\partial x_2} & \lambda \dfrac{d\phi_p}{dx_3} \\ \lambda\phi_p \dfrac{\partial}{\partial x_1} & \lambda\phi_p \dfrac{\partial}{\partial x_2} & (\lambda+2\mu) \dfrac{d\phi_p}{dx_3} \\ \mu\phi_p \dfrac{\partial}{\partial x_2} & \mu\phi_p \dfrac{\partial}{\partial x_1} & 0 \\ 0 & \mu \dfrac{d\phi_p}{dx_3} & \mu\phi_p \dfrac{\partial}{\partial x_2} \\ \mu \dfrac{d\phi_p}{dx_3} & 0 & \mu\phi_p \dfrac{\partial}{\partial x_1} \end{bmatrix} \begin{Bmatrix} V_1^p \\ V_2^p \\ V_3^p \end{Bmatrix} \tag{3.6}$$

or

$$\tau_k = \mathbf{B}_{ki}^p\, V_i^p \qquad (k = 1, 2, \ldots, 6;\ i = 1, 2, 3). \tag{3.7}$$

In the above equations, summation convention is implied over the repeated index p=1,2,...,N, and $\mathbf{B}_{ki}^p$ denotes the differential operator in the constitutive relation (3.6). Equation (3.6) can also be used to describe the stresses in a typical element of the finite plate which correspond to the displacement field $(v_1^p,\ v_2^p,\ v_3^p)$.

In a way similar to that of defining the fundamental solution, a stress matrix $S_{ks}(x_1, x_2, x_3; \xi_1, \xi_2)$ is introduced, where the subscript s is given in equation (3.4). Its columns are the six stress components (k=1,...,6) at an arbitrary point (x_1, x_2, x_3) in V, which are produced by a unit concentrated load in the x_j direction at the n-th node of point (ξ_1, ξ_2). This stress matrix is expressed in terms of the fundamental solution as

$$[\mathbf{S}(x_1, x_2, x_3; \xi_1, \xi_2)] = \left[\left[\mathbf{B}^1(x_3)\right] \left[\mathbf{B}^2(x_3)\right] \cdots \left[\mathbf{B}^N(x_3)\right] \right] \ [\mathbf{U}(x_1, x_2; \xi_1, \xi_2)] \tag{3.8}$$

where the operator $\mathbf{B}_{ki}^{p}$ at each node p is given in equation (3.7).

The differential equations of an infinite multilayered plate, which is subjected to unit loads, are obtained in a similar way. In this case, the definitions of (2.32) are written for each numerical layer as

$$(\delta p_I^n)_e = -(\lambda_e + \mu_e) M_{np}^e \frac{\partial^2 (V_M^p)_e}{\partial x_I \partial x_M} - \mu_e M_{np}^e \frac{\partial^2 (V_I^p)_e}{\partial x_M \partial x_M}$$

$$+ (\mu_e D_{np}^e - \lambda_e C_{np}^e) \frac{\partial (V_3^p)_e}{\partial x_I} + \mu_e K_{np}^e (V_I^p)_e \qquad (3.9)$$

$$(\delta p_3^n)_e = -\mu_e M_{np}^e \frac{\partial^2 (V_3^p)_e}{\partial x_M \partial x_M} + (\lambda_e D_{np}^e - \mu_e C_{np}^e) \frac{\partial (V_M^p)_e}{\partial x_M}$$

$$+ (\lambda_e + 2\mu_e) K_{np}^e (V_3^p)_e \qquad (3.10)$$

where I, M=1,2; e=1,2,...,L and n, p=1,2,...,N. Then, setting the coefficients of the actual displacement components $(v_i^n)_e$ in the first domain integral of (2.36), equal to unit loads of the form of (3.3), the differential equations are derived in the following concise form

$$(\delta p_i^n)_e = (P_i^n)_e \quad (n=2,3,...,N;\ e=1,2,...,L) \qquad (3.11)$$

$$\left(\delta p_i^N\right)_e + \left(\delta p_i^1\right)_{e+1} = \hat{P}_i^e \ \text{ and } \ \left(V_i^N\right)_e = \left(V_i^1\right)_{e+1} \quad (e=1,2,...,L-1) \qquad (3.12)$$

where $(\delta p_i^n)_e$ (i=1,2,3) are given in equations (3.9) and (3.10). $(P_i^n)_e$ denote the components of unit nodal forces that act at nodes within the numerical layer, while $\hat{P}_i^e$ denote the components of unit forces that act at the common node between adjacent layers. All the unit loads in equations (3.11) and (3.12) are expressed mathematically in the same way as the load in equation (3.3).

3.2 FOURIER TRANSFORM OF THE DIFFERENTIAL EQUATIONS

Equations (3.1) and (3.2) form a system of second order linear partial differential equations. The number of the unknowns and corresponding number of equations depend on the number of nodes in each element. The solution of this system can be obtained in a systematic way by transforming the differential equations to the two-dimensional Fourier domain and solving the corresponding N ordinary algebraic equations for the N unknown displacements. The solution in the physical space can then be obtained through the inverse transform. According to Sneddon (1951, 1975), the following two-dimensional Fourier transform is defined

$$\bar{f}(\alpha_1, \alpha_2) = \mathfrak{F}[f(x_1, x_2)] = \frac{1}{2\pi} \int_{-\infty}^{+\infty} \int_{-\infty}^{+\infty} f(x_1, x_2)\, e^{i(\alpha_1 x_1 + \alpha_2 x_2)}\, dx_1\, dx_2 \tag{3.13}$$

where $i = \sqrt{-1}$, and its inverse transform is

$$f(x_1, x_2) = \mathfrak{F}^{-1}\left[\bar{f}(\alpha_1, \alpha_2)\right] = \frac{1}{2\pi} \int_{-\infty}^{+\infty} \int_{-\infty}^{+\infty} \bar{f}(\alpha_1, \alpha_2)\, e^{-i(\alpha_1 x_1 + \alpha_2 x_2)}\, d\alpha_1\, d\alpha_2, \tag{3.14}$$

if $f(x_1, x_2)$ satisfies Dirichlet's conditions for $-\infty < x_1, x_2 < \infty$ and if the integral

$$\int_{-\infty}^{+\infty} \int_{-\infty}^{+\infty} f(x_1, x_2)\, dx_1\, dx_2$$

is absolutely convergent. The transforms of the derivatives that appear in (3.1), (3.2) and (3.3) of the fundamental problem are given by

$$\overline{\frac{\partial f}{\partial x_I}} = -i\, \alpha_I\, \bar{f}, \quad \text{for} \lim_{|x_I| \to \infty} f(x_1, x_2) \to 0, \tag{3.15}$$

$$\overline{\frac{\partial^2 f}{\partial^2 x_I}} = -\alpha_I^2\, \bar{f}, \quad \text{for} \lim_{|x_I| \to \infty} f(x_1, x_2) \to 0 \quad \text{and} \lim_{|x_I| \to \infty} \frac{\partial f(x_1, x_2)}{\partial x_I} \to 0, \tag{3.16}$$

$$\overline{\frac{\partial^2 f}{\partial x_1 \partial x_2}} = -\alpha_1 \alpha_2 \bar{f}, \quad \text{for} \lim_{|x_1|\to\infty} f(x_1, x_2) \to 0 \quad \text{and} \lim_{|x_2|\to\infty} f(x_1, x_2) \to 0 \,. \quad (3.17)$$

For the case of an infinite layer subjected to a concentrated load the displacements and the tractions vanish at infinity and therefore the displacement vector V_i^p is such that all the above conditions are fulfilled (equation 2.12).

Application of the above definitions (3.13, 3.15, 3.16 and 3.17) to the governing equations (3.1) and (3.2), yields

$$(\lambda+\mu)\,\alpha_I\,\alpha_M\,M_{np}\,\bar{V}_M^p + \mu\,\alpha_M\,\alpha_M\,M_{np}\,\bar{V}_I^p + i\,\alpha_I\,(\lambda\,C_{np} - \mu\,D_{np})\bar{V}_3^p + \mu\,K_{np}\,\bar{V}_I^p = \bar{P}_I^n \quad (3.18)$$

$$\mu\,\alpha_M\,\alpha_M\,M_{np}\,\bar{V}_3^p + i\,\alpha_M\,(\mu\,C_{np} - \lambda\,D_{np})\,\bar{V}_M^p + (\lambda+2\mu)\,K_{np}\,\bar{V}_3^p = \bar{P}_3^n \quad (3.19)$$

and application to the equations (3.6) and (3.7) for the stresses, yields

$$\begin{Bmatrix} \bar{\tau}_1 \\ \bar{\tau}_2 \\ \bar{\tau}_3 \\ \bar{\tau}_4 \\ \bar{\tau}_5 \\ \bar{\tau}_6 \end{Bmatrix} = \sum_{p=1}^{N} \begin{bmatrix} -i\alpha_1(\lambda+2\mu)\phi_p & -i\alpha_2\lambda\phi_p & \lambda\dfrac{d\phi_p}{dx_3} \\ -i\alpha_1\lambda\phi_p & -i\alpha_2(\lambda+2\mu)\phi_p & \lambda\dfrac{d\phi_p}{dx_3} \\ -i\alpha_1\lambda\phi_p & -i\alpha_2\lambda\phi_p & (\lambda+2\mu)\dfrac{d\phi_p}{dx_3} \\ -i\alpha_2\mu\phi_p & -i\alpha_1\mu\phi_p & 0 \\ 0 & \mu\dfrac{d\phi_p}{dx_3} & -i\alpha_2\mu\phi_p \\ \mu\dfrac{d\phi_p}{dx_3} & 0 & -i\alpha_1\mu\phi_p \end{bmatrix} \begin{Bmatrix} \bar{V}_1^p \\ \bar{V}_2^p \\ \bar{V}_3^p \end{Bmatrix} \quad (3.20)$$

or $$\bar{\tau}_k = \bar{\mathbf{B}}_{ki}^p\,\bar{V}_i^p \qquad (k = 1, 2, \ldots, 6) \,. \quad (3.21)$$

Equations (3.18) and (3.19) can be rewritten in a matrix form giving the following system of algebraic equations

$$\begin{bmatrix} [\bar{\mathbf{K}}^{pp}] & [\bar{\mathbf{K}}^{pz}] \\ [\bar{\mathbf{K}}^{zp}] & [\bar{\mathbf{K}}^{zz}] \end{bmatrix} \begin{Bmatrix} \{\bar{\mathbf{V}}^{p}\} \\ \{\bar{\mathbf{V}}^{z}\} \end{Bmatrix} = \begin{Bmatrix} \{\bar{\mathbf{P}}^{p}\} \\ \{\bar{\mathbf{P}}^{z}\} \end{Bmatrix} \tag{3.22}$$

where

$$\{\bar{\mathbf{V}}^{p}\} = \begin{Bmatrix} \begin{Bmatrix} \bar{V}_1^1 \\ \bar{V}_2^1 \end{Bmatrix} \\ \begin{Bmatrix} \bar{V}_1^2 \\ \bar{V}_2^2 \end{Bmatrix} \\ \vdots \\ \begin{Bmatrix} \bar{V}_1^N \\ \bar{V}_2^N \end{Bmatrix} \end{Bmatrix}, \qquad \{\bar{\mathbf{V}}^{z}\} = \begin{Bmatrix} \bar{V}_3^1 \\ \bar{V}_3^2 \\ \vdots \\ \bar{V}_3^N \end{Bmatrix}, \tag{3.23}$$

$$\{\bar{\mathbf{P}}^{p}\} = \begin{Bmatrix} \begin{Bmatrix} \bar{P}_1^1 \\ \bar{P}_2^1 \end{Bmatrix} \\ \begin{Bmatrix} \bar{P}_1^2 \\ \bar{P}_2^2 \end{Bmatrix} \\ \vdots \\ \begin{Bmatrix} \bar{P}_1^N \\ \bar{P}_2^N \end{Bmatrix} \end{Bmatrix}, \qquad \{\bar{\mathbf{P}}^{z}\} = \begin{Bmatrix} \bar{P}_3^1 \\ \bar{P}_3^2 \\ \vdots \\ \bar{P}_3^N \end{Bmatrix}. \tag{3.24}$$

The components of the force vectors in equations (3.24) are obtained from the Fourier transform of the unit loads of equation (3.3). Their transformed components are

$$\bar{P}_i^n = \frac{1}{2\pi} \int_{-\infty}^{+\infty} \int_{-\infty}^{+\infty} \delta(x)\, \delta(y)\, e^{i(\alpha_1 x_1 + \alpha_2 x_2)}\, dx_1\, dx_2 = \frac{1}{2\pi} e^{i(\alpha_1 \xi_1 + \alpha_2 \xi_2)}. \tag{3.25}$$

The stiffness equation of a typical numerical layer, whose form is shown in (3.22), can be used to construct the stiffness equation of the multilayered plate that consists of L such layers and extends to infinity in the plane Ω. The element stiffness matrices are assembled using the continuity conditions that were introduced in (3.11) and (3.12). Denoting by e the typical layer, the transformed interface conditions are

$$\left\{\begin{array}{c}\bar{V}_1^N\\ \bar{V}_2^N\\ \bar{V}_3^N\end{array}\right\}_e = \left\{\begin{array}{c}\bar{V}_1^1\\ \bar{V}_2^1\\ \bar{V}_3^1\end{array}\right\}_{e+1} \quad \text{and} \quad \left\{\begin{array}{c}\bar{P}_1^N\\ \bar{P}_2^N\\ \bar{P}_3^N\end{array}\right\}_e + \left\{\begin{array}{c}\bar{P}_1^1\\ \bar{P}_2^1\\ \bar{P}_3^1\end{array}\right\}_{e+1} = \left\{\begin{array}{c}\bar{\hat{P}}_1\\ \bar{\hat{P}}_2\\ \bar{\hat{P}}_3\end{array}\right\}_e \tag{3.26}$$

where e=1,2,...,(L–1) and $\left(\bar{\hat{P}}_i\right)_e$ denotes the components of the unit load applied at the interface between layers e and (e+1) and is given in equation (3.25). The final form of the assembled equations is going to be

$$\left[\bar{\mathbf{K}}(\alpha_1,\alpha_2)\right]\left\{\bar{\mathbf{V}}(\alpha_1,\alpha_2;\xi_1,\xi_2)\right\} = \left\{\bar{\mathbf{P}}(\xi_1,\xi_2)\right\} \tag{3.27}$$

where $\left[\bar{\mathbf{K}}\right]$ is the transformed stiffness matrix of the multilayered plate, $\left\{\bar{\mathbf{V}}\right\}$ is the vector of all the transformed nodal displacements and $\left\{\bar{\mathbf{P}}\right\}$ is the vector of all the nodal forces. The dimension of these vectors is, 3 [L (N–1)+1].

3.3 FUNDAMENTAL SOLUTION IN THE FOURIER DOMAIN

The formulation presented up to this point is general and refers to a N-node numerical layer with $3N$ degrees of freedom at every point in the plane Ω. However, a closed-form solution to the system of equations (3.22) can be obtained only if specific interpolation functions are chosen for the approximation of the displacements through the thickness of the layer. The degree of the polynomials in (2.18) is determined by considering requirements on the accuracy of the solution, the type of loading, the cross sectional geometry of the multilayered plate, and whether the problem is studied at a micro- or macro-mechanical level. In the sequel, it is assumed that the displacements vary linearly through the thickness $2h$ of the element, and thus, the finite element interpolation functions are

$$\phi_1(x_3) = \frac{h-x_3}{2h} \quad \text{and} \quad \phi_2(x_3) = \frac{h+x_3}{2h}\ . \tag{3.28}$$

Substitution of these functions into expressions (2.21) to (2.24), yields (Reddy, 1993),

$$[K]=\frac{1}{2h}\begin{bmatrix} 1 & -1 \\ -1 & 1 \end{bmatrix},\ [M]=\frac{h}{3}\begin{bmatrix} 2 & 1 \\ 1 & 2 \end{bmatrix} \text{ and } [C]=[D]^{\mathrm{T}}=\frac{1}{2}\begin{bmatrix} -1 & 1 \\ -1 & 1 \end{bmatrix}. \quad (3.29)$$

Making use of the element matrices given in (3.29) and by means of equations (3.18) and (3.19), the matrices in the transformed stiffness equation (3.22) become

$$\left[\bar{\mathbf{K}}^{pp}\right] = \frac{h}{3}(\lambda+2\mu) \times \begin{bmatrix} 2\left(\alpha_1^2+A_2\alpha_2^2\right) & 2A_3\alpha_1\alpha_2 & \alpha_1^2+A_2\alpha_2^2 & A_3\alpha_1\alpha_2 \\ 2A_3\alpha_1\alpha_2 & 2\left(A_2\alpha_1^2+\alpha_2^2\right) & A_3\alpha_1\alpha_2 & A_2\alpha_1^2+\alpha_2^2 \\ \alpha_1^2+A_2\alpha_2^2 & A_3\alpha_1\alpha_2 & 2\left(\alpha_1^2+A_2\alpha_2^2\right) & 2A_3\alpha_1\alpha_2 \\ A_3\alpha_1\alpha_2 & A_2\alpha_1^2+\alpha_2^2 & 2A_3\alpha_1\alpha_2 & 2\left(A_2\alpha_1^2+\alpha_2^2\right) \end{bmatrix} + \frac{\mu}{2h}\begin{bmatrix} 1 & 0 & -1 & 0 \\ 0 & 1 & 0 & -1 \\ -1 & 0 & 1 & 0 \\ 0 & -1 & 0 & 1 \end{bmatrix} \quad (3.30)$$

$$\left[\bar{\mathbf{K}}^{pz}\right] = i\,\frac{1}{2}\begin{bmatrix} (\mu-\lambda)\alpha_1 & (\mu+\lambda)\alpha_1 \\ (\mu-\lambda)\alpha_2 & (\mu+\lambda)\alpha_2 \\ -(\mu+\lambda)\alpha_1 & (\lambda-\mu)\alpha_1 \\ -(\mu+\lambda)\alpha_2 & (\lambda-\mu)\alpha_2 \end{bmatrix} \quad (3.31)$$

$$\left[\bar{\mathbf{K}}^{zp}\right] = i\,\frac{1}{2}\begin{bmatrix} (\lambda-\mu)\alpha_1 & (\lambda-\mu)\alpha_2 & (\mu+\lambda)\alpha_1 & (\mu+\lambda)\alpha_2 \\ -(\mu+\lambda)\alpha_1 & -(\mu+\lambda)\alpha_2 & (\mu-\lambda)\alpha_1 & (\mu-\lambda)\alpha_2 \end{bmatrix} \quad (3.32)$$

$$\left[\bar{\mathbf{K}}^{zz}\right] = \frac{h}{3}\mu\begin{bmatrix} 2 & 1 \\ 1 & 2 \end{bmatrix}\left(\alpha_1^2+\alpha_2^2\right)+\frac{(\lambda+2\mu)}{2h}\begin{bmatrix} 1 & -1 \\ -1 & 1 \end{bmatrix} \quad (3.33)$$

with $i=\sqrt{-1}$ and

$$\left.\begin{aligned} A_1 &= \frac{\lambda}{\lambda+2\mu} = \frac{\nu}{(1-\nu)}, \quad A_2 = \frac{\mu}{\lambda+2\mu} = \frac{(1-2\nu)}{2(1-\nu)} \\ A_3 &= A_1 + A_2 = \frac{\lambda+\mu}{\lambda+2\mu} = \frac{1}{2(1-\nu)} \end{aligned}\right\} \tag{3.34}$$

Equations (3.22) form a system of six ordinary algebraic equations in six unknowns. The system is solved for each unit load and the six corresponding displacement vectors are grouped into a 6×6 matrix $\left[\bar{\mathbf{U}}\right]$. This matrix is the fundamental solution in the Fourier domain of a single infinite layer with linear variation of the displacements through the thickness. This matrix can also be viewed as the flexibility matrix of the layer. The structure of this matrix is shown schematically in the following equation,

$$\left[\bar{\mathbf{U}}(\alpha_1,\alpha_2;\xi_1,\xi_2)\right] = \begin{array}{c} \overbrace{\phantom{\bar{P}_1^1\ \bar{P}_2^1\ \bar{P}_3^1}}^{\text{node 1}}\ \overbrace{\phantom{\bar{P}_1^2\ \bar{P}_2^2\ \bar{P}_3^2}}^{\text{node 2}} \\ \bar{P}_1^1\ \bar{P}_2^1\ \bar{P}_3^1\ \ \bar{P}_1^2\ \bar{P}_2^2\ \bar{P}_3^2 \\ \left[\begin{array}{cccccc} \bar{U}_{11} & \bar{U}_{12} & \bar{U}_{13} & \bar{U}_{14} & \bar{U}_{15} & \bar{U}_{16} \\ \bar{U}_{21} & \bar{U}_{22} & \bar{U}_{23} & \bar{U}_{24} & \bar{U}_{25} & \bar{U}_{26} \\ \bar{U}_{31} & \bar{U}_{32} & \bar{U}_{33} & \bar{U}_{34} & \bar{U}_{35} & \bar{U}_{36} \\ \bar{U}_{41} & \bar{U}_{42} & \bar{U}_{43} & \bar{U}_{44} & \bar{U}_{45} & \bar{U}_{46} \\ \bar{U}_{51} & \bar{U}_{52} & \bar{U}_{53} & \bar{U}_{54} & \bar{U}_{55} & \bar{U}_{56} \\ \bar{U}_{61} & \bar{U}_{62} & \bar{U}_{63} & \bar{U}_{64} & \bar{U}_{65} & \bar{U}_{66} \end{array}\right] \begin{array}{l} \leftarrow \\ \leftarrow \\ \leftarrow \\ \leftarrow \\ \leftarrow \\ \leftarrow \end{array} \begin{array}{l} \left.\begin{array}{l} \bar{V}_1^1 \\ \bar{V}_2^1 \\ \bar{V}_3^1 \end{array}\right\} \text{node 1} \\ \left.\begin{array}{l} \bar{V}_1^2 \\ \bar{V}_2^2 \\ \bar{V}_3^2 \end{array}\right\} \text{node 2} \end{array} \end{array} \tag{3.35}$$

The fundamental solution $U_{ij}(x_1,x_2;\xi_1,\xi_2)$ is obtained by taking the inverse transform of $\bar{U}_{ij}(\alpha_1,\alpha_2;\xi_1,\xi_2)$, and it represents the displacement in the direction and nodal position of the i-th degree of freedom at point (x_1,x_2) of the middle plane Ω, due to a unit concentrated load along the direction and nodal position of the j-th degree of freedom at point (ξ_1,ξ_2) on plane Ω. The components of the solution in the physical space are

$$\left\{\begin{array}{c} U_{11} \\ U_{22} \end{array}\right\} = \left\{\begin{array}{c} U_{44} \\ U_{55} \end{array}\right\} = \frac{h}{\pi\mu}\left\{\begin{array}{c} \mathrm{f}_{10} \\ \mathrm{f}_{10} \end{array}\right\} + \frac{h}{4\pi\mu}\left(-4A_3 + \frac{A_4}{4}\right)\left\{\begin{array}{c} \mathrm{f}_{73} \\ \mathrm{f}_{75} \end{array}\right\}$$
$$- \frac{3h}{4\pi\mu}\left\{\begin{array}{c} \mathrm{f}_{75} - \mathrm{f}_{93} \\ \mathrm{f}_{73} - \mathrm{f}_{91} \end{array}\right\} - \frac{h}{4\pi\mu}\frac{A_4}{4}\left\{\begin{array}{c} \mathrm{f}_{81} \\ \mathrm{f}_{83} \end{array}\right\} \qquad (3.36a)$$

$$U_{12} = U_{21} = U_{45} = U_{54} = \frac{h}{4\pi\mu}\left(-4A_3 + \frac{A_4}{4}\right)\mathrm{f}_{74} + \frac{3h}{4\pi\mu}\left(\mathrm{f}_{74} - \mathrm{f}_{92}\right)$$
$$- \frac{h}{4\pi\mu}\frac{A_4}{4}\mathrm{f}_{82} \qquad (3.36b)$$

$$U_{24} = U_{42} = U_{15} = U_{51} = \frac{h}{4\pi\mu}\left(2A_3 + \frac{A_4}{4}\right)\mathrm{f}_{74} + \frac{3h}{4\pi\mu}\left(-\mathrm{f}_{74} + \mathrm{f}_{92}\right)$$
$$- \frac{h}{4\pi\mu}\frac{A_4}{4}\mathrm{f}_{82} \qquad (3.36c)$$

$$\left\{\begin{array}{c} U_{14} \\ U_{25} \end{array}\right\} = \left\{\begin{array}{c} U_{41} \\ U_{52} \end{array}\right\} = -\frac{h}{2\pi\mu}\left\{\begin{array}{c} \mathrm{f}_{10} \\ \mathrm{f}_{10} \end{array}\right\} + \frac{h}{4\pi\mu}\left(2A_3 + \frac{A_4}{4}\right)\left\{\begin{array}{c} \mathrm{f}_{73} \\ \mathrm{f}_{75} \end{array}\right\}$$
$$+ \frac{3h}{4\pi\mu}\left\{\begin{array}{c} \mathrm{f}_{75} - \mathrm{f}_{93} \\ \mathrm{f}_{73} - \mathrm{f}_{91} \end{array}\right\} - \frac{h}{4\pi\mu}\frac{A_4}{4}\left\{\begin{array}{c} \mathrm{f}_{81} \\ \mathrm{f}_{83} \end{array}\right\} \qquad (3.36d)$$

$$\left\{\begin{array}{c} U_{61} \\ U_{62} \\ U_{64} \\ U_{65} \end{array}\right\} = -\left\{\begin{array}{c} U_{16} \\ U_{26} \\ U_{46} \\ U_{56} \end{array}\right\} = -\left\{\begin{array}{c} U_{34} \\ U_{35} \\ U_{31} \\ U_{32} \end{array}\right\} = \left\{\begin{array}{c} U_{43} \\ U_{53} \\ U_{13} \\ U_{23} \end{array}\right\} =$$
$$= \frac{hA_1}{16\pi\mu A_3}\left\{\begin{array}{c} \mathrm{f}_{41} - \mathrm{f}_{51} \\ \mathrm{f}_{42} - \mathrm{f}_{52} \\ \mathrm{f}_{41} - \mathrm{f}_{51} \\ \mathrm{f}_{42} - \mathrm{f}_{52} \end{array}\right\} + \frac{3hA_2}{4\pi\mu}\left\{\begin{array}{c} \mathrm{f}_{71} \\ \mathrm{f}_{72} \\ -\mathrm{f}_{71} \\ -\mathrm{f}_{72} \end{array}\right\} \qquad (3.36e)$$

$$U_{33} = U_{66} = \frac{h}{4\pi\mu}\left(\mathrm{f}_{10} + 3A_2\,\mathrm{f}_{30}\right) + \frac{3h}{4\pi\mu}\,\mathrm{f}_{20} \qquad (3.36f)$$

$$U_{36} = U_{63} = \frac{h}{4\pi\mu}\left(\mathrm{f}_{10} + 3A_2\,\mathrm{f}_{30}\right) - \frac{3h}{4\pi\mu}\,\mathrm{f}_{20} \qquad (3.36g)$$

where

$$A_4 = \frac{A_1^2}{A_3} = \frac{\lambda^2}{(\lambda+\mu)(\lambda+2\mu)} = \frac{2\nu^2}{1-\nu} \tag{3.37}$$

and $f_{\alpha\beta}$ are functions of $x = x_1 - \xi_1$ and $y = x_2 - \xi_2$, having Fourier transforms

$$\left.\begin{aligned}
&\bar{f}_{10} = \frac{P}{\bar{\rho}^2}, \quad \bar{f}_{20} = \frac{P}{(c^2+\bar{\rho}^2)}, \quad \bar{f}_{30} = \frac{P}{\bar{\rho}^4} \\
&\begin{Bmatrix} \bar{f}_{41} \\ \bar{f}_{42} \end{Bmatrix} = \frac{iP}{\bar{\rho}^2} \begin{Bmatrix} \bar{\alpha}_1 \\ \bar{\alpha}_2 \end{Bmatrix}, \quad \begin{Bmatrix} \bar{f}_{51} \\ \bar{f}_{52} \end{Bmatrix} = \frac{iP}{(c^2+\bar{\rho}^2)} \begin{Bmatrix} \bar{\alpha}_1 \\ \bar{\alpha}_2 \end{Bmatrix} \\
&\begin{Bmatrix} \bar{f}_{71} \\ \bar{f}_{72} \end{Bmatrix} = \frac{iP}{\bar{\rho}^4} \begin{Bmatrix} \bar{\alpha}_1 \\ \bar{\alpha}_2 \end{Bmatrix}, \quad \begin{Bmatrix} \bar{f}_{73} \\ \bar{f}_{74} \\ \bar{f}_{75} \end{Bmatrix} = \frac{P}{\bar{\rho}^4} \begin{Bmatrix} \bar{\alpha}_1^2 \\ \bar{\alpha}_1\bar{\alpha}_2 \\ \bar{\alpha}_2^2 \end{Bmatrix} \\
&\begin{Bmatrix} \bar{f}_{81} \\ \bar{f}_{82} \\ \bar{f}_{83} \end{Bmatrix} = \frac{P}{\bar{\rho}^2(c^2+\bar{\rho}^2)} \begin{Bmatrix} \bar{\alpha}_1^2 \\ \bar{\alpha}_1\bar{\alpha}_2 \\ \bar{\alpha}_2^2 \end{Bmatrix}, \quad \begin{Bmatrix} \bar{f}_{91} \\ \bar{f}_{92} \\ \bar{f}_{93} \end{Bmatrix} = \frac{P}{\bar{\rho}^2(3+\bar{\rho}^2)} \begin{Bmatrix} \bar{\alpha}_1^2 \\ \bar{\alpha}_1\bar{\alpha}_2 \\ \bar{\alpha}_2^2 \end{Bmatrix}
\end{aligned}\right\} \tag{3.38}$$

in which $i = \sqrt{-1}$,

$$P = e^{i(\alpha_1\xi_1 + \alpha_2\xi_2)} \tag{3.39}$$

and

$$c = \sqrt{\frac{12(\lambda+\mu)}{(\lambda+2\mu)}} = 2\sqrt{3A_3} \ . \tag{3.40}$$

The quantities $\bar{\alpha}_I = h\alpha_I$ are the dimensionless transform parameters and

$$\bar{\rho} = h\rho = h\sqrt{\alpha_1^2+\alpha_2^2} \ . \tag{3.41}$$

Equations (3.36) also apply in the Fourier domain if the symbols 'U' and 'f' are replaced by the corresponding symbols of the transformed quantities '$\bar{U}$' and '$\bar{f}$', respectively.

Substitution of the transformed fundamental solution (3.35) into expression (3.20) for the stresses produces a 6×6 matrix of the following form

$$\left[\bar{\mathbf{S}}\right]=\left[\left[\bar{\mathbf{B}}^{1}\right]\left[\bar{\mathbf{B}}^{2}\right]\right]\left[\bar{\mathbf{U}}\right] \tag{3.42}$$

where the operator $\left[\bar{\mathbf{B}}^{p}\right]$ (p=1,2) is given in equations (3.20) and (3.21). The k-th column of $\left[\bar{\mathbf{S}}\right]$ represents the six transformed stress components at an arbitrary point of the layer due to a unit concentrated load in the direction and nodal position of the k-th degree of freedom. This is the same load that caused the displacement field of the k-th column of $\left[\bar{\mathbf{U}}\right]$ in (3.35). The components of matrix $[\mathbf{S}(x_1,x_2,x_3;\xi_1,\xi_2)]$, which is the inverse transform of $\left[\bar{\mathbf{S}}\right]$, are given in the following concise form of matrix multiplications

$$\begin{bmatrix} S_{11} & S_{14} \\ S_{21} & S_{24} \\ S_{12} & S_{15} \\ S_{22} & S_{25} \end{bmatrix} = \frac{1}{8\pi}\left(\frac{A_5}{A_3}\begin{Bmatrix} -f_{77} \\ f_{77} \\ f_{76} \\ -f_{76} \end{Bmatrix} + A_4\begin{Bmatrix} -f_{85} \\ f_{85} \\ f_{84} \\ -f_{84} \end{Bmatrix} - \frac{1}{A_3}\begin{Bmatrix} 2A_3 f_{41} \\ A_1 f_{41} \\ A_1 f_{42} \\ 2A_3 f_{42} \end{Bmatrix}\right)\begin{Bmatrix} 1 & 1 \end{Bmatrix}$$

$$-\frac{A_4}{8\pi}\begin{Bmatrix} 0 \\ f_{51} \\ f_{52} \\ 0 \end{Bmatrix}\begin{Bmatrix} 1 & 1 \end{Bmatrix} + \frac{3}{2\pi}\frac{x_3}{h}\left(\begin{Bmatrix} -A_2 f_{77} + f_{95} \\ A_2 f_{77} - f_{95} \\ A_2 f_{76} - f_{94} \\ -A_2 f_{76} + f_{94} \end{Bmatrix}\right.$$

$$\left. + \frac{1}{2}\begin{Bmatrix} f_{41} \\ A_1 f_{41} \\ A_1 f_{42} \\ f_{42} \end{Bmatrix}\right)\begin{Bmatrix} 1 & -1 \end{Bmatrix} \tag{3.43a}$$

$$\begin{bmatrix} S_{31} & S_{34} \\ S_{32} & S_{35} \end{bmatrix} = \frac{A_1}{4\pi}\left(-\begin{bmatrix} f_{51} & f_{51} \\ f_{52} & f_{52} \end{bmatrix} + 3\frac{x_3}{h}\begin{bmatrix} f_{41} & -f_{41} \\ f_{42} & -f_{42} \end{bmatrix}\right) \tag{3.43b}$$

$$\begin{bmatrix} S_{41} & S_{44} \\ S_{42} & S_{45} \end{bmatrix} = \frac{1}{2\pi}\left(\frac{A_5}{4A_3}\begin{Bmatrix} f_{76} \\ f_{77} \end{Bmatrix} + \frac{A_4}{4}\begin{Bmatrix} f_{84} \\ f_{85} \end{Bmatrix} - \frac{1}{2}\begin{Bmatrix} f_{42} \\ f_{41} \end{Bmatrix}\right)\{\, 1 \;\; 1 \,\}$$

$$+\frac{3}{2\pi}\frac{x_3}{h}\left(\frac{1}{2}\begin{Bmatrix} f_{62} \\ f_{61} \end{Bmatrix} - \begin{Bmatrix} f_{94} \\ f_{95} \end{Bmatrix} + A_2\begin{Bmatrix} f_{76} \\ f_{77} \end{Bmatrix}\right)\{\, 1 \;\; -1 \,\} \qquad (3.43c)$$

$$\begin{bmatrix} S_{51} & S_{52} & S_{54} & S_{55} \\ S_{61} & S_{62} & S_{64} & S_{65} \end{bmatrix} = \frac{3}{4\pi}\begin{bmatrix} f_{92} & -f_{91} & -f_{92} & f_{91} \\ -f_{93} & f_{92} & f_{93} & -f_{92} \end{bmatrix}$$

$$+\frac{x_3}{h}\frac{3A_1}{4\pi}\begin{bmatrix} f_{82} & f_{83} & f_{82} & f_{83} \\ f_{81} & f_{82} & f_{81} & f_{82} \end{bmatrix} \qquad (3.43d)$$

$$\begin{bmatrix} S_{13} & S_{16} \\ S_{23} & S_{26} \\ S_{43} & S_{46} \end{bmatrix} = \frac{3A_1}{2\pi}\begin{Bmatrix} f_{83} \\ f_{81} \\ -f_{82} \end{Bmatrix}\{\, -1 \;\; 1 \,\}$$

$$+\frac{3}{2\pi}\frac{x_3}{h}\left(\begin{Bmatrix} 1 \\ A_1 \\ 0 \end{Bmatrix}\frac{f_{10}}{2} + A_2\begin{Bmatrix} -f_{75} \\ f_{75} \\ f_{74} \end{Bmatrix}\right)\{\, 1 \;\; 1 \,\} \qquad (3.43e)$$

$$\begin{Bmatrix} S_{33} \\ S_{36} \end{Bmatrix} = \frac{3}{4\pi}\left(4A_3\begin{Bmatrix} -1 \\ 1 \end{Bmatrix} f_{20} + \frac{x_3}{h}A_1\begin{Bmatrix} 1 \\ 1 \end{Bmatrix} f_{10}\right) \qquad (3.43f)$$

$$\begin{bmatrix} S_{53} & S_{56} \\ S_{63} & S_{66} \end{bmatrix} = \frac{1}{4\pi}\left(-\begin{bmatrix} f_{42} & f_{42} \\ f_{41} & f_{41} \end{bmatrix} + 3\frac{x_3}{h}\begin{bmatrix} f_{52} & -f_{52} \\ f_{51} & -f_{51} \end{bmatrix}\right) \qquad (3.43g)$$

where A_1, A_2 and A_3 is defined in (3.34), A_4 is defined in (3.37), and

$$A_5 = 3A_1 + 2A_2 = \frac{3\lambda + 2\mu}{\lambda + 2\mu} = \frac{1+\nu}{1-\nu}\,. \qquad (3.44)$$

The inverse Fourier transforms of the functions $f_{\alpha\beta}(x, y)$, which appear in equations (3.43) and are not listed in (3.38), are

$$\left.\begin{aligned}
&\left\{\begin{matrix}\bar{f}_{61}\\ \bar{f}_{62}\end{matrix}\right\} = \frac{i\,P}{(3+\bar{\rho}^2)}\left\{\begin{matrix}\bar{\alpha}_1\\ \bar{\alpha}_2\end{matrix}\right\}, \quad \left\{\begin{matrix}\bar{f}_{76}\\ \bar{f}_{77}\end{matrix}\right\} = \frac{i\,P}{\bar{\rho}^4}\left\{\begin{matrix}\bar{\alpha}_1^2\,\bar{\alpha}_2\\ \bar{\alpha}_1\,\bar{\alpha}_2^2\end{matrix}\right\}\\
&\left\{\begin{matrix}\bar{f}_{84}\\ \bar{f}_{85}\end{matrix}\right\} = \frac{P}{\bar{\rho}^2(c^2+\bar{\rho}^2)}\left\{\begin{matrix}i\,\bar{\alpha}_1^2\,\bar{\alpha}_2\\ i\,\bar{\alpha}_1\,\bar{\alpha}_2^2\end{matrix}\right\}\\
&\left\{\begin{matrix}\bar{f}_{94}\\ \bar{f}_{95}\end{matrix}\right\} = \frac{i\,P}{\bar{\rho}^2(3+\bar{\rho}^2)}\left\{\begin{matrix}\bar{\alpha}_1^2\,\bar{\alpha}_2\\ \bar{\alpha}_1\,\bar{\alpha}_2^2\end{matrix}\right\}
\end{aligned}\right\} \tag{3.45}$$

where $i = \sqrt{-1}$ and P is given in (3.39). Although, expressions (3.43) are written in the physical space, they are also valid in the Fourier space if S_{ij} and all functions $f_{\alpha\beta}$ are replaced by the corresponding transformed quantities.

3.4 INVERSE FOURIER TRANSFORM OF THE SINGLE LAYER FUNDAMENTAL SOLUTION

In order to derive the fundamental solution and corresponding stresses in the physical space we have to obtain the inverse Fourier transform of the functions $\bar{f}_{\alpha\beta}(\alpha_1, \alpha_2; \xi_1, \xi_2)$ using the definition (3.14),

$$f(x,y) = \frac{1}{2\pi}\int_{-\infty}^{+\infty}\int_{-\infty}^{+\infty} \bar{f}(\alpha_1, \alpha_2; \xi_1, \xi_2)\; e^{-i(\alpha_1 x_1 + \alpha_2 x_2)}\, d\alpha_1\, d\alpha_2 \tag{3.46}$$

where f in the above equation may represent any of the functions $f_{\alpha\beta}(x,y)$.

Depending on the structure of functions $\bar{f}_{\alpha\beta}$ in equations (3.38) and (3.45), their inverse transforms can be cast into the following four categories,

$$f(x,y) = \frac{1}{2\pi}\int_{-\infty}^{+\infty}\int_{-\infty}^{+\infty} F(\bar{\rho})\; P\; e^{-i(\alpha_1 x_1 + \alpha_2 x_2)}\, d\alpha_1\, d\alpha_2 \tag{3.47a}$$

$$f(x,y) = \frac{1}{2\pi}\int_{-\infty}^{+\infty}\int_{-\infty}^{+\infty} \bar{\alpha}_n\; F(\bar{\rho})\; P\, e^{-i(\alpha_1 x_1 + \alpha_2 x_2)}\, d\alpha_1\, d\alpha_2 \tag{3.47b}$$

$$(n = 1, 2)$$

$$f(x,y) = \frac{1}{2\pi}\int_{-\infty}^{+\infty}\int_{-\infty}^{+\infty} \bar{\alpha}_m\,\bar{\alpha}_n\,F(\bar{\rho})\,P\,e^{-i(\alpha_1 x_1+\alpha_2 x_2)}\,d\alpha_1\,d\alpha_2 \qquad (3.47c)$$

$$(m,n=1,2)$$

$$f(x,y) = \frac{1}{2\pi}\int_{-\infty}^{+\infty}\int_{-\infty}^{+\infty} \bar{\alpha}_m^2\,\bar{\alpha}_n\,F(\bar{\rho})\,P\,e^{-i(\alpha_1 x_1+\alpha_2 x_2)}\,d\alpha_1\,d\alpha_2 \qquad (3.47d)$$

$$(m,n=1,2;\, m\neq n)$$

in which

$$\bar{f} = \mathrm{P}\,F(\bar{\rho}),\quad \bar{f} = \mathrm{P}\,\bar{\alpha}_n\,F(\bar{\rho}),\quad \bar{f} = \mathrm{P}\,\bar{\alpha}_m\,\bar{\alpha}_n\,F(\bar{\rho}) \quad \text{and} \quad \bar{f} = \mathrm{P}\,\bar{\alpha}_m^2\,\bar{\alpha}_n\,F(\bar{\rho}),$$

respectively, and P is given in (3.39). The integrals of equations (3.47) are written in cylindrical coordinates and the exponential terms are expressed in terms of the modified Bessel functions of the first kind (Watson, 1945), as

$$\mathrm{P}\,e^{-i(\alpha_1 x_1+\alpha_2 x_2)} = e^{-i(\alpha_1 x+\alpha_2 y)} = e^{-i\rho R\cos(\phi-\theta)}$$

$$= I_0(-i\rho R) + 2\sum_{k=1}^{\infty} I_k(-i\rho R)\cos[k(\phi-\theta)] \qquad (3.48)$$

where $\alpha_1 = \rho\cos\phi$, $\alpha_2 = \rho\sin\phi$, $x = R\cos\theta$, $y = R\sin\theta$, and R is the distance between points (x_1, x_2) and (ξ_1, ξ_2),

$$R = \sqrt{(x_1-\xi_1)^2+(x_2-\xi_2)^2} = \sqrt{x^2+y^2}\,. \qquad (3.49)$$

Substituting equation (3.48) into the integrals of (3.47) and using the relation between the modified Bessel functions of the first kind I_k and the Bessel functions of the first kind J_k, $I_k(-i\rho R) = e^{-k\frac{\pi}{2}i}J_k(\rho R)$, the inverse transforms of (3.47) become

$$\bar{f} = \mathrm{P}\,F(\bar{\rho}) \qquad \rightarrow\ f(x,y) = \frac{1}{h^2}\int_0^{\infty}\bar{\rho}\,F(\bar{\rho})\,J_0\!\left(\bar{\rho}\,\frac{R}{h}\right)d\bar{\rho} \qquad (3.50a)$$

$$\bar{f} = \mathrm{P}\left\{\begin{matrix}\bar{\alpha}_1\\ \bar{\alpha}_2\end{matrix}\right\}F(\bar{\rho}) \quad \rightarrow\ f(x,y) = \frac{-i}{h^2 R}\left\{\begin{matrix}x\\ y\end{matrix}\right\}\int_0^{\infty}\bar{\rho}^2\,F(\bar{\rho})\,J_1\!\left(\bar{\rho}\,\frac{R}{h}\right)d\bar{\rho} \qquad (3.50b)$$

$$\bar{f} = \mathrm{P}\left\{\begin{array}{c}\bar{\alpha}_1^2\\ \bar{\alpha}_1\bar{\alpha}_2\\ \bar{\alpha}_2^2\end{array}\right\} F(\bar{\rho}) \;\rightarrow$$

$$f(x,y) = \frac{1}{2h^2}\left\{\begin{array}{c}1\\0\\1\end{array}\right\} \int_0^\infty \bar{\rho}^3 F(\bar{\rho})\, J_0\left(\bar{\rho}\,\frac{R}{h}\right) d\bar{\rho}$$

$$+\frac{1}{2h^2R^2}\left\{\begin{array}{c}y^2-x^2\\-2xy\\x^2-y^2\end{array}\right\} \int_0^\infty \bar{\rho}^3 F(\bar{\rho})\, J_2\left(\bar{\rho}\,\frac{R}{h}\right) d\bar{\rho} \qquad (3.50c)$$

$$\bar{f} = \mathrm{P}\left\{\begin{array}{c}\bar{\alpha}_1^2\bar{\alpha}_2\\ \bar{\alpha}_1\bar{\alpha}_2^2\end{array}\right\} F(\bar{\rho}) \;\rightarrow$$

$$f(x,y) = \frac{-i}{4h^2R}\left\{\begin{array}{c}y\\x\end{array}\right\} \int_0^\infty \bar{\rho}^4 F(\bar{\rho})\, J_1\left(\bar{\rho}\,\frac{R}{h}\right) d\bar{\rho}$$

$$+\frac{i}{4h^2R^3}\left\{\begin{array}{c}y\,(3x^2-y^2)\\x\,(3y^2-x^2)\end{array}\right\} \int_0^\infty \bar{\rho}^4 F(\bar{\rho})\, J_3\left(\bar{\rho}\,\frac{R}{h}\right) d\bar{\rho}\ , \qquad (3.50d)$$

respectively, which involve Hankel transforms of zero up to the third order (Sneddon, 1951).

The inverse Fourier transforms of the functions $\bar{f}_{\alpha\beta}$ are obtained using expressions (3.50) and the properties of Bessel functions which are listed in Appendix A. The resulting expressions are

$$f_{10} = \frac{1}{h^2}\int_0^\infty \frac{1}{\bar{\rho}} J_0\left(\bar{\rho}\,\frac{R}{h}\right) d\bar{\rho}\ , \quad f_{20} = \frac{1}{h^2} K_0\left(\frac{cR}{h}\right) \qquad (3.51a,b)$$

$$f_{30} = \frac{1}{h^2}\int_0^\infty \frac{1}{\bar{\rho}^3} J_0\left(\bar{\rho}\,\frac{R}{h}\right) d\bar{\rho}\ , \quad \left\{\begin{array}{c}f_{41}\\f_{42}\end{array}\right\} = \frac{1}{hR^2}\left\{\begin{array}{c}x\\y\end{array}\right\} \qquad (3.51c,d)$$

$$\left\{\begin{array}{c}f_{51}\\f_{52}\end{array}\right\} = \frac{c}{h^2R} K_1\left(c\frac{R}{h}\right)\left\{\begin{array}{c}x\\y\end{array}\right\} \qquad (3.51e)$$

$$\begin{Bmatrix} f_{61} \\ f_{62} \end{Bmatrix} = \frac{\sqrt{3}}{h^2 R} K_1\left(\sqrt{3}\,\frac{R}{h}\right) \begin{Bmatrix} x \\ y \end{Bmatrix} \tag{3.51f}$$

$$\begin{Bmatrix} f_{71} \\ f_{72} \end{Bmatrix} = \frac{1}{2h^3} \begin{Bmatrix} x \\ y \end{Bmatrix} \int_0^\infty \frac{1}{\bar{\rho}} J_0\left(\bar{\rho}\,\frac{R}{h}\right) d\bar{\rho} + \frac{1}{4h^3} \begin{Bmatrix} x \\ y \end{Bmatrix} \tag{3.51g}$$

$$\begin{Bmatrix} f_{73} \\ f_{74} \\ f_{75} \end{Bmatrix} = \frac{1}{2h^2} \begin{Bmatrix} 1 \\ 0 \\ 1 \end{Bmatrix} \int_0^\infty \frac{1}{\bar{\rho}} J_0\left(\bar{\rho}\,\frac{R}{h}\right) d\bar{\rho} + \frac{1}{4h^2 R^2} \begin{Bmatrix} y^2 - x^2 \\ -2x\,y \\ x^2 - y^2 \end{Bmatrix} \tag{3.51h}$$

$$\begin{Bmatrix} f_{76} \\ f_{77} \end{Bmatrix} = \frac{(x^2 - y^2)}{2h\,R^4} \begin{Bmatrix} -y \\ x \end{Bmatrix} \tag{3.51i}$$

$$\begin{Bmatrix} f_{81} \\ f_{82} \\ f_{83} \end{Bmatrix} = \frac{1}{c^2 R^4} \left[1 - c\frac{R}{h} K_1\left(c\frac{R}{h}\right)\right] \begin{Bmatrix} -x^2 + y^2 \\ -2xy \\ x^2 - y^2 \end{Bmatrix} + \frac{1}{h^2 R^2} K_0\left(c\frac{R}{h}\right) \begin{Bmatrix} x^2 \\ xy \\ y^2 \end{Bmatrix} \tag{3.51j}$$

$$\begin{Bmatrix} f_{84} \\ f_{85} \end{Bmatrix} = \frac{2}{cR^5} \left[\frac{h}{cR} - \frac{cR}{2h} K_0\left(c\frac{R}{h}\right) - K_1\left(c\frac{R}{h}\right)\right] \begin{Bmatrix} y\,(y^2 - 3x^2) \\ x\,(x^2 - 3y^2) \end{Bmatrix} + \frac{c\,x\,y}{h^2 R^3} K_1\left(c\frac{R}{h}\right) \begin{Bmatrix} x \\ y \end{Bmatrix} \tag{3.51k}$$

$$\begin{Bmatrix} f_{91} \\ f_{92} \\ f_{93} \end{Bmatrix} = \frac{1}{3R^4} \left[1 - \sqrt{3}\frac{R}{h} K_1\left(\sqrt{3}\frac{R}{h}\right)\right] \begin{Bmatrix} -x^2 + y^2 \\ -2xy \\ x^2 - y^2 \end{Bmatrix} + \frac{1}{h^2 R^2} K_0\left(\sqrt{3}\frac{R}{h}\right) \begin{Bmatrix} x^2 \\ xy \\ y^2 \end{Bmatrix} \tag{3.51l}$$

$$\begin{Bmatrix} f_{94} \\ f_{95} \end{Bmatrix} = \frac{2}{\sqrt{3}\,R^5}\left[\frac{h}{\sqrt{3}\,R} - \frac{\sqrt{3}\,R}{2h}K_0\left(\sqrt{3}\,\frac{R}{h}\right) - K_1\left(\sqrt{3}\,\frac{R}{h}\right)\right]$$
$$\times\begin{Bmatrix} y\,(y^2-3x^2) \\ x\,(x^2-3y^2) \end{Bmatrix} + \frac{\sqrt{3}\,xy}{h^2R^3}K_1\left(\sqrt{3}\,\frac{R}{h}\right)\begin{Bmatrix} x \\ y \end{Bmatrix} \qquad (3.51m)$$

In the analytical expressions obtained above there are some functions which involve the following two integrals,

$$G_1 = \int_0^\infty \frac{1}{\bar{\rho}}\,J_0\left(\bar{\rho}\,\frac{R}{h}\right)d\bar{\rho} \qquad (3.52)$$

and

$$G_2 = \int_0^\infty \frac{1}{\bar{\rho}^3}\,J_0\left(\bar{\rho}\,\frac{R}{h}\right)d\bar{\rho}\,. \qquad (3.53)$$

These integrals are special because their integrands exhibit a singular behavior for $\bar{\rho} \to 0$, although they are well behaved for $\bar{\rho} \to \infty$. Expansion of their integrands in ascending power series of $\bar{\rho}$ reveals terms of the form

$$\frac{1}{\bar{\rho}}\,J_0\left(\bar{\rho}\,\frac{R}{h}\right) = \frac{1}{\bar{\rho}} + \sum_{k=1}^{\infty}\frac{(-1)^k}{(k!)^2}\left(\frac{R^2}{4h^2}\right)^k\bar{\rho}^{2k-1} \qquad (3.54)$$

$$\frac{1}{\bar{\rho}^3}\,J_0\left(\bar{\rho}\,\frac{R}{h}\right) = \frac{1}{\bar{\rho}^3} - \frac{R^2}{4h^2}\frac{1}{\bar{\rho}} + \sum_{k=2}^{\infty}\frac{(-1)^k}{(k!)^2}\left(\frac{R^2}{4h^2}\right)^k\bar{\rho}^{2k-3} \qquad (3.55)$$

and it is apparent that both expressions tend to infinity as $\bar{\rho} \to 0$ because of the terms $\bar{\rho}^{-1}$ and $\bar{\rho}^{-3}$.

The singular behavior of the integrands in equations (3.52) and (3.53) indicates that the expressions for some of the components of the fundamental solution U_{ij} and the corresponding stresses S_{ij}, in their present form, are non-convergent and that the solution should be reexamined. A thorough study of these components and the construction of the revised solution are going to be the topic of the next section.

3.5 SINGLE LAYER FUNDAMENTAL SOLUTION IN THE PHYSICAL SPACE

The construction of the final solution to our problem is suggested by inspecting the structure of expressions obtained by Dougall (1904) and by the observation of Benitez and Rosakis (1987), that simple subtraction of the singular terms that appear in the expansions (3.54) and (3.55) from the original integrands in (3.52) and (3.53) yields integrands which are convergent. More specifically, subtraction of

$$G_1^*(\bar{\rho}) = \int_0^\infty \frac{e^{-\bar{\rho}}}{\bar{\rho}}\, d\bar{\rho} \tag{3.56}$$

from the integral G_1 of equation (3.52) and

$$G_2^*(\bar{\rho}, R) = \int_0^\infty \left(\frac{1}{\bar{\rho}^3} - \frac{R^2}{4h^2} \frac{e^{-\bar{\rho}}}{\bar{\rho}} \right) d\bar{\rho} \tag{3.57}$$

from the integral G_2 of (3.53), results in new integrals which are convergent since their integrands are well behaved for every $\bar{\rho} \in [0, \infty)$. The inclusion of the multiplying factor $e^{-\bar{\rho}}$ in the $\bar{\rho}^{-1}$ terms of (3.54) and (3.55) ensures the integrability of the final expressions for $G_1 - G_1^*$ and $G_2 - G_2^*$, as it is shown in Appendix B.

The integrals introduced in equations (3.56) and (3.57) give rise to a new set of functions $\mathrm{f}^*_{\alpha\beta}(x, y)$ which are constructed by eliminating in the expressions (3.51) of the functions $\mathrm{f}_{\alpha\beta}(x, y)$ all the terms that do not involve the singular integrals G_1 and G_2, and by replacing in the retained terms the two singular integrals with G_1^* and G_2^*, respectively. These operations give

$$\mathrm{f}^*_{10} = \frac{1}{h^2} G_1^*, \tag{3.58a}$$

$$\mathrm{f}^*_{30} = \frac{1}{h^2} G_2^*, \tag{3.58b}$$

$$\begin{Bmatrix} f^*_{71} \\ f^*_{72} \end{Bmatrix} = \frac{1}{2h^3} \begin{Bmatrix} x \\ y \end{Bmatrix} G_1^*, \tag{3.58c}$$

and

$$\begin{Bmatrix} f^*_{73} \\ f^*_{75} \end{Bmatrix} = \frac{1}{2h^2} \begin{Bmatrix} 1 \\ 1 \end{Bmatrix} G_1^*, \tag{3.58d}$$

while all the other functions $f^*_{\alpha\beta}$ vanish. Consequently, substitution of these functions into equations (3.36) produces a displacement matrix $U^*_{ij}(x,y)$, which is

$$[\mathbf{U}^*] = \begin{bmatrix} U^*_{11} & 0 & -U^*_{31} & U^*_{41} & 0 & -U^*_{31} \\ 0 & U^*_{11} & -U^*_{32} & 0 & U^*_{41} & -U^*_{32} \\ U^*_{31} & U^*_{32} & U^*_{33} & -U^*_{31} & -U^*_{32} & U^*_{33} \\ U^*_{41} & 0 & U^*_{31} & U^*_{11} & 0 & U^*_{31} \\ 0 & U^*_{41} & U^*_{32} & 0 & U^*_{11} & U^*_{32} \\ U^*_{31} & U^*_{32} & U^*_{33} & -U^*_{31} & -U^*_{32} & U^*_{33} \end{bmatrix} \tag{3.59}$$

with

$$U^*_{11} = \frac{1}{8\pi\mu h}\left(5 - 4A_3 + \frac{A_4}{4}\right) G_1^* , \tag{3.60a}$$

$$U^*_{41} = \frac{1}{8\pi\mu h}\left(-1 + 2A_3 + \frac{A_4}{4}\right) G_1^* , \tag{3.60b}$$

$$U^*_{31} = \frac{3A_2}{8\pi\mu h}\frac{x}{h} G_1^* , \quad U^*_{32} = \frac{3A_2}{8\pi\mu h}\frac{y}{h} G_1^* , \tag{3.60c,d}$$

and

$$U^*_{33} = \frac{1}{4\pi\mu h}(G_1^* + 3A_2\, G_2^*) , \tag{3.60e}$$

where A_2, A_3 and A_4 are given in equations (3.34) and (3.37). Substitution of the functions (3.58) into the stress expressions (3.43), produces a stress matrix whose non-zero components are the following,

$$S^*_{13} = S^*_{16} = S^*_{23} = S^*_{26} = \frac{3A_3\, x_3}{4\pi h^3}\, G_1^* , \quad S^*_{33} = S^*_{36} = \frac{3A_1\, x_3}{4\pi h^3}\, G_1^* . \tag{3.61}$$

The displacement and stress matrices are constructed independently of each other, on the basis of the observation that subtraction of these matrices from the fundamental solution (3.36) and stress components (3.43) yields new matrices, which are both relieved from the non-convergent integrals. However, it can be shown that the displacement fields U_{ij}^{*} of equations (3.59) and (3.60) give rise to stresses which are identical to those of (3.61), and therefore it is

$$[\mathbf{S}^{*}(x,y,x_3)] = \left[\left[\mathbf{B}^{1}(x_3)\right] \left[\mathbf{B}^{2}(x_3)\right] \right] \ [\mathbf{U}^{*}(x,y)]. \tag{3.62}$$

Equation (3.62) demonstrates that the displacement components U_{ij}^{*} of each column of the fundamental matrix are compatible with the stress field described by the corresponding column of S_{ij}^{*}.

It is also observed that direct substitutions of the six displacement fields described by matrix U_{ij}^{*} into the governing equations (3.1) and (3.2) yield zero nodal forces for every point $(x_1, x_2) \in \Omega$. The physical interpretation of this is that all displacement fields correspond to zero body forces and to zero traction boundary conditions at $x_3 = -h$ and $x_3 = h$. Hence, the displacements U_{ij}^{*} and stresses S_{ij}^{*} form a self-equilibrating system and they can be subtracted from U_{ij} and S_{ij}, respectively, to give the final solution, which is convergent and satisfies the same field equations as the original solution. The proposed solution can still be expressed by equations (3.36) and (3.43), and the non-singular functions $f_{\alpha\beta}$ by equations (3.51), but the functions f_{10}, f_{30}, f_{71}, f_{72}, f_{73} and f_{75}, which initially involved the singular integrals, are now given by the following expressions,

$$f_{10} = \frac{1}{h^2} \ln\left(\frac{2h}{R}\right), \tag{3.63a}$$

$$f_{30} = -\frac{R^2}{4h^4}\left[1+\ln\left(\frac{2h}{R}\right)\right], \tag{3.63b}$$

$$\begin{Bmatrix} f_{71} \\ f_{72} \end{Bmatrix} = \frac{1}{2h^3}\left[\frac{1}{2}+\ln\left(\frac{2h}{R}\right)\right]\begin{Bmatrix} x \\ y \end{Bmatrix}, \tag{3.63c}$$

and

$$\begin{Bmatrix} f_{73} \\ f_{75} \end{Bmatrix} = \frac{1}{2h^2}\ln\left(\frac{2h}{R}\right)\begin{Bmatrix} 1 \\ 1 \end{Bmatrix} + \frac{y^2-x^2}{4h^2R^2}\begin{Bmatrix} 1 \\ -1 \end{Bmatrix}. \tag{3.63d}$$

The above functions are obtained by replacing the singular integrals G_1^* and G_2^* in expressions (3.51a,c,g,h) with $G_1 - G_1^*$ and $G_2 - G_2^*$, respectively, and making use of equations (B.6) and (B.13) from Appendix B.

3.6 BASIC FEATURES AND PROPERTIES OF THE FUNDAMENTAL SOLUTION

In the sequel, we present the basic features of the modified solution. Properties regarding symmetry of the fundamental solution and the effect of the relative position of points (x_1, x_2) and (ξ_1, ξ_2) on the solution can be found in Appendix C.

According to the presented formulation the stress matrix S_{ij} was obtained by transforming the constitutive relations into the Fourier space, substituting into the transformed expressions the displacements $\bar{U}_{ij}$, and finally inverting the transformed stresses $\bar{S}_{ij}$ back into the physical space and making the appropriate modifications to treat the singular integrals. The stresses S_{ij} and the displacements U_{ij}, both being expressed in terms of the modified functions $f_{\alpha\beta}$, are still related through the constitutive relations, and it is

$$[\mathbf{S}] = \left[\left[\mathbf{B}^1\right]\left[\mathbf{B}^2\right]\right][\mathbf{U}] \tag{3.64}$$

where the stresses are given in (3.43), the displacements in (3.36) and the operators $[\mathbf{B}^p]$ (p=1,2) are given in equations (3.6) and (3.7). This can be

verified by substituting the displacements into the right-hand side of the above equation and using the recurrence formulae for the modified Bessel functions of the second kind from Appendix A.

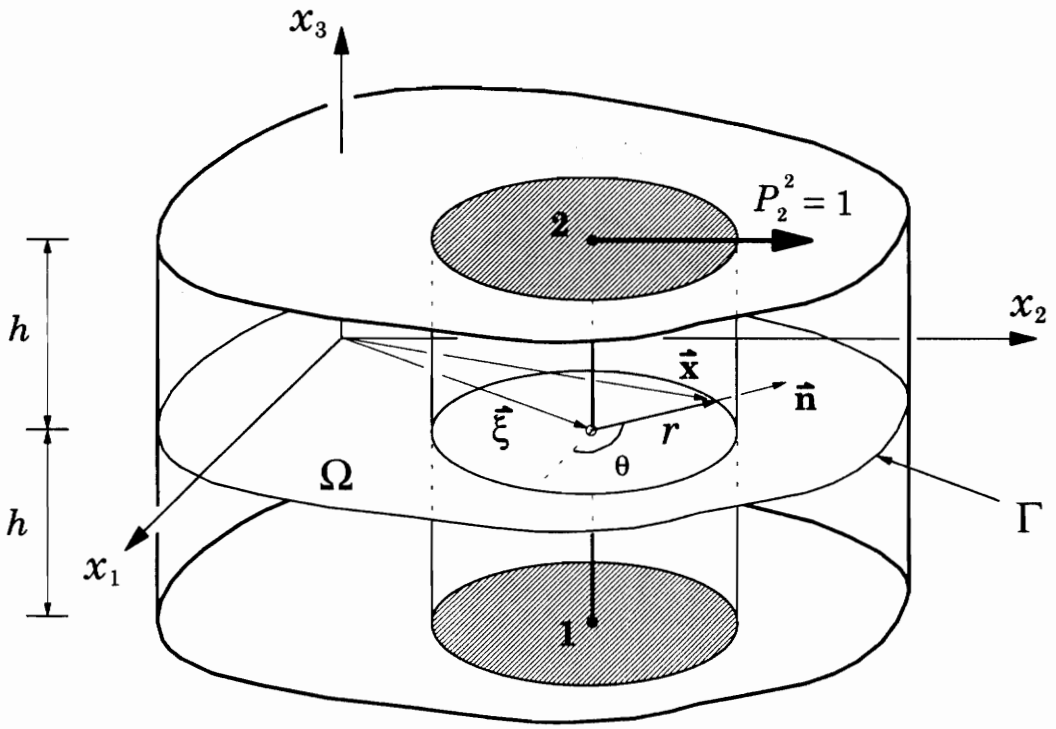

Figure 3.2 Cylindrical surface of arbitrary radius r with unit concentrated load applied at node 2 in the x_2 direction.

The fundamental solution $U_{ij}(x_1, x_2; \xi_1, \xi_2)$ satisfies the field equations (3.1) and (3.2) of the discrete problem at any point $(x_1, x_2) \in \Omega$, except at $(x_1, x_2) = (\xi_1, \xi_2)$ where the concentrated load is applied. This can be proved by replacing the nodal displacements V_k^p in (3.1) and (3.2) with the components of the fundamental solution, according to the relations

$$V_k^1 = U_{kj} \quad \text{and} \quad V_k^2 = U_{mj} \tag{3.65}$$

in which m=3+k and k=1,2,3. The components U_{ij} are given in (3.36) and the functions $f_{\alpha\beta}(x_1, x_2; \xi_1, \xi_2)$ are given in (3.51) and (3.63). The left-hand side of the equilibrium equations (3.1) and (3.2) becomes zero at every point in Ω, except at point (ξ_1, ξ_2), for all values of j=1,2,...,6 in equation (3.65), *i.e.*, for all six displacement fields of U_{ij}. When the field point (x_1, x_2) approaches point (ξ_1, ξ_2), where the unit loads are applied, the distance $R \to 0$, and thus the expressions for the fundamental solution become singular due to the logarithmic terms and the modified Bessel functions of the second kind in the expressions (3.51) and (3.63) for the functions $f_{\alpha\beta}$. In this case we prove that the integral of the tractions over the side surface of a cylinder having arbitrary radius r=R, height $2h$ and center axis perpendicular to the plane Ω at point (ξ_1, ξ_2), is equal to minus the unit point load that is applied at one of the nodes of (ξ_1, ξ_2). This condition ensures the equilibrium for the limiting case $\vec{\mathbf{x}}(x_1, x_2) \to \vec{\xi}(\xi_1, \xi_2)$. Denoting the side surface of the cylinder by S_c, the force resultants on its side surface are found to be:

in the x_1 direction,

$$\int_{S_c} n_i \, \sigma_{i1} \, dS = \int_{-h}^{h} \int_{-\pi}^{\pi} (n_1 \, S_{1j} + n_2 \, S_{4j}) \, r \, d\theta \, dx_3 = \begin{cases} -1\,, & \text{for } j=1,4 \\ 0\,, & \text{for } j=2,3,5,6 \end{cases} \tag{3.66}$$

in the x_2 direction,

$$\int_{S_c} n_i \, \sigma_{i2} \, dS = \int_{-h}^{h} \int_{-\pi}^{\pi} (n_1 \, S_{4j} + n_2 \, S_{2j}) \, r \, d\theta \, dx_3 = \begin{cases} -1\,, & \text{for } j=2,5 \\ 0\,, & \text{for } j=1,3,4,6 \end{cases} \tag{3.67}$$

in the x_3 direction,

$$\int_{S_c} n_i \, \sigma_{i3} \, dS = \int_{-h}^{h} \int_{-\pi}^{\pi} (n_1 \, S_{6j} + n_2 \, S_{5j}) \, r \, d\theta \, dx_3 = \begin{cases} -1\,, & \text{for } j=3,6 \\ 0\,, & \text{for } j=1,2,4,5 \end{cases} \tag{3.68}$$

where $n_1 = \cos\theta$, $n_2 = \sin\theta$, $n_3 = 0$ are the components of the unit outward normal vector on the surface S_c, $S_{kj}(x_1, x_2, x_3; \xi_1, \xi_2)$ are the stress components at $\vec{\mathbf{x}}$ due to a unit load at point (ξ_1, ξ_2). Note that the force resultants in equations (3.66), (3.67) and (3.68) are independent of r, and thus the results hold also for the case $R = r \to 0$. Figure 3.2 shows the fictitious cylinder at point $\vec{\xi}$ and a unit load applied in the x_2 direction at node 2. In this case it is j=5 and the integrals (3.66), (3.67) and (3.68) yield: 0, −1 and 0, respectively.

This completes the derivation and evaluation of the fundamental solution $U_{ij}(x_1, x_2; \xi_1, \xi_2)$ for a single layer whose displacement field varies linearly through the thickness. This solution will be used in the sequel to construct the Boundary Integral Equation Model (BIEM) for the typical numerical layer (element).

3.7 DERIVATIVES OF THE FUNDAMENTAL SOLUTION

The components $U_{ij}(x_1, x_2; \xi_1, \xi_2)$ (i, j=1,2,...,6) of the fundamental solution are expressed in equations (3.36) in terms of the functions $f_{\alpha\beta}(x_1, x_2; \xi_1, \xi_2)$, where the values of the subscripts α and β are those in the definitions (3.51) and (3.63). The $f_{\alpha\beta}$ and, consequently, the fundamental solution U_{ij} depend on the relative position of the field point $\vec{\mathbf{x}}(x_1, x_2)$, and the point $\vec{\xi}(\xi_1, \xi_2)$ where the unit loads are applied. The distance between the two points has been introduced as

$$x = x_1 - \xi_1 \quad \text{and} \quad y = x_2 - \xi_2, \tag{3.69}$$

along the x_1 and x_2 directions, respectively.

The integral statements developed in Chapter 2 involve integrands which contain either the components of the fundamental solution (equation 2.33), or their derivatives with respect to the independent parameters x_1 and x_2 (equation 2.31). In order to use these statements in the development of the boundary integral model, it is necessary to obtain first the expressions for the derivatives of U_{ij} with respect to the coordinates of points (x_1, x_2) and (ξ_1, ξ_2). Derivatives with respect to $\vec{\xi}$ will be required in order to evaluate the strains and stresses, after the displacement field (solution) has been expressed in an integral form. Since, the dependence of the fundamental solution on the coordinates of the two points, or their relative position, is introduced through the functions $f_{\alpha\beta}$, we only have to obtain expressions for the derivatives of these functions. The expressions for the derivatives of the fundamental solution will then be given from the same equations (3.36) as the components of the fundamental solution, if the functions are replaced by their derivatives.

The derivatives with respect to x_1 and x_2, or ξ_1 and ξ_2 are related to the derivatives with respect to x and y through the following expressions

$$\frac{\partial f_{\alpha\beta}(x_1, x_2; \xi_1, \xi_2)}{\partial x} = \frac{\partial f_{\alpha\beta}}{\partial x_1} = -\frac{\partial f_{\alpha\beta}}{\partial \xi_1} \tag{3.70a}$$

and

$$\frac{\partial f_{\alpha\beta}(x_1, x_2; \xi_1, \xi_2)}{\partial y} = \frac{\partial f_{\alpha\beta}}{\partial x_2} = -\frac{\partial f_{\alpha\beta}}{\partial \xi_2}, \tag{3.70b}$$

which arise from equation (3.69). The derivatives of the functions $f_{\alpha\beta}$ with respect to x and y, can be easily obtained from equations (3.51) and (3.63), and most of the derivatives can be expressed in terms of the same functions $f_{\alpha\beta}$:

$$\frac{\partial f_{10}}{\partial x} = -\frac{1}{h} f_{41}, \quad \frac{\partial f_{10}}{\partial y} = -\frac{1}{h} f_{42} \tag{3.71}$$

$$\frac{\partial f_{20}}{\partial x} = -\frac{1}{h} f_{51}, \quad \frac{\partial f_{20}}{\partial y} = -\frac{1}{h} f_{52} \tag{3.72}$$

$$\frac{\partial f_{30}}{\partial x} = -\frac{1}{h} f_{71}, \quad \frac{\partial f_{30}}{\partial y} = -\frac{1}{h} f_{72} \tag{3.73}$$

$$\frac{\partial f_{41}}{\partial x} = -\frac{\partial f_{42}}{\partial y} = \frac{y^2 - x^2}{h R^4}, \quad \frac{\partial f_{41}}{\partial y} = \frac{\partial f_{42}}{\partial x} = -\frac{2xy}{h R^4} \tag{3.74}$$

$$\frac{\partial f_{51}}{\partial x} = \frac{\partial f_{41}}{\partial x} - \frac{c^2}{h} f_{81}, \quad \frac{\partial f_{51}}{\partial y} = \frac{\partial f_{52}}{\partial x} = \frac{\partial f_{41}}{\partial y} - \frac{c^2}{h} f_{82}, \quad \frac{\partial f_{52}}{\partial y} = \frac{\partial f_{42}}{\partial y} - \frac{c^2}{h} f_{83} \tag{3.75}$$

$$\frac{\partial f_{61}}{\partial x} = \frac{\partial f_{41}}{\partial x} - \frac{3}{h} f_{91}, \quad \frac{\partial f_{61}}{\partial y} = \frac{\partial f_{62}}{\partial x} = \frac{\partial f_{41}}{\partial y} - \frac{3}{h} f_{92}, \quad \frac{\partial f_{62}}{\partial y} = \frac{\partial f_{42}}{\partial y} - \frac{3}{h} f_{93} \tag{3.76}$$

$$\left.\begin{aligned}
&\frac{\partial f_{71}}{\partial x} = \frac{1}{h} f_{73}, \quad \frac{\partial f_{71}}{\partial y} = \frac{\partial f_{72}}{\partial x} = \frac{1}{h} f_{74}, \quad \frac{\partial f_{72}}{\partial y} = \frac{1}{h} f_{75} \\
&\frac{\partial f_{73}}{\partial x} = \frac{1}{h}\left(f_{77} - f_{41}\right), \quad \frac{\partial f_{73}}{\partial y} = \frac{\partial f_{74}}{\partial x} = -\frac{1}{h} f_{76} \\
&\frac{\partial f_{74}}{\partial y} = \frac{\partial f_{75}}{\partial x} = -\frac{1}{h} f_{77}, \quad \frac{\partial f_{75}}{\partial y} = \frac{1}{h}\left(f_{76} - f_{42}\right) \\
&\frac{\partial f_{76}}{\partial x} = \frac{xy\,(x^2 - 3y^2)}{h R^6}, \quad \frac{\partial f_{76}}{\partial y} = \frac{\partial f_{77}}{\partial x} = \frac{8x^2y^2 - R^4}{2h R^6} \\
&\frac{\partial f_{77}}{\partial y} = \frac{xy\,(y^2 - 3x^2)}{h R^6}
\end{aligned}\right\} \tag{3.77}$$

$$\left.\begin{aligned}
&\frac{\partial f_{81}}{\partial x} = \frac{1}{h}\left(f_{85} - f_{51}\right), \quad \frac{\partial f_{81}}{\partial y} = \frac{\partial f_{82}}{\partial x} = -\frac{1}{h} f_{84}, \\
&\frac{\partial f_{82}}{\partial y} = \frac{\partial f_{83}}{\partial x} = -\frac{1}{h} f_{85}, \quad \frac{\partial f_{83}}{\partial y} = \frac{1}{h}\left(f_{84} - f_{52}\right)
\end{aligned}\right\} \tag{3.78}$$

$$\left.\begin{aligned} &\frac{\partial f_{91}}{\partial x} = \frac{1}{h}\left(f_{95} - f_{61}\right), \quad \frac{\partial f_{91}}{\partial y} = \frac{\partial f_{92}}{\partial x} = -\frac{1}{h} f_{94} \\ &\frac{\partial f_{92}}{\partial y} = \frac{\partial f_{93}}{\partial x} = -\frac{1}{h} f_{95}, \quad \frac{\partial f_{93}}{\partial y} = \frac{1}{h}\left(f_{94} - f_{62}\right) \end{aligned}\right\} \tag{3.79}$$

It should be pointed out that, in the expressions (3.36) for the fundamental solution, the functions f_{41}, f_{42} and f_{51}, f_{52} appear always as differences of the form $(f_{41}-f_{51})$ and $(f_{42}-f_{52})$, and thus, although the derivatives of each function with respect to x or y are not defined for $\vec{\mathbf{x}}(x_1, x_2) \to \vec{\xi}(\xi_1, \xi_2)$, the derivatives of their differences are defined and their limit goes to zero (see equations 3.75). In the above expressions we have also used the following useful properties

$$f_{73} + f_{75} = f_{10}, \quad f_{73} - f_{75} = \frac{y^2 - x^2}{2h^2 R^2},$$

$$f_{81} + f_{83} = f_{20} = \frac{1}{h^2} K_0\left(\frac{cR}{h}\right) \quad \text{and} \quad f_{91} + f_{93} = \frac{1}{h^2} K_0\left(\frac{\sqrt{3}\, R}{h}\right).$$

The derivatives of the functions f_{84} and f_{85} cannot be expressed in terms of other functions $f_{\alpha\beta}$, and they are given by the following equations :

$$\frac{\partial f_{84}}{\partial x} = \frac{xy}{h R^6}\left[\left(\frac{cR}{h}\right)^2\left((3y^2 - 5x^2)\frac{h}{cR} K_1\left(\frac{cR}{h}\right) - x^2 K_0\left(\frac{cR}{h}\right)\right)\right.$$
$$\left. -24(x^2 - y^2)\left(\frac{1}{2} K_0\left(\frac{cR}{h}\right) + \frac{h}{cR} K_1\left(\frac{cR}{h}\right) - \left(\frac{h}{cR}\right)^2\right)\right], \tag{3.80a}$$

$$\frac{\partial f_{85}}{\partial x} = \frac{\partial f_{84}}{\partial y} = \frac{1}{h R^6}\left[(R^4 - 8x^2 y^2)\left(-6\left(\frac{h}{cR}\right)^2 + 6\frac{h}{cR} K_1\left(\frac{cR}{h}\right)\right.\right.$$
$$\left. +3 K_0\left(\frac{cR}{h}\right) + \frac{cR}{h} K1\left(\frac{cR}{h}\right)\right)$$
$$\left. -x^2 y^2\left(\frac{cR}{h}\right)^2 K_0\left(\frac{cR}{h}\right)\right], \tag{3.80b}$$

$$\frac{\partial f_{85}}{\partial y} = \frac{x\,y}{h\,R^6}\left[\left(\frac{c\,R}{h}\right)^2\left((3x^2-5y^2)\,\frac{h}{c\,R}\,K_1\left(\frac{c\,R}{h}\right)-y^2\,K_0\left(\frac{c\,R}{h}\right)\right)\right.$$

$$\left.+24\,(x^2-y^2)\left(\frac{1}{2}K_0\left(\frac{c\,R}{h}\right)+\frac{h}{c\,R}\,K_1\left(\frac{c\,R}{h}\right)-\left(\frac{h}{c\,R}\right)^2\right)\right]\ . \quad (3.80c)$$

The derivatives of the functions f_{94} and f_{95} can be obtained from equations (3.80), if the parameter c, which is given in (3.40), is replaced by $\sqrt{3}$.

Chapter 4

BOUNDARY INTEGRAL EQUATION MODEL

4.1 LAYERWISE BOUNDARY INTEGRAL EQUATIONS FOR THE TYPICAL NUMERICAL LAYER

The variational statement for the typical numerical layer has been derived in Chapter 2 and is given in equation (2.33). For the case of a linear numerical layer (N=2), each point $\vec{x}(x_1, x_2)$ on the mid-plane Ω_e of the e-th layer is associated with two nodes which are placed at the bottom and top surface of the element (Figure 3.1 and Figure 3.2). Therefore, node 1 is located on the plane $x_3 = -h_e$, while node 2 is located on the plane $x_3 = h_e$. The variational statement (2.33) may be written for the two-node model as

$$\int_{\Omega_e} \left(\delta p_i^1 \, v_i^1 + \delta p_i^2 \, v_i^2 \right) d\Omega = \int_{\Omega_e} \left[\left(\hat{t}_i^1 + F_i^1 \right) \delta v_i^1 + \left(\hat{t}_i^2 + F_i^2 \right) \delta v_i^2 \right] d\Omega +$$

$$+ \oint_{\Gamma_e} \left(\hat{Q}_i^1 \, \delta v_i^1 + \hat{Q}_i^2 \, \delta v_i^2 \right) d\Gamma - \oint_{\Gamma_e} \left(\delta t_i^1 \, v_i^1 + \delta t_i^2 \, v_i^2 \right) d\Gamma. \tag{4.1}$$

As it was also discussed in Chapter 2, the virtual quantities in the above statement can be replaced by the solution of the problem of a linear numerical layer (element) which extends to infinity in its plane and is subjected to a concentrated unit load along one of the three directions. This solution is the fundamental solution that was developed in the previous chapter, and more specifically, for the choice of a single unit load $\delta p_i^n(\vec{x}) = \delta(x_I - \xi_I)$ (I=1,2), the components of the corresponding virtual displacements δv_j^p are given in the matrix $U_{\alpha\beta}^e(x_I - \xi_I)$ in column $\beta = 3(n-1)+i$, where i=1,2,3 denotes the three directions for the load, n,p=1,2 denote the two nodes, and $\alpha = 3(p-1)+j$ (see equation 3.35 or C.1 of Appendix C) refers to the displacement components at the two nodes. The corresponding virtual tractions can be obtained from the fundamental solution using equation (2.31),

$$\delta t_I^q = n_I \, \lambda_e \left(M_{qp}^e \frac{\partial \delta v_J^p}{\partial x_J} + C_{qp}^e \, \delta v_3^p \right) + n_J \, \mu_e \, M_{qp}^e \left(\frac{\partial \delta v_I^p}{\partial x_J} + \frac{\partial \delta v_J^p}{\partial x_I} \right) \tag{4.2a}$$

$$\delta t_3^q = n_I \, \mu_e \left(C_{qp}^e \, \delta v_I^p + M_{qp}^e \frac{\partial \delta v_3^p}{\partial x_I} \right) \tag{4.2b}$$

where I, J, q, p=1,2 and δv_j^p are the displacements produced by the unit load δp_i^n. It is apparent that, for each of the six unit loads, equations (4.2) produce six traction components on the boundary Γ_e of the element (three at each node). All these traction components can be cast into a 6×6 matrix, which is called *traction matrix,* and it is denoted by $T_{\alpha\beta}^e(x_I - \xi_I)$. This matrix has the same structure as the displacement matrix $U_{\alpha\beta}^e(x_I - \xi_I)$ and its components are given in terms of the virtual tractions as

$$T_{\alpha\beta}^e(x_I - \xi_I) = \delta t_k^q \tag{4.3}$$

where k=1,2,3, q=1,2, $\alpha = 3(q-1)+k$, and $\beta = 3(n-1)+i$ depending on the position of the unit load δp_i^n. The traction matrix is expressed in terms of the functions $f_{\alpha\beta}(x,y)$, which are given in equations (3.51) and (3.63), and the components of the outward normal vector at the boundary Γ_e. The superscript e denotes that these quantities are written for the e-th numerical layer, and that they involve the material properties and the geometric characteristics related to this layer.

4.2 TRACTION MATRIX FOR THE INFINITE NUMERICAL LAYER

The components of the traction matrix $T^e_{\alpha\beta}(x_I - \xi_I)$ (I=1,2; α,β=1,2,...,6) are obtained using the definitions (4.2) and (4.3), and the relations between the virtual displacements and the fundamental solution $U^e_{\alpha\beta}(x_I - \xi_I)$, which are

$$\delta v_i^p = U^e_{\alpha\beta}(x_I - \xi_I). \tag{4.4}$$

In the above equation $\alpha = 1, 2, ..., 6$ is the row number in the fundamental solution matrix and $\alpha = 3(p-1)+i$, where $p = 1, 2$ refers to the nodal point, and $i = 1, 2, 3$ denotes the direction of the displacement component. The subscript β is the column number and $\beta = 3(s-1)+j$, with $s = 1, 2$ and $j = 1, 2, 3$ denoting a unit load at node s in the x_j–direction. The traction matrix is then obtained from the following expressions,

$$T^e_{\alpha(I,q)\beta} = n_I \lambda_e \left(M^e_{qp} \frac{\partial U^e_{\alpha(J,p)\beta}}{\partial x_J} + C^e_{qp} U^e_{\alpha(3,p)\beta} \right)$$

$$+ n_J \mu_e M^e_{qp} \left(\frac{\partial U^e_{\alpha(I,p)\beta}}{\partial x_J} + \frac{\partial U^e_{\alpha(J,p)\beta}}{\partial x_I} \right) \tag{4.5a}$$

$$T^e_{\alpha(3,q)\beta} = n_I \mu_e \left(C^e_{qp} U^e_{\alpha(I,p)\beta} + M^e_{qp} \frac{\partial U^e_{\alpha(3,p)\beta}}{\partial x_I} \right) \tag{4.5b}$$

where $I, J = 1, 2$, $\alpha(j,p) = 3(p-1)+j$ depends on the values of the node number p=1,2 and the direction x_j (j=1,2,3), and $\beta = 1, 2, ..., 6$. Substituting into (4.5) the expressions (3.36) for the displacement components of the fundamental solution and using the properties of the derivatives of functions $f_{\kappa\zeta}(x,y)$ introduced in (3.71–3.80), we arrive at the following equations for the components of the traction matrix $T^e_{\alpha\beta}(x,y)$ ($\alpha, \beta = 1, 2, ..., 6$) :

$$\begin{Bmatrix} T_{11} \\ T_{22} \\ T_{14} \\ T_{25} \end{Bmatrix} = \frac{h}{8\pi} \left(-4 \begin{Bmatrix} n_1 f_{41} \\ n_2 f_{42} \\ 0 \\ 0 \end{Bmatrix} - 2 \begin{Bmatrix} n_2 (f_{42} + f_{62}) \\ n_1 (f_{41} + f_{61}) \\ n_2 (f_{42} - f_{62}) \\ n_1 (f_{41} - f_{61}) \end{Bmatrix} \right.$$
$$+ (n_1 f_{77} - n_2 f_{76}) \begin{Bmatrix} -A_6 \\ A_6 \\ -A_7 \\ A_7 \end{Bmatrix} + A_4 (n_1 f_{85} - n_2 f_{84}) \begin{Bmatrix} -1 \\ 1 \\ -1 \\ 1 \end{Bmatrix}$$
$$\left. + 4 (n_1 f_{95} - n_2 f_{94}) \begin{Bmatrix} -1 \\ 1 \\ 1 \\ -1 \end{Bmatrix} \right) \qquad (4.6a)$$

$$\begin{Bmatrix} T_{12} \\ T_{15} \end{Bmatrix} = \frac{h}{8\pi} \left(-2 n_2 \begin{Bmatrix} f_{41} + f_{61} \\ f_{41} - f_{61} \end{Bmatrix} - n_1 \begin{Bmatrix} A_4 f_{52} + A_6 f_{42} \\ A_4 (f_{52} - f_{42}) \end{Bmatrix} \right.$$
$$+ (n_1 f_{76} + n_2 f_{77}) \begin{Bmatrix} A_6 \\ A_7 \end{Bmatrix} + A_4 (n_1 f_{84} + n_2 f_{85}) \begin{Bmatrix} 1 \\ 1 \end{Bmatrix}$$
$$\left. + 4 (n_1 f_{94} + n_2 f_{95}) \begin{Bmatrix} 1 \\ -1 \end{Bmatrix} \right) \qquad (4.6b)$$

$$\begin{Bmatrix} T_{13} \\ T_{16} \end{Bmatrix} = \frac{h}{2\pi} \left[\left(-\tfrac{1}{2} n_1 f_{10} + A_2 (n_1 f_{75} - n_2 f_{74}) \right) \begin{Bmatrix} 1 \\ 1 \end{Bmatrix} \right.$$
$$\left. + 3 A_1 (n_1 f_{83} - n_2 f_{82}) \begin{Bmatrix} -1 \\ 1 \end{Bmatrix} \right] \qquad (4.6c)$$

$$\begin{Bmatrix} T_{21} \\ T_{24} \end{Bmatrix} = \frac{h}{8\pi}\left(-2n_1\begin{Bmatrix} \mathrm{f}_{42}+\mathrm{f}_{62} \\ \mathrm{f}_{42}-\mathrm{f}_{62} \end{Bmatrix} - n_2\begin{Bmatrix} A_4\,\mathrm{f}_{51}+A_6\,\mathrm{f}_{41} \\ A_4(\mathrm{f}_{51}-\mathrm{f}_{41}) \end{Bmatrix}\right.$$
$$+(n_1\,\mathrm{f}_{76}+n_2\,\mathrm{f}_{77})\begin{Bmatrix} A_6 \\ A_7 \end{Bmatrix} + A_4(n_1\,\mathrm{f}_{84}+n_2\,\mathrm{f}_{85})\begin{Bmatrix} 1 \\ 1 \end{Bmatrix}$$
$$\left.+4(n_1\,\mathrm{f}_{94}+n_2\,\mathrm{f}_{95})\begin{Bmatrix} 1 \\ -1 \end{Bmatrix}\right) \tag{4.6d}$$

$$\begin{Bmatrix} T_{23} \\ T_{26} \end{Bmatrix} = \frac{h}{2\pi}\left[\left(-\tfrac{1}{2}n_2\,\mathrm{f}_{10}-A_2(n_1\,\mathrm{f}_{74}-n_2\,\mathrm{f}_{73})\right)\begin{Bmatrix} 1 \\ 1 \end{Bmatrix}\right.$$
$$\left.+3A_1(n_1\,\mathrm{f}_{82}-n_2\,\mathrm{f}_{81})\begin{Bmatrix} 1 \\ -1 \end{Bmatrix}\right] \tag{4.6e}$$

$$\begin{Bmatrix} T_{31} \\ T_{34} \end{Bmatrix} = \frac{h}{4\pi}\left(-A_1(n_1\,\mathrm{f}_{81}+n_2\,\mathrm{f}_{82})\begin{Bmatrix} 1 \\ 1 \end{Bmatrix}+3(n_1\,\mathrm{f}_{93}-n_2\,\mathrm{f}_{92})\begin{Bmatrix} -1 \\ 1 \end{Bmatrix}\right) \tag{4.6f}$$

$$\begin{Bmatrix} T_{32} \\ T_{35} \end{Bmatrix} = \frac{h}{4\pi}\left(-A_1(n_1\,\mathrm{f}_{82}+n_2\,\mathrm{f}_{83})\begin{Bmatrix} 1 \\ 1 \end{Bmatrix}+3(n_1\,\mathrm{f}_{92}-n_2\,\mathrm{f}_{91})\begin{Bmatrix} 1 \\ -1 \end{Bmatrix}\right) \tag{4.6g}$$

$$\begin{Bmatrix} T_{33} \\ T_{36} \end{Bmatrix} = \frac{h}{4\pi}\left(-(n_1\,\mathrm{f}_{41}+n_2\,\mathrm{f}_{42})\begin{Bmatrix} 1 \\ 1 \end{Bmatrix}+(n_1\,\mathrm{f}_{51}+n_2\,\mathrm{f}_{52})\begin{Bmatrix} -1 \\ 1 \end{Bmatrix}\right) \tag{4.6h}$$

$$\{T_{41}\ T_{42}\ T_{43}\ T_{44}\ T_{45}\ T_{46}\} = \{T_{14}\ T_{15}\ -T_{16}\ T_{11}\ T_{12}\ -T_{13}\} \tag{4.6i}$$

$$\{T_{51}\ T_{52}\ T_{53}\ T_{54}\ T_{55}\ T_{56}\} = \{T_{24}\ T_{25}\ -T_{26}\ T_{21}\ T_{22}\ -T_{23}\} \tag{4.6j}$$

$$\{T_{61}\ T_{62}\ T_{63}\ T_{64}\ T_{65}\ T_{66}\} = \{-T_{34}\ -T_{35}\ T_{36}\ -T_{31}\ -T_{32}\ T_{33}\} \tag{4.6k}$$

where n_1 and n_2 are the components of the outward normal unit vector along the x_1 and x_2 directions . The functions $\mathrm{f}_{\kappa\zeta}(x,y)$ are given in equations (3.51) and (3.63), and the coefficients A_1, A_2, A_3, A_4 and A_5, which depend on the material constants of the e-th numerical layer, have been defined in equations (3.34), (3.37) and (3.44). The coefficients A_6 and A_7 are defined as

$$A_6 = 4A_1 - A_4 \quad \text{and} \quad A_7 = 4 - A_4. \tag{4.7}$$

The thirty-six components of the traction matrix in equation (4.6) are not independent. The independent components are only eighteen, and these are the components of the upper half of the matrix. The components of the lower half of the matrix are expressed in terms of the those of the upper half and thus, the 6×6 traction matrix may also be written in the following form

$$\left[\mathbf{T}\,(x_1,x_2;\xi_1,\xi_2)\right] = \begin{array}{c} \overbrace{}^{\text{node 1}} \quad \overbrace{}^{\text{node 2}} \\ \begin{matrix} P_1^1 & P_2^1 & P_3^1 & P_1^2 & P_2^2 & P_3^2 \end{matrix} \\ \left[\begin{matrix} T_{11} & T_{12} & T_{13} & T_{14} & T_{15} & T_{16} \\ T_{21} & T_{22} & T_{23} & T_{24} & T_{25} & T_{26} \\ T_{31} & T_{32} & T_{33} & T_{34} & T_{35} & T_{36} \\ T_{14} & T_{15} & -T_{16} & T_{11} & T_{12} & -T_{13} \\ T_{24} & T_{25} & -T_{26} & T_{21} & T_{22} & -T_{23} \\ -T_{34} & -T_{35} & T_{36} & -T_{31} & -T_{32} & T_{33} \end{matrix}\right] \end{array} \begin{array}{l} \left.\right\} \text{node 1} \\ \left.\right\} \text{node 2} \end{array} \tag{4.8}$$

4.3 DISPLACEMENTS AT POINTS IN THE DOMAIN OF THE LAYER

Incorporating the definitions (4.3) of the virtual tractions and (4.4) of the virtual displacements in the virtual statement (4.1), we obtain the boundary integral equations for the typical numerical layer

$$\int_{\Omega_e} \delta\left(\vec{x}-\vec{\xi}\right)\, v_\alpha(\vec{x})\, d\Omega(\vec{x}) = v_\alpha\left(\vec{\xi}\right) =$$

$$\int_{\Omega_e} \left[\hat{t}_\beta(\vec{x}) + F_\beta(\vec{x})\right] U^e_{\beta\alpha}\left(\vec{x},\vec{\xi}\right)\, d\Omega(\vec{x})$$

$$+ \oint_{\Gamma_e} \hat{Q}_\beta(\vec{x})\; U^e_{\beta\alpha}\left(\vec{x},\vec{\xi}\right)\, d\Gamma(\vec{x}) - \oint_{\Gamma_e} v_\beta(\vec{x})\; T^e_{\beta\alpha}\left(\vec{x},\vec{\xi}\right) d\Gamma(\vec{x}) \tag{4.9}$$

in which $\alpha, \beta = 1, 2, ..., 6$ and the points $\vec{x}, \vec{\xi} \in \Omega_e$ are the point of integration and the reference point, respectively. In the above equation, all the nodal displacements associated with the arbitrary point $\vec{x}$ in the plane of the element have been combined into one vector $u_\beta(\vec{x})$ which is defined as

$$\{u(\vec{x})\} = \left\{u_1^1(\vec{x}) \quad u_2^1(\vec{x}) \quad u_3^1(\vec{x}) \quad u_1^2(\vec{x}) \quad u_2^2(\vec{x}) \quad u_3^2(\vec{x})\right\}^{\mathrm{T}}. \tag{4.10a}$$

In a similar way, we introduce the traction components $\hat{t}_\beta(\vec{x})$, which are external loads applied at the bottom $(x_3 = -h_e)$ or top $(x_3 = h_e)$ surface of the layer, the equivalent nodal values of the body forces $F_\beta(\vec{x})$, and the boundary tractions $\hat{Q}_\beta(\vec{x})$. These vectors with dimensions 6×1, are defined as

$$\{F(\vec{x})\} = \left\{F_1^1(\vec{x}) \quad F_2^1(\vec{x}) \quad F_3^1(\vec{x}) \quad F_1^2(\vec{x}) \quad F_2^2(\vec{x}) \quad F_3^2(\vec{x})\right\}^{\mathrm{T}} \tag{4.10b}$$

$$\left\{\hat{Q}(\vec{x})\right\} = \left\{\hat{Q}_1^1(\vec{x}) \quad \hat{Q}_2^1(\vec{x}) \quad \hat{Q}_3^1(\vec{x}) \quad \hat{Q}_1^2(\vec{x}) \quad \hat{Q}_2^2(\vec{x}) \quad \hat{Q}_3^2(\vec{x})\right\}^{\mathrm{T}} \tag{4.10c}$$

$$\left\{\hat{t}(\vec{x})\right\} = \left\{\hat{t}_1(\vec{x}, -h_e) \quad \hat{t}_2(\vec{x}, -h_e) \quad \hat{t}_3(\vec{x}, -h_e) \quad \hat{t}_1(\vec{x}, h_e) \quad \hat{t}_2(\vec{x}, h_e) \quad \hat{t}_3(\vec{x}, h_e)\right\}^{\mathrm{T}} \tag{4.10d}$$

where $\vec{x}(x_1, x_2)$ is a point in the domain Ω_e of the e-th numerical layer and $2h_e$ is the thickness of the layer. The BIE which is described by equation (4.9) is also called *Somigliana-type identity* and relates the displacements at an arbitrary point $\vec{\xi}$ *in the domain* Ω_e of the layer with the external tractions applied on its side boundary and on the top and bottom faces, and also with the displacements along its boundary Γ_e. We should also notice that the integral equation (4.9) is very similar to equation (2.16), which was obtained in Chapter 2 for the two- and three-dimensional elasticity problems.

The boundary integral equation (4.9) cannot be used in its present form to obtain solutions for the single layer, unless the boundary displacements and tractions are known throughout the boundary Γ_e. Note that at this stage, the surface tractions are considered to be prescribed over the bottom and top

surface of the layer, but the boundary quantities, *i.e.* displacements and tractions, are not known everywhere on the boundary Γ_e. This indicates that, in order to find the boundary quantities, we must derive an integral expression which relates directly the displacements on the boundary to the other boundary quantities of the boundary integrals in (4.9). Such an expression can be obtained by letting the point $\vec{\xi} \in \Omega_e$ to approach the boundary Γ_e, and in this case the left-hand side of (4.9) will describe boundary displacements which will be related through (4.9) to the other boundary quantities on Γ_e.

4.4 DISPLACEMENTS AT POINTS ON THE BOUNDARY OF THE LAYER

Assuming that the body can be represented as shown in Figure 4.1, *i.e.* with the point $P \equiv \vec{\xi}(\xi_1, \xi_2)$ as an internal point surrounded by part of a circle of radius ε (Brebbia *et al.*, 1984), equation (4.9) can be written as

$$
\begin{aligned}
u_\alpha(P) = & \oint_{\Gamma_e - \bar{\Gamma} + \Gamma^*} \left[\hat{Q}_\beta(Q)\, U^e_{\beta\alpha}(Q,P) - u_\beta(Q)\, T^e_{\beta\alpha}(Q,P) \right] d\Gamma(Q) \\
& + \int_{\Omega_e + \Omega^*} \left[\hat{t}_\beta(q) + F_\beta(q) \right] U^e_{\beta\alpha}(q,P)\, d\Omega(q) \qquad (4.11)
\end{aligned}
$$

where $q(x_1, x_2) \in \Omega_e + \Omega^*$ and $Q(x_1, x_2) \in \Gamma_e$. The domain of the problem has become $\Omega_e + \Omega^*$ and the corresponding boundary is the $\Gamma_e + \Gamma^*$. It is also assumed that the solution state is regular, which means that the displacements, tractions and body forces are regular throughout the domain $\Omega_e + \Omega^*$ (Cruse, 1967).

Let us now study separately the limit of each integral in equation (4.11) as $\varepsilon \to 0$. First, we are going to examine the domain integral of the surface tractions and body forces which can be written as

$$\int_{\Omega_e+\Omega^*} g_\beta(q)\, U^e_{\beta\alpha}(q,P)\, d\Omega(q) = \int_{\Omega_e} g_\beta(q)\, U^e_{\beta\alpha}(q,P)\, d\Omega(q)$$

$$+ \lim_{\varepsilon\to 0} \int_{\Omega^*} [g_\beta(q) - g_\beta(P)]\, U^e_{\beta\alpha}(q,P)\, d\Omega(q)$$

$$+ g_\beta(P) \lim_{\varepsilon\to 0} \int_{\Omega^*} U^e_{\beta\alpha}(q,P)\, d\Omega(q) \qquad (4.12)$$

in which $g_\beta(q) = \hat{t}_\beta(q) + F_\beta(q)$ is introduced for the sake of mathematical convenience. In the above expression the limit $\varepsilon \to 0$ of integrals over Ω^*, implies that the domain point $q \in \Omega^*$ approaches the boundary point P.

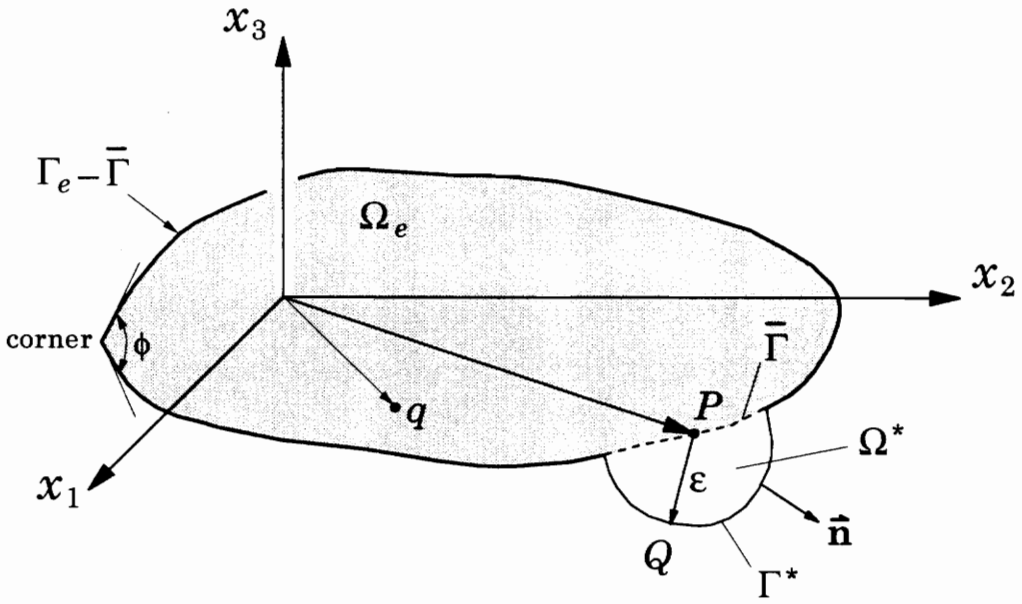

Figure 4.1 Singular point $P(\xi_1, \xi_2)$ on the boundary surrounded by part of circle of radius ε.

Denoting the distance of these two points by R, *i.e.* $R = |q - P|$, and writing the domain integrals in polar coordinates with the origin at point P, we find that the two integrals over Ω^* present no special singularities, and they become

$$\lim_{\varepsilon\to 0}\int_{\Omega^*}[g_\beta(q)-g_\beta(P)]\,U^e_{\beta\alpha}(q,P)\,d\Omega(q)=$$

$$\int_0^{\phi}\left[\lim_{\varepsilon\to 0}\int_0^{\varepsilon}[g_\beta(q)-g_\beta(P)]\,U^e_{\beta\alpha}(q,P)\,R\,dR\right]d\theta=0 \qquad (4.13a)$$

$$\lim_{\varepsilon\to 0}\int_{\Omega^*}U^e_{\beta\alpha}(q,P)\,d\Omega(q)=\int_0^{\phi}\left[\lim_{\varepsilon\to 0}\int_0^{\varepsilon}U^e_{\beta\alpha}(q,P)\,R\,dR\right]d\theta=0 \qquad (4.13b)$$

where $\phi=\pi$, when the point P is on a smooth part of the boundary Γ^e, or, when the point P is at a corner of Γ^e, ϕ is the angle between the two sides of this corner (Figure 4.1). In the case however of the integrals (4.13), the results are independent of the angle ϕ. For the evaluation of the integrals in (4.13), we have used the functions $f_{\kappa\zeta}(x,y)$ in the form given in equations (3.51) and (3.63), but in these equations, the relative position of the points $q(x_1,x_2)$ and $P(\xi_1,\xi_2)$ has been expressed in polar coordinates as

$$x=x_1-\xi_1=R\cos\theta \quad \text{and} \quad y=x_2-\xi_2=R\sin\theta, \qquad (4.14)$$

and the modified Bessel functions have been evaluated from the following expressions

$$K_0\left(c\frac{R}{h}\right)\to\ln\left(\frac{h}{cR}\right) \quad \text{and} \quad K_1\left(c\frac{R}{h}\right)\to\frac{h}{cR}, \qquad (4.15)$$

which are valid for small arguments.

The next step in this analysis is to examine the limit of the integrals over the boundary $\Gamma_e-\bar{\Gamma}+\Gamma^*$ in the equation (4.11) as the distance between the points P and Q goes to zero (*i.e.*, $\varepsilon\to 0$). The first of the boundary integrals in (4.11), which involves the components of the fundamental solution, can be written as

$$\oint_{\Gamma_e-\bar{\Gamma}+\Gamma^*} \hat{Q}_\beta(Q)\, U^e_{\beta\alpha}(Q,P)\, d\Gamma(Q) =$$

$$\lim_{\varepsilon\to 0} \int_{\Gamma^*} \left[\hat{Q}_\beta(Q) - \hat{Q}_\beta(P)\right] U^e_{\beta\alpha}(Q,P)\, d\Gamma(Q)$$

$$+ \lim_{\varepsilon\to 0} \hat{Q}_\beta(P) \int_{\Gamma^*} U^e_{\beta\alpha}(Q,P)\, d\Gamma(Q) + \lim_{\varepsilon\to 0} \int_{\Gamma_e-\bar{\Gamma}} \hat{Q}_\beta(Q)\, U^e_{\beta\alpha}(Q,P)\, d\Gamma(Q)\ . \quad (4.16)$$

The first integral of the right-hand side of (4.16) vanishes from the continuity of $\hat{Q}_\beta$, and the second one is evaluated using the expressions of the fundamental solution in polar coordinates and equation (4.15). The second integral of (4.16) yields,

$$\lim_{\varepsilon\to 0} \hat{Q}_\beta(P) \int_{\Gamma^*} U^e_{\beta\alpha}(Q,P)\, d\Gamma(Q) = \hat{Q}_\beta(P) \int_0^{\phi} \lim_{R=\varepsilon\to 0} \left[U^e_{\beta\alpha}(Q,P)\, R\right] d\theta = 0 \quad (4.17)$$

where $\phi = \pi$ for smooth boundary and $\phi \neq \pi$ for a corner. Referring to the last integral of (4.16), it is easy to verify by using the regularity of the solution state and the expressions for the fundamental solution, that it approaches the total integral on Γ_e as the radius ε is taken in the limit toward zero. This integral presents no special singularity and it can be interpreted in the normal sense of integration. Therefore, the left-hand side integral of equation (4.16) finally becomes

$$\oint_{\Gamma_e-\bar{\Gamma}+\Gamma^*} \hat{Q}_\beta(Q)\, U^e_{\beta\alpha}(Q,P)\, d\Gamma(Q) = \lim_{\varepsilon\to 0} \int_{\Gamma_e-\bar{\Gamma}} \hat{Q}_\beta(Q)\, U^e_{\beta\alpha}(Q,P)\, d\Gamma(Q)$$

$$= \int_{\Gamma_e} \hat{Q}_\beta(Q)\, U^e_{\beta\alpha}(Q,P)\, d\Gamma(Q) \quad (4.18)$$

In a similar way, the second boundary integral in equation (4.11), which involves the components of the traction matrix, can be written as

$$\oint_{\Gamma_e-\bar{\Gamma}+\Gamma^*} v_\beta(Q)\; T^e_{\beta\alpha}(Q,P)\, d\Gamma(Q) =$$

$$\lim_{\varepsilon\to 0}\int_{\Gamma^*}[v_\beta(Q)-v_\beta(P)]\; T^e_{\beta\alpha}(Q,P)\, d\Gamma(Q)$$

$$+\lim_{\varepsilon\to 0} v_\beta(P)\int_{\Gamma^*} T^e_{\beta\alpha}(Q,P)\, d\Gamma(Q)+\lim_{\varepsilon\to 0}\int_{\Gamma_e-\bar{\Gamma}} v_\beta(Q)\; T^e_{\beta\alpha}(Q,P)\, d\Gamma(Q)\ , \quad (4.19)$$

and using the continuity of the displacements,

$$\oint_{\Gamma_e-\bar{\Gamma}+\Gamma^*} v_\beta(Q)\; T^e_{\beta\alpha}(Q,P)\, d\Gamma(Q) = \lim_{\varepsilon\to 0}\int_{\Gamma_e-\bar{\Gamma}} v_\beta(Q)\; T^e_{\beta\alpha}(Q,P)\, d\Gamma(Q)$$

$$+ v_\beta(P)\lim_{\varepsilon\to 0}\int_{\Gamma^*} T^e_{\beta\alpha}(Q,P)\, d\Gamma(Q) \quad . \quad (4.20)$$

The first integral on the right hand of (4.20) is seen to be taken in the Cauchy principal value sense, the existence of which can be proved if $\hat{Q}_\beta(Q)$ satisfies a *Hölder condition* at point Q, in the form

$$\left|\hat{Q}_\beta(Q)-\hat{Q}_\beta(P)\right| \le B\,R^a, \qquad B,a>0 \quad (4.21)$$

where $R=|Q-P|$. A function that satisfies *Hölder condition* (Kellogg, 1929) is evidently continuous but not necessarily differentiable. Introducing a polar coordinate system at point P, equation (4.20) yields

$$\oint_{\Gamma_e-\bar{\Gamma}+\Gamma^*} v_\beta(Q)\; T^e_{\beta\alpha}(Q,P)\, d\Gamma(Q) =$$

$$\int_{\Gamma_e} v_\beta(Q)\; T^e_{\beta\alpha}(Q,P)\, d\Gamma(Q) + v_\beta(P)\lim_{R=\varepsilon\to 0}\int_0^{\phi} T^e_{\beta\alpha}(Q,P)\; R\; d\theta\ . \quad (4.22)$$

The last integral of (4.22), can be evaluated using the definitions (4.6) for the components of the traction matrix $T^e_{\alpha\beta}(Q,P)$, along with equations (4.14) and

(4.15). The components of the outward normal vector on the boundary Γ^*, which appear in these expressions, are given as

$$n_1 = \cos\theta \quad \text{and} \quad n_2 = \sin\theta \ . \tag{4.23}$$

In this case, the value of the angle ϕ (Figure 4.1) plays a crucial role, since the expressions for the traction components depend on the tangent at point $P \in \Gamma^*$ (Hartmann, 1980). For *smooth boundary* at the neighborhood of P, it is $\phi = \pi$, and

$$\lim_{R=\varepsilon\to 0} \int_0^{\pi} T^e_{\beta\alpha}(Q,P)\ R\ d\theta \ = \ -\tfrac{1}{2}\delta_{\beta\alpha} \ , \tag{4.24}$$

$\delta_{\beta\alpha}$ being the *Kronecker delta*, while, if P is at the vertex of a corner ($\phi \neq \pi$), one has to evaluate the last integral in (4.22), and then find the limit as $\varepsilon \to 0$.

Incorporating now the results of (4.12), (4.13), (4.18) and (4.22), in the integral statement (4.11), the following equation arises as $\varepsilon \to 0$

$$\begin{aligned} c_{\beta\alpha}(P)\, v_\beta(P) = & \oint_{\Gamma_e} \left[\hat{Q}_\beta(Q)\ U^e_{\beta\alpha}(Q,P) - v_\beta(Q)\ T^e_{\beta\alpha}(Q,P) \right] d\Gamma(Q) \\ & + \int_{\Omega_e} \left[\hat{t}_\beta(q) + F_\beta(q) \right] U^e_{\beta\alpha}(q,P)\ d\Omega(q) \end{aligned} \tag{4.25}$$

$$(P, Q \in \Gamma_e ; \ q \in \Omega_e ; \ \alpha, \beta = 1, 2, ..., 6)$$

where the matrix $c_{\beta\alpha}(P)$ is generally defined as

$$c_{\beta\alpha}(P) \ = \ \delta_{\beta\alpha} \ + \ \lim_{R=\varepsilon\to 0} \int_0^{\phi} T^e_{\beta\alpha}(R,\theta)\ R\ d\theta \ . \tag{4.26}$$

and the contour integral with kernel $T^e_{\beta\alpha}(Q,P)$ is to be interpreted in the Cauchy principal value sense. Equation (4.25) is valid for points P on the

boundary of the numerical layer and provides a relation that must be satisfied between boundary displacements, boundary tractions, and surface tractions ($\hat{t}_\beta$ and F_β). Taking into consideration that the surface tractions are either known for the case of single layers, or they can be determined from equilibrium and displacement compatibility requirements for the case of multilayered systems, this equation becomes a boundary integral equation for the evaluation of *the unknown boundary data* when the boundary conditions are defined. This important feature is the one that makes equation (4.25) most attractive and can be fully explored for numerical solutions.

4.5 BOUNDARY INTEGRAL REPRESENTATION OF THE 3-D DISPLACEMENT FIELD IN A LAYER

The boundary integral equations in (4.9) and (4.25) give a complete description of the nodal displacements for the typical numerical layer. These are displacements at the top and bottom surface of the layer for the case of linear variation of the displacement components through the layer's thickness. The first of these equations relates displacements at points *in the domain* Ω_e to the surface tractions $\hat{t}_\beta(\vec{x})$, the body forces $F_\beta(\vec{x})$, the boundary tractions $\hat{Q}_\beta(\vec{x})$ and the boundary displacements $\upsilon_\beta(\vec{x})$, while the second one relates displacements at points *on the boundary* Γ_e to the aforementioned quantities. These two equations along with the fundamental solution that has already been derived in the previous chapter are the starting equations for the application of the boundary element method. The two equations can be combined in one general expression which may then be applied for any position of the arbitrary point $\vec{\xi} \in (\Omega_e + \Gamma_e)$ of the e-th numerical layer,

$$c_{\beta\alpha}\left(\vec{\xi}\right)v_\beta\left(\vec{\xi}\right) = \oint_{\Gamma_e} \hat{Q}_\beta(\vec{x})\; U^e_{\beta\alpha}\left(\vec{x},\vec{\xi}\right) d\Gamma(\vec{x}) \;-\; \oint_{\Gamma_e} v_\beta(\vec{x})\; T^e_{\beta\alpha}\left(\vec{x},\vec{\xi}\right) d\Gamma(\vec{x})$$

$$+ \int_{\Omega_e} \left[\hat{t}_\beta(\vec{x}) + F_\beta(\vec{x})\right] U^e_{\beta\alpha}\left(\vec{x},\vec{\xi}\right) d\Omega(\vec{x})\,. \qquad (4.27)$$

$$(\alpha, \beta = 1, 2, \ldots, 6)$$

The c-matrix, in the above equation, depends on the position of the reference point $\vec{\xi}$, and it is defined in the following way

$$c_{\beta\alpha}\left(\vec{\xi}\right) = \begin{cases} \delta_{\beta\alpha}\,, & \text{for } \vec{\xi} \in \Omega_e \\ \frac{1}{2}\delta_{\beta\alpha}\,, & \text{for } \vec{\xi} \in \Gamma_e \quad \text{(smooth point)} \\ \delta_{\beta\alpha} + \lim\limits_{\varepsilon\to 0} \int\limits_{\Gamma^*} T^e_{\beta\alpha}\left(\vec{x},\vec{\xi}\right) d\Gamma(\vec{x})\,, & \text{for } \vec{\xi} \in \Gamma_e \quad \text{(corner point)} \\ 0\,, & \text{for } \vec{\xi} \notin \Omega_e + \Gamma_e \end{cases} \qquad (4.28)$$

where Γ^* denotes a part of the circumference of a circle which has center at the reference point $\vec{\xi}$ (corner point) and radius $\varepsilon = \left|\vec{x} - \vec{\xi}\right|$, as it is also shown in Figure 4.1.

Finally, the three-dimensional displacement field for the typical numerical layer can be obtained by substituting the nodal displacements of (4.27) into the displacement approximation (2.18),

$$u_i(\xi_1, \xi_2, \xi_3) = v_i(\xi_1, \xi_2)\; \phi^e_1(\xi_3) + v_{3+i}(\xi_1, \xi_2)\; \phi^e_2(\xi_3) \qquad (4.29)$$

where $i = 1, 2, 3$, and $\phi^e_I(\xi_3)$ are the linear Lagrange interpolation functions (equation 2.18) which are given in terms of the ξ_3 coordinate as

$$\phi^e_1(\xi_3) = \frac{h_e - \xi_3}{2h_e} \qquad \text{and} \qquad \phi^e_2(\xi_3) = \frac{h_e + \xi_3}{2h_e} \qquad (4.30)$$

with $2h_e$ the thickness of the e-th numerical layer (see equations 3.28).

4.6 STRESSES AND STRAINS IN THE TYPICAL NUMERICAL LAYER

The linear strain-displacement relations and the constitutive relations are given by equations (2.2) and (2.3), respectively, and they can be written for the arbitrary point (ξ_1, ξ_2, ξ_3) in the three-dimensional layer as

$$\varepsilon_{ij}(\xi_1, \xi_2, \xi_3) = \frac{1}{2}\left(\frac{\partial u_i}{\partial \xi_j} + \frac{\partial u_j}{\partial \xi_i}\right), \tag{4.31}$$

and $$\sigma_{ij}(\xi_1, \xi_2, \xi_3) = \lambda_e \, \delta_{ij} \, \varepsilon_{kk} + 2\mu_e \, \varepsilon_{ij} = \lambda_e \delta_{ij} \frac{\partial u_k}{\partial \xi_k} + \mu_e \left(\frac{\partial u_i}{\partial \xi_j} + \frac{\partial u_j}{\partial \xi_i}\right), \tag{4.32}$$

where $i, j, k = 1, 2, 3$, and the subscript e denotes that the elastic constants λ_e and μ_e are those of the e-th layer. The derivatives of the displacement components $u_i(\xi_1, \xi_2, \xi_3)$ that appear in the above equations can be obtained in terms of the derivatives of the nodal displacements by differentiating both sides of equation (4.29) with respect to the coordinates ξ_i $(i = 1,2,3)$,

$$\frac{\partial u_i(\xi_1, \xi_2, \xi_3)}{\partial \xi_I} = \frac{\partial v_i(\xi_1, \xi_2)}{\partial \xi_I} \, \phi_1^e(\xi_3) + \frac{\partial v_{3+i}(\xi_1, \xi_2)}{\partial \xi_I} \, \phi_2^e(\xi_3) \tag{4.33a}$$

$$\frac{\partial u_i(\xi_1, \xi_2, \xi_3)}{\partial \xi_3} = v_i(\xi_1, \xi_2) \, \frac{d\phi_1^e(\xi_3)}{d\xi_3} + v_{3+i}(\xi_1, \xi_2) \, \frac{d\phi_2^e(\xi_3)}{d\xi_3} \tag{4.33b}$$

where $I = 1, 2$ and ϕ_I^e are the linear Lagrange interpolation functions of (4.30). The nodal displacements $v_\alpha(\xi_1, \xi_2)$ are given in an integral form in equation (4.27).

Equation (4.27) is a continuous representation of the nodal displacements at any point $\vec{\xi}$ on the mid-plane Ω_e of the layer. Consequently, the derivatives of the nodal displacements can be obtained by differentiating the right-hand side of (4.27) with respect to the coordinates of point $\vec{\xi}(\xi_1, \xi_2) \in \Omega_e$. The differentiation can be carried out directly inside the integrals. This is

obviously possible for the boundary integrals of (4.27), because the reference point $\vec{\xi}$ is located in the domain Ω_e and the integration point $\vec{x}$ is always on the boundary Γ_e, but the domain integrals need special attention, since in their case both, the reference and integration points, are in the domain (Partridge and Brebbia, 1990). However, the validity of this operation can be proved assuming a cylindrical volume with center at $\vec{\xi}$ and radius $\varepsilon = \left|\vec{x} - \vec{\xi}\right|$, as shown in Figure 3.2, and finding the limit as $\varepsilon \to 0$ by means of the Leibnitz formula and the Hölder condition (see Section 4.4). The resulting expressions for the derivatives become

$$\begin{aligned}\frac{\partial}{\partial \xi_I} v_\alpha\left(\vec{\xi}\right) = & \oint_{\Gamma_e} \hat{Q}_\beta(\vec{x}) \, \frac{\partial}{\partial \xi_I}\left[U^e_{\beta\alpha}\left(\vec{x}, \vec{\xi}\right)\right] d\Gamma(\vec{x}) \\ & - \oint_{\Gamma_e} v_\beta(\vec{x}) \, \frac{\partial}{\partial \xi_I}\left[T^e_{\beta\alpha}\left(\vec{x}, \vec{\xi}\right)\right] d\Gamma(\vec{x}) \\ & + \int_{\Omega_e} \left[\hat{t}_\beta(\vec{x}) + F_\beta(\vec{x})\right] \frac{\partial}{\partial \xi_I}\left[U^e_{\beta\alpha}\left(\vec{x}, \vec{\xi}\right)\right] d\Omega(\vec{x}) \end{aligned} \tag{4.34}$$

where $I = 1, 2$; $\alpha, \beta = 1, 2, ..., 6$, and $\vec{\xi}(\xi_1, \xi_2) \in \Omega_e$.

It is very interesting and also useful, to notice that the stress components at the bottom and top surface of the layer may also be found using the surface tractions $\hat{t}_\beta(\vec{\xi})$, since both these surfaces are parallel to the x_1x_2–plane. The stresses at a point on the bounding surfaces of the layer are related to the tractions through the expressions

$$\sigma_{3i}(\xi_1, \xi_2, -h_e) = -\hat{t}_i(\xi_1, \xi_2), \tag{4.35a}$$

and

$$\sigma_{3i}(\xi_1, \xi_2, h_e) = \hat{t}_{3+i}(\xi_1, \xi_2), \tag{4.35b}$$

where $i = 1, 2, 3$ and h_e is half of the e-th layer's thickness.

Based on equations (4.35), we can also express the derivative with respect to ξ_3 of the displacement component u_3 at points of the top and bottom surface, in terms of the surface tractions,

$$\left.\frac{\partial u_3}{\partial \xi_3}\right|_{\xi_3=-h_e} = \frac{1}{\lambda_e + 2\mu_e}\left[-\hat{t}_3(\xi_1,\xi_2) - \lambda_e \frac{\partial v_M}{\partial \xi_M}\right] \tag{4.36a}$$

$$\left.\frac{\partial u_3}{\partial \xi_3}\right|_{\xi_3=h_e} = \frac{1}{\lambda_e + 2\mu_e}\left[\hat{t}_6(\xi_1,\xi_2) - \lambda_e \frac{\partial v_{3+M}}{\partial \xi_M}\right] \tag{4.36b}$$

in which $M = 1, 2$. Consequently, substitution of these expressions in (4.32), yields the in-plane stress components at the faces of the layer, which may be written in the following form,

$$\sigma_{IJ}(\xi_1,\xi_2,-h_e) = \frac{\lambda_e}{\lambda_e + 2\mu_e}\delta_{IJ}\left[-\hat{t}_3(\xi_1,\xi_2) + 2\,\mu_e \frac{\partial v_M}{\partial \xi_M}\right] + \mu_e\left(\frac{\partial v_I}{\partial \xi_J} + \frac{\partial v_J}{\partial \xi_I}\right) \tag{4.37a}$$

$$\sigma_{IJ}(\xi_1,\xi_2,h_e) = \frac{\lambda_e}{\lambda_e + 2\mu_e}\delta_{IJ}\left[\hat{t}_6(\xi_1,\xi_2) + 2\,\mu_e \frac{\partial v_{3+M}}{\partial \xi_M}\right] + \mu_e\left(\frac{\partial v_{3+I}}{\partial \xi_J} + \frac{\partial v_{3+J}}{\partial \xi_I}\right) \tag{4.37b}$$

where the indices $I, J, M = 1, 2$.

It becomes apparent from the previous analysis that using the constitutive relations and the integral representation of the nodal displacements, we can derive *continuous* representations of the stress and strain components at *any point* in the typical numerical layer.

Chapter 5

BOUNDARY ELEMENT MODEL

5.1 INTRODUCTION

In the previous chapter we established the integral representation of the displacements at the nodal points of the typical numerical layer (equation 4.27). These nodal points are located at the top and bottom surface of the layer, since the boundary integral model was developed under the assumption of linear displacement variation through the thickness of the layer. The displacements were grouped in a vector $\upsilon_\alpha(\xi_1, \xi_2)$ $(\alpha = 1, 2, ..., 6)$, in which the first three components are the displacements at point $(\xi_1, \xi_2, -h_e)$, while the other three components are the displacements at point (ξ_1, ξ_2, h_e), where $2h_e$ is the thickness of the e-th layer (equation 4.10a). Similar definitions were also adopted for the surface tractions $\hat{t}_\alpha(\xi_1, \xi_2)$ and the boundary tractions $\hat{Q}_\alpha(\xi_1, \xi_2)$ (equations 4.10c,d). All these vectors being introduced into equations (4.27) and (4.29) can fully describe the three-dimensional displacement field in a numerical layer, and also, by means of equations (4.31–4.34), they

can produce the components of the strain and stress tensors at any point in the layer. Having established this notation, we can now refer to the layer with its mid-plane Ω_e and the corresponding boundary Γ_e, and we may consider that each point in the two-dimensional region Ω_e is associated with six displacement components and the corresponding six traction components.

In the first part of this chapter a numerical procedure for the solution of the boundary value problem of a single layer will be developed under the assumption that the surface tractions are fully prescribed. In the sequel, the same procedure will be extended to the problem of a multilayered system by utilizing appropriate boundary conditions at the interfaces between the numerical layers. In this case, the surface tractions will not be known and they will be obtained through the numerical procedure as part of the solution.

5.2 BOUNDARY ELEMENT MODEL FOR THE TYPICAL NUMERICAL LAYER

Equation (4.27), written for points $\vec{\xi}(\xi_1, \xi_2)$ on the boundary of the layer, becomes the integral representation of the solution for the boundary-value problem of a single layer. Instead of attempting closed form solutions to this equation, which is a difficult task and only attainable for simple geometries and boundary conditions, the boundary element method (BEM) employs a numerical approach. The basic steps involved in this approach constitute the numerical essence of the technique (Banerjee and Butterfield, 1981; Brebbia *et al.*, 1984; Hartmann, 1989), and they are summarized below:

(i) The boundary Γ_e of the two-dimensional model of the layer is discretized into series of elements over which the displacements and

tractions are chosen to be piecewise interpolated between the element nodal points.

(ii) Equation (4.27) is applied in a discretized form to each nodal point $\vec{\xi}(\xi_1, \xi_2) \in \Gamma_e$ and the integrals are computed by a numerical quadrature scheme over each boundary element. Assuming that there are N_b nodal points on the boundary, a system of $6N_b$ linear algebraic equations involving the set of $6N_b$ nodal tractions and $6N_b$ nodal displacements is obtained.

(iii) Boundary conditions are imposed and consequently $6N_b$ nodal values (tractions or displacements along each direction per node) are prescribed. The system of $6N_b$ equations can therefore be solved by standard methods to determine the remaining boundary data.

(iv) Values of the displacement, strain and stress components at any internal point can readily be computed by numerical quadrature using the appropriate equations in a discretized form (*i.e.*, equations 4.27 and 4.31–34).

Body forces or surface tractions can be included in the model by a numerical integration scheme which leads to an additional contribution to the independent term of the system of equations, and similar contribution to the internal quantities. The domain terms can be treated in an efficient and systematic way by discretizing Ω_e into domain elements, preferably triangular, and employing a finite element-type model for the approximation of the domain integrals.

The boundary Γ_e of the layer is divided into N_b intervals, not necessarily equal, referred to as *boundary elements* (Figure 5.1). The elements on the external boundary are numbered consecutively counterclockwise, while on the internal boundaries, *i.e.* boundaries of holes or inclusions within the

domain Ω_e, clockwise. The numbering direction is determined according to the direction of the outward unit normal vector on the boundary. In order to capture more accurately the geometry of the boundary, each boundary element is approximated by a parabolic arc. The values of the unknown functions υ_α and $\hat{Q}_\alpha$ are assumed constant over the element (step function assumption) and equal to the values at the nodal points (Brebbia and Niku, 1987). The domain Ω_e of the layer is divided into M triangular elements (Cruse, 1969) as it is shown Figure 5.1, and the surface tractions $\hat{t}_\alpha$ and the body forces F_α are approximated over each element using linear two-dimensional Lagrange interpolation functions (Reddy, 1993).

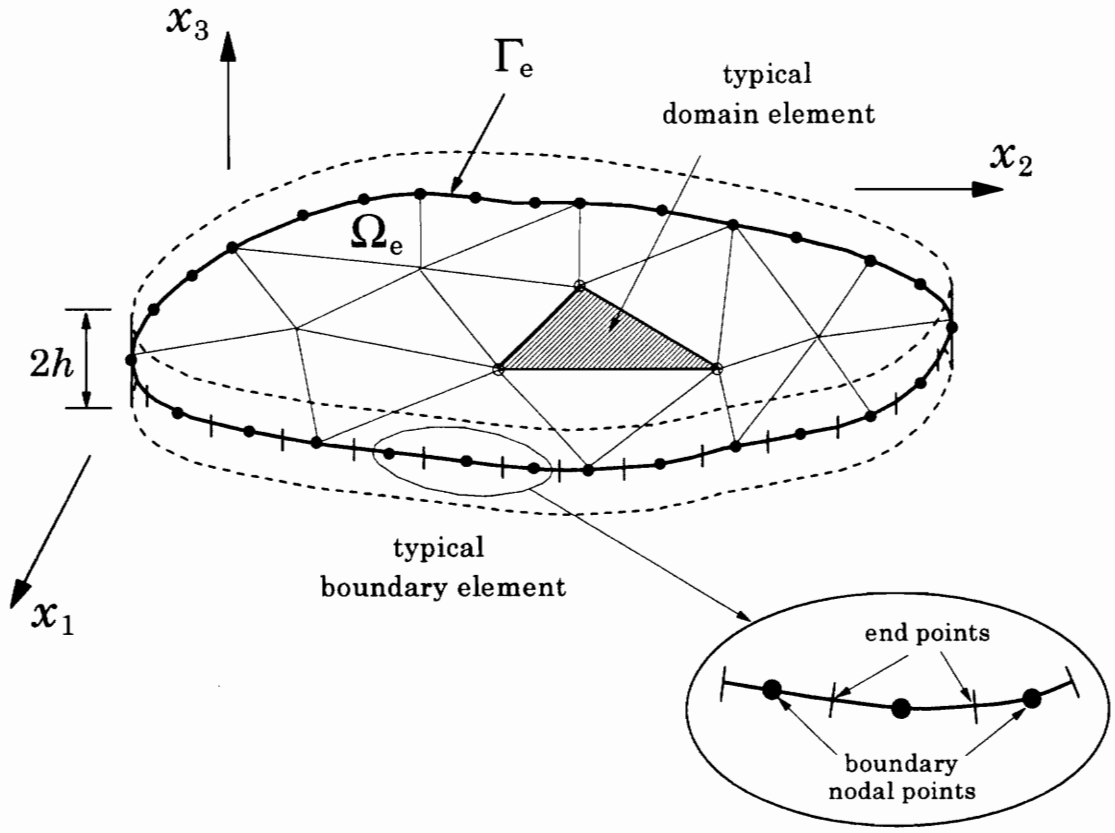

Figure 5.1 Boundary and domain discretization of the typical numerical layer.

The boundary integral equation (4.27) of the typical numerical layer can now be written in the following discretized form,

$$\left[c\left(\vec{\xi}\right)\right]^{\mathrm{T}}\left\{v\left(\vec{\xi}\right)\right\} = \sum_{n=1}^{N_b}\int_{\Gamma_e^n}\left[U^e\left(\vec{x},\vec{\xi}\right)\right]^{\mathrm{T}}\left\{\hat{Q}(\vec{x})\right\}d\Gamma(\vec{x}) - \sum_{n=1}^{N_b}\int_{\Gamma_e^n}\left[T^e\left(\vec{x},\vec{\xi}\right)\right]^{\mathrm{T}}\{v(\vec{x})\}\,d\Gamma(\vec{x}) + \sum_{m=1}^{M}\int_{\Omega_e^m}\left[U^e\left(\vec{x},\vec{\xi}\right)\right]^{\mathrm{T}}\left(\left\{\hat{t}(\vec{x})\right\}+\{F(\vec{x})\}\right)d\Omega(\vec{x}) \qquad (5.1)$$

where Γ_e^n denotes the n-th boundary element and Ω_e^m denotes the m-th triangular element. In equation (5.1), we have adopted matrix notation instead of indicial notation that was used in the previous chapters. The surface tractions and the body forces are assumed to be linear element-wise, so, for a point $\vec{x}\in\Omega_e^m$, they are expressed in terms of the nodal values as

$$\left\{\hat{t}(\vec{x})\right\} = \sum_{k=1}^{3}\phi_k(\vec{x})\left\{\hat{t}\right\}_k^m \quad \text{and} \quad \{F(\vec{x})\} = \sum_{k=1}^{3}\phi_k(\vec{x})\{F\}_k^m\,, \qquad (5.2)$$

where the superscript m denotes the domain element and the subscript k (k =1,2,3) is the local node number. The shape functions $\phi_k(x_1,x_2)$ are the linear interpolation functions for the three-node triangular element (Reddy, 1993). The boundary quantities are constant over each element (Brebbia and Niku, 1987; Katsikadelis and Kokkinos, 1987), and therefore it is

$$\{v(\vec{x})\} = \{v\}_n \quad \text{and} \quad \left\{\hat{Q}(\vec{x})\right\} = \left\{\hat{Q}\right\}_n\,, \ \text{for}\ \vec{x}\in\Gamma_e^n. \qquad (5.3)$$

This actually means that when the point $\vec{x}$ is on the n-th boundary element, the values of the tractions or the displacements are constant and equal to the value at the nodal point.

Substituting the nodal approximations of (5.2) and (5.3) into the discretized integral equation (5.1), we find the following matrix equation for the nodal displacements and tractions (it resembles a flexibility-type equation)

$$[c]_p^{\mathrm{T}}\,\{v\}_p = \sum_{n=1}^{N_b}\left(\int_{\Gamma_e^n}[U^e]_{pn}^{\mathrm{T}}\,d\Gamma(\vec{x})\right)\left\{\hat{Q}\right\}_n - \sum_{n=1}^{N_b}\left(\int_{\Gamma_e^n}[T^e]_{pn}^{\mathrm{T}}\,d\Gamma(\vec{x})\right)\{v\}_n$$

$$+\sum_{m=1}^{M}\sum_{k=1}^{3}\left(\int_{\Omega_e^m}\left[U^e\left(\vec{x},\vec{\xi}\right)\right]^{\mathrm{T}}\phi_k(\vec{x})\,d\Omega(\vec{x})\right)\left(\left\{\hat{t}\right\}_k^m + \{F\}_k^m\right) \qquad (5.4)$$

where the subscript p of the fundamental displacement and traction matrices denotes that the *field point* $\vec{\xi}$, which is also called *reference point*, coincides with the p-th boundary nodal point, while the subscript n denotes that the *source point* $\vec{x}$, which is also called *integration point*, lies on the n-th boundary element. Referring to the c-matrix, the subscript p denotes that the components of this matrix are evaluated at the p-th boundary nodal point according to the definition (4.28). Note that in equation (5.4) the dimensions of all the vectors and all the matrices are 6×1 and 6×6, respectively.

The boundary and domain integrals of equation (5.4) are evaluated using special integration techniques, that will be presented in detail in the next chapter. All these integrals are *regular* when the field point does not belong to the element (boundary or domain element) over which the integration is performed, but they become *singular* when the field point is on the element of integration. The singular line integrals are evaluated using a purely numerically technique developed in Section 6.1. The domain integrals are transformed analytically to regular line integrals over the boundary of each domain element using a technique presented in Section 6.2, and then, these line integrals are evaluated numerically.

For the sake of mathematical convenience, we introduce the following two matrices:

$$[G]^e_{pn} = \int_{\Gamma^n_e} [U^e]^{\mathrm{T}}_{pn}\, d\Gamma(\vec{x}) \quad \text{and} \quad [H]^e_{pn} = \int_{\Gamma^n_e} [T^e]^{\mathrm{T}}_{pn}\, d\Gamma(\vec{x}), \tag{5.5}$$

which represent the influence of the displacements and tractions of the n-th boundary element (n is the nodal point of Γ^n_e) on the displacements of the p-th boundary nodal point ($p \equiv \vec{\xi}$). In addition, we define

$$[D]^{em}_{pk} = \int_{\Omega^m_e} \left[U^e\left(\vec{x}, \vec{\xi}\right) \right]^{\mathrm{T}} \phi_k(\vec{x})\, d\Omega(\vec{x}) , \tag{5.6}$$

where point $\vec{\xi}$ coincides with the p-th boundary nodal point. The matrix $[D]^{em}_{pk}$ represents the effect of tractions distributed over the m-th domain element on the nodal displacements of the p-th boundary element. The subscript k (k=1,2,3) refers to the three nodes of the triangular domain element and the superscript e denotes the numerical layer. Substitution of the definitions (5.5) and (5.6) into equation (5.4) yields the matrix equation,

$$\begin{aligned} \tfrac{1}{2}\{v\}_p = & \sum_{n=1}^{N_b} [G]^e_{pn} \left\{\hat{Q}\right\}_n - \sum_{n=1}^{N_b} [H]^e_{pn} \{v\}_n \\ & + \sum_{m=1}^{M} \sum_{k=1}^{3} [D]^{em}_{pk} \left(\left\{\hat{t}\right\}^k_m + \{F\}^k_m \right) . \end{aligned} \tag{5.7}$$

The above equation relates the displacement vector at node p of the boundary element model to the displacements and boundary tractions of all the boundary nodal points (including also point p), the surface tractions at the nodal points of the domain, and the body forces. Note that equation (5.7) was written assuming that the boundary Γ_e is smooth at the boundary nodal point p, which is true for most of the cases. If, however, the boundary is not smooth at

this nodal point, *i.e.* if p is a corner point, one must compute the coefficients of the c-matrix, which are given in an integral form in equation (4.28), and then use the results in (5.4). In general, this procedure may be avoided by setting, in the discretization of the boundary, any corner points at the end-points of the boundary elements.

5.2–1 Boundary Element Model for Points on the Boundary of the Layer

Furthermore, equation (5.7) can be applied for every node on the boundary, and the resulting N_b matrix equations can be grouped in one equation which constitutes the *boundary element model for the single layer* and has the following form,

$$\tfrac{1}{2}\{v\}^e = [G]^e \left\{\hat{Q}\right\}^e - [H]^e \{v\}^e + [D]^e \left(\left\{\hat{t}\right\}^e + \{F\}^e\right) \tag{5.8}$$

where the vectors $\{v\}^e$ and $\left\{\hat{Q}\right\}^e$ have $6N_b$ components and they are defined as

$$\{v\}^e = \begin{Bmatrix} \{v\}_1 \\ \{v\}_2 \\ \vdots \\ \{v\}_{N_b} \end{Bmatrix}^e \quad \text{and} \quad \left\{\hat{Q}\right\}^e = \begin{Bmatrix} \left\{\hat{Q}\right\}_1 \\ \left\{\hat{Q}\right\}_2 \\ \vdots \\ \left\{\hat{Q}\right\}_{N_b} \end{Bmatrix}^e . \tag{5.9}$$

The vectors $\left\{\hat{t}\right\}^e$ and $\{F\}^e$ have $6N_d$ components, N_d being the total number of nodes in the domain mesh, and they are defined as

$$\left\{\hat{t}\right\}^e = \begin{Bmatrix} \left\{\hat{t}\right\}_1 \\ \left\{\hat{t}\right\}_2 \\ \vdots \\ \left\{\hat{t}\right\}_{N_d} \end{Bmatrix}^e \quad \text{and} \quad \{F\}^e = \begin{Bmatrix} \{F\}_1 \\ \{F\}_2 \\ \vdots \\ \{F\}_{N_d} \end{Bmatrix}^e . \tag{5.10}$$

The vectors in equation (5.10) denote the surface tractions and the body forces at the N_d nodes of the discretized domain. The subscripts of the vectors on the right-hand side of these equations are the global node numbers in the domain mesh. In equation (5.8), the dimensions of matrices $[H]^e$ and $[G]^e$ are $6N_b \times 6N_b$ and they have the following structure

$$[G]^e = \begin{bmatrix} [G]^e_{11} & [G]^e_{12} & \cdots & [G]^e_{1N_b} \\ [G]^e_{21} & [G]^e_{22} & \cdots & [G]^e_{2N_b} \\ \vdots & \vdots & \ddots & \vdots \\ & & [G]^e_{pn} & \\ & & & \ddots \\ [G]^e_{N_b1} & [G]^e_{N_b2} & \cdots & [G]^e_{N_bN_b} \end{bmatrix}, \tag{5.11a}$$

and

$$[H]^e = \begin{bmatrix} [H]^e_{11} & [H]^e_{12} & \cdots & [H]^e_{1N_b} \\ [H]^e_{21} & [H]^e_{22} & \cdots & [H]^e_{2N_b} \\ \vdots & \vdots & \ddots & \vdots \\ & & [H]^e_{pn} & \\ & & & \ddots \\ [H]^e_{N_b1} & [H]^e_{N_b2} & \cdots & [H]^e_{N_bN_b} \end{bmatrix}. \tag{5.11b}$$

The matrix $[D]^e$ with dimensions $6N_b \times 6N_d$ is constructed by assembling the element matrices $[D]^{em}_{pk}$ $(m = 1, 2, ..., M;\ p = 1, 2, ..., N_b;\ k = 1, 2, 3)$ through the correspondence between element node numbers and global node numbers (*connectivity matrix*). This process is usually referred to as *assembly of the element matrices* (Reddy, 1993).

5.2–2 Boundary Element Model for Points in the Domain of the Layer

The boundary integral equations for points $\vec{\xi}$ in the domain Ω_e of the layer are given in (4.27), in which the coefficients of the c-matrix take values according to the definition (4.28). Equation (4.27) may also be written in

matrix form, in which $[c(\vec{\xi})]$ is going to be the identity matrix since point $\vec{\xi} \in \Omega_e$, and it will have the form

$$\{v^*\}_q = \sum_{n=1}^{N_b} [G^*]_{qn}^e \left\{\hat{Q}\right\}_n - \sum_{n=1}^{N_b} [H^*]_{qn}^e \{v\}_n + \sum_{m=1}^{M} \sum_{k=1}^{3} [D^*]_{qk}^{em} \left(\left\{\hat{t}\right\}_m^k + \{F\}_m^k\right) \tag{5.12}$$

where the asterisk (*) denotes that the corresponding quantities, displacement vector or coefficient matrix, refer to a field point in the domain of the layer. The coefficient matrices $[G^*]_{qn}^e$, $[H^*]_{qn}^e$ and $[D^*]_{qk}^{em}$ are evaluated from equations (5.5) and (5.6) by making the field point $\vec{\xi}$ to coincide with node q in the discretized domain. If the global node numbers are assigned, first, to all the nodes in the domain Ω_e (excluding Γ_e), and, then, to those nodes of the mesh that lie on the boundary Γ_e, the subscript q in the equation (5.12) will take the values $q = 1, 2, ..., K$, where K is the total number of nodes in the domain. Equation (5.12) can be applied for every node in the domain Ω_e, and the resulting matrix equations can be written in the following compact form

$$\{v^*\}^e = [G^*]^e \left\{\hat{Q}\right\}^e - [H^*]^e \{v\}^e + [D^*]^e \left(\left\{\hat{t}\right\}^e + \{F\}^e\right) \tag{5.13}$$

where the vectors $\{v\}^e$, $\left\{\hat{Q}\right\}^e$, $\left\{\hat{t}\right\}^e$ and $\{F\}^e$ have been defined in (5.9) and (5.10), and the vector $\{v^*\}^e$ is composed of the displacement vectors of all the nodes inside Ω_e, *i.e.*,

$$\{v^*\}^e = \begin{Bmatrix} \{v^*\}_1 \\ \{v^*\}_2 \\ \vdots \\ \{v^*\}_K \end{Bmatrix}^e . \tag{5.14}$$

The coefficient matrices $[G^*]^e$ and $[H^*]^e$ with dimensions $6K \times 6N_b$ have the same structure as the corresponding matrices for the boundary nodal points which are given in equations (5.11). The coefficient matrix $[D^*]^e$ with dimensions $6K \times 6N_d$ is constructed in the same way as the matrix $[D]^e$ of equation (5.8).

The generalized displacement vector for the $(N_d - K)$ nodes of the finite element mesh that lie on the boundary Γ_e can be obtained by applying the matrix equations (5.4) or (5.7) at these points. However, it is more convenient and there is no loss of generality to assume that these $(N_d - K)$ nodes coincide with nodal points of the boundary element model (Figure 5.1). In this case the nodal displacements of all the nodes on the boundary and in the domain of the discretized layer are evaluated using equations (5.8) and (5.13), respectively.

These two matrix equations fully describe the typical numerical layer and they can be seen as the element equations of a model for which each numerical layer is one super-element. The solution of the boundary value problem for a single layer is obtained from equation (5.8). In this case we do not have to discretize the whole domain Ω_e into triangular elements, but only that part of it on which there are externally applied tractions and/or body forces. Equation (5.8) constitutes a system of $6N_b$ simultaneous linear algebraic equations in $12N_b$ unknowns (boundary tractions and displacements). The additional $6N_b$ equations, which are required to establish the unknowns, are extracted from the imposed boundary conditions ($6N_b$ nodal values). The system of $6N_b$ equations can be solved to obtain the remaining boundary data, and the displacements at points in the domain may then be evaluated from equations (5.12) or (5.13).

5.3 BOUNDARY ELEMENT MODEL FOR A MULTILAYERED SYSTEM

5.3–1 Boundary Conditions at the Interfaces of the Layers

Consider now a multilayered system which is divided into L numerical layers through its thickness. These layers are numbered consecutively with direction from the bottom to the top of the multilayered system. The boundaries and the domains of all the numerical layers are discretized into boundary elements and domain elements, respectively, as it was presented for the case of a single layer. Each of the boundaries Γ_e $(e = 1, 2, ..., L)$ is divided into N_b boundary elements, and each of the domains Ω_e is divided into M triangular elements with N_d nodal points in the mesh. The boundary and domain discretization is identical for all the layers.

The boundary displacements for each layer are given in equations (5.8) in terms of the boundary tractions, the body forces and the surface tractions. These equations, however, cannot be solved independently for the unknown boundary quantities, due to the following two reasons: first, the boundary conditions are not known explicitly at the element level, but they are prescribed at the side surface of the multilayered system (global system), and second, the surface tractions at the interfaces between numerical layers are also not known. There are, though, additional conditions, *continuity conditions*, that must be satisfied at these interfaces, and they are established from the following physical considerations:

(i) *Equilibrium at the interface.* The surface tractions at the interface separating two different numerical layers are equal in magnitude and opposite in direction, in the absence of externally applied loads

at these planes. Their vector sum is equal to the external load in the presence of body forces.

(ii) *Equilibrium on the boundary.* The boundary tractions developed on the common boundary between two layers have to balance the externally applied tractions along this boundary.

(iii) *Displacement continuity.* The displacements at any point, either on the boundary or in the domain, of the interface between adjacent layers remain continuous across the interface. It is assumed that the layers are firmly bonded together and that there is no delamination.

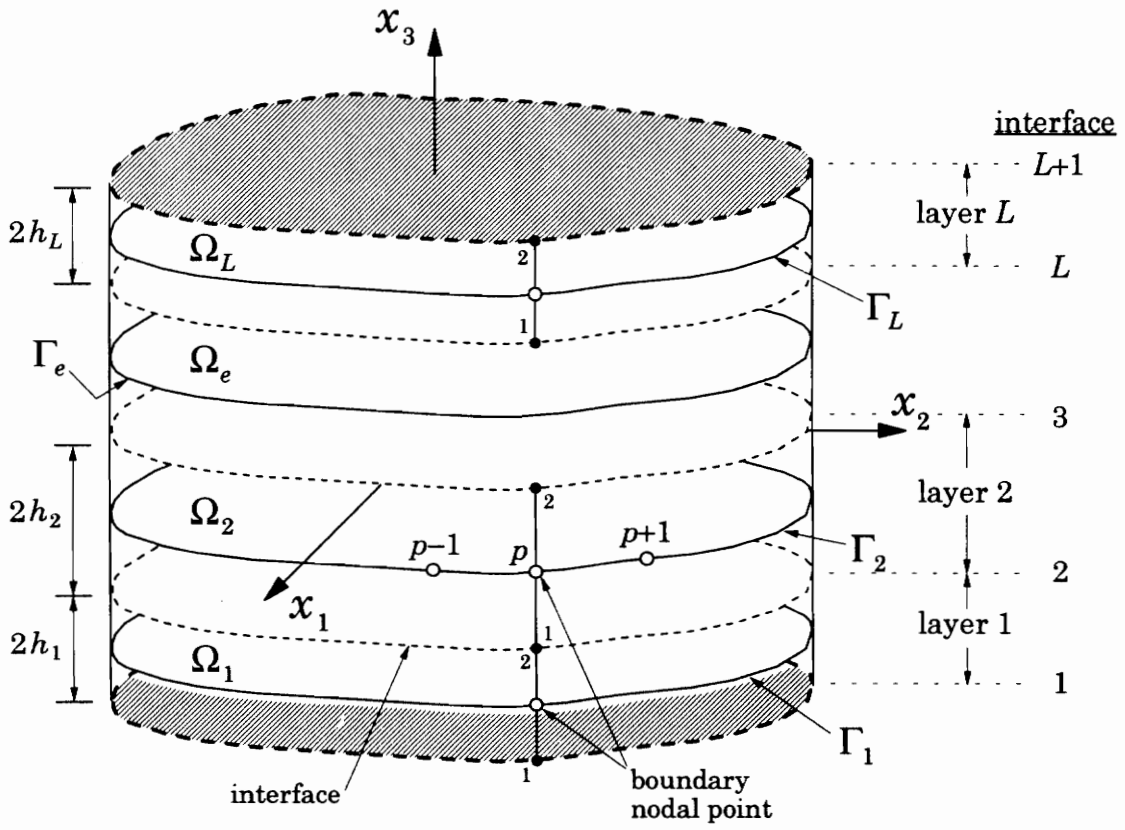

Figure 5.2 Multilayered system divided into L numerical layers.

In order to express the continuity conditions in algebraic form, we need first to introduce a new notation for the vectors and matrices of equations (5.8) and (5.13). In this new notation it is assumed that for each layer all the nodal displacements associated with the bottom surface of the layer are placed in the upper half of the corresponding vector of generalized displacements, while all the nodal displacements associated with the top surface of the layer are placed in the lower half of the vector, and in the same order as those of the upper half. For example, the new vectors for the displacements at boundary nodal point p and the generalized displacements for all the boundary nodal points of the layer will have the following forms,

$$\{v\}_p = \begin{Bmatrix} v_1^1 \\ v_2^1 \\ v_3^1 \\ --- \\ v_1^2 \\ v_2^2 \\ v_3^2 \end{Bmatrix}_p = \begin{Bmatrix} \{v^1\}_p \\ --- \\ \{v^2\}_p \end{Bmatrix} \quad \text{and} \quad \{v\}^e = \begin{Bmatrix} \{v^1\}_1 \\ \{v^1\}_2 \\ \vdots \\ \{v^1\}_{N_b} \\ --- \\ \{v^2\}_1 \\ \{v^2\}_2 \\ \vdots \\ \{v^2\}_{N_b} \end{Bmatrix}^e = \begin{Bmatrix} \{v\}_1^e \\ --- \\ \{v\}_2^e \end{Bmatrix}, \quad (5.15)$$

respectively (Figure 5.2). The same concept applies to the rearrangement of terms in the generalized vectors $\{v^*\}^e$, $\left\{\hat{Q}\right\}^e$, $\left\{\hat{t}\right\}^e$, and $\{F\}^e$, and all the coefficient matrices in equations (5.8) and (5.13). The revised forms of these two equations are given below,

$$\frac{1}{2}\begin{Bmatrix} \{v\}_1^e \\ \{v\}_2^e \end{Bmatrix} = \begin{bmatrix} [G]_{11}^e & [G]_{12}^e \\ [G]_{21}^e & [G]_{22}^e \end{bmatrix} \begin{Bmatrix} \left\{\hat{Q}\right\}_1^e \\ \left\{\hat{Q}\right\}_2^e \end{Bmatrix} - \begin{bmatrix} [H]_{11}^e & [H]_{12}^e \\ [H]_{21}^e & [H]_{22}^e \end{bmatrix} \begin{Bmatrix} \{v\}_1^e \\ \{v\}_2^e \end{Bmatrix}$$

$$+ \begin{bmatrix} [D]_{11}^e & [D]_{12}^e \\ [D]_{21}^e & [D]_{22}^e \end{bmatrix} \left(\begin{Bmatrix} \left\{\hat{t}\right\}_1^e \\ \left\{\hat{t}\right\}_2^e \end{Bmatrix} + \begin{Bmatrix} \{F\}_1^e \\ \{F\}_2^e \end{Bmatrix} \right) \quad (5.16)$$

$$\begin{Bmatrix} \{v^*\}_1^e \\ \{v^*\}_2^e \end{Bmatrix} = \begin{bmatrix} [G^*]_{11}^e & [G^*]_{12}^e \\ [G^*]_{21}^e & [G^*]_{22}^e \end{bmatrix} \begin{Bmatrix} \{\hat{Q}\}_1^e \\ \{\hat{Q}\}_2^e \end{Bmatrix} - \begin{bmatrix} [H^*]_{11}^e & [H^*]_{12}^e \\ [H^*]_{21}^e & [H^*]_{22}^e \end{bmatrix} \begin{Bmatrix} \{v\}_1^e \\ \{v\}_2^e \end{Bmatrix}$$

$$+ \begin{bmatrix} [D^*]_{11}^e & [D^*]_{12}^e \\ [D^*]_{21}^e & [D^*]_{22}^e \end{bmatrix} \left(\begin{Bmatrix} \{\hat{t}\}_1^e \\ \{\hat{t}\}_2^e \end{Bmatrix} + \begin{Bmatrix} \{F\}_1^e \\ \{F\}_2^e \end{Bmatrix} \right) \tag{5.17}$$

where the superscript e denotes the numerical layer and it is $e = 1, 2, ..., L$. Both equations have been partitioned with respect to nodal quantities on the bottom (subscript 1) and top (subscript 2) surfaces of the layer (Figure 5.2), and they incorporate the new notation for the generalized vectors. The dimensions of matrices $[H]_{IJ}^e$ and $[G]_{IJ}^e$ are $3N_b \times 3N_b$, where the indices $I, J = 1, 2$, the dimensions of $[H^*]_{IJ}^e$ and $[G^*]_{IJ}^e$ are $3N_d \times 3N_b$, and the dimensions of $[D]_{IJ}^e$ and $[D^*]_{IJ}^e$ are $3N_b \times 3N_d$ and $3N_d \times 3N_d$, respectively. The vectors $\{v\}_I^e$ and $\left\{\hat{Q}\right\}_I^e$ of the boundary displacements and tractions have dimensions $3N_b \times 1$, while the vectors $\{v^*\}_I^e$ and $\left\{\hat{t}\right\}_I^e$ of the domain nodal quantities have dimensions $3N_d \times 1$.

The boundary tractions $\left\{\hat{Q}\right\}_I^e$ and the surface tractions $\left\{\hat{t}\right\}_I^e$ represent all the prescribed loads at boundary and domain nodal points of the bottom ($I = 1$) and top ($I = 2$) surface of a single layer. In a multilayered system, however, these quantities will not be known since they are going to be the *internal tractions* (also called *interlaminar tractions*) developed at the interface between adjacent layers. Actually, what will be known, are the external loads applied at the global nodes which are the common nodes on the interface between the layers. It is therefore, more convenient to make reference to the tractions using the number of the interface instead of using the number of the layer. For this reason, it is necessary to revise the notation for the tractions and define as $\{t\}_e$ the internal boundary tractions on the e-th interface, *i.e.* the top surface of the $(e-1)$-th layer, and accordingly, define as $\{s\}_e$ the

internal surface tractions at domain points of the same interface. The externally applied loads at boundary nodal points of the e-th interface will be denoted by $\{q\}_e$, while, the external loads at domain nodal points they will be denoted by $\{p\}_e$. For these four vectors, the subscript e takes the values $e = 1, 2, ..., (L+1)$ since it refers to the interface and not to the layer. The aforementioned definitions can be expressed mathematically in the following way

$$\left\{\hat{Q}\right\}_2^{e-1} = \{t\}_e \qquad \text{and} \qquad \left\{\hat{t}\right\}_2^{e-1} = \{s\}_e \,, \tag{5.18a,b}$$

where $e = 2, 3, ..., L$ denotes the interface between adjacent numerical layers.

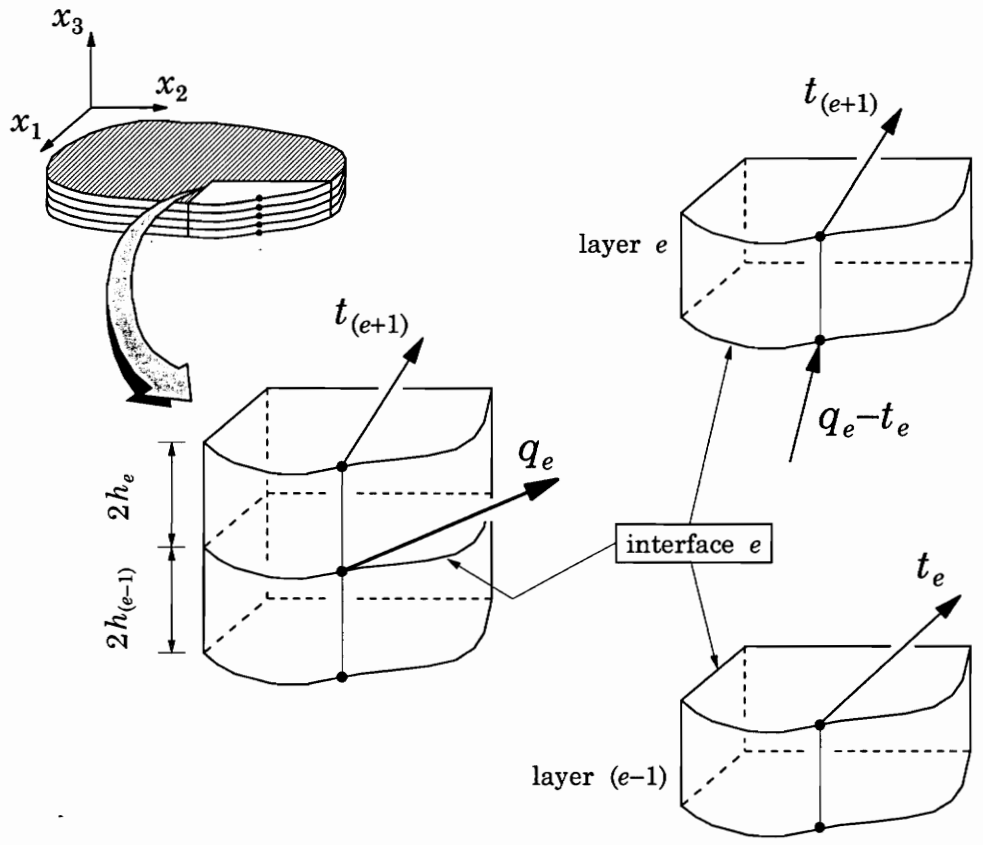

Figure 5.3 Traction equilibrium conditions at *boundary* nodal points on the e-th interface of the multilayered system.

The equilibrium conditions along the boundary of the e-th interface between the layers $(e-1)$ and e are written as

$$\left\{\hat{Q}\right\}_2^{e-1} + \left\{\hat{Q}\right\}_1^{e} = \{q\}_e \tag{5.19}$$

where $\{q\}_e$ is the vector of the external loads applied at all the boundary nodes of the e-th interface. These nodal equilibrium conditions are depicted graphically in Figure 5.3. The equilibrium conditions at the common domain nodes of the $(e-1)$ and e layers have the form

$$\left\{\hat{t}\right\}_2^{e-1} + \left\{\hat{t}\right\}_1^{e} = \{p\}_e \tag{5.20}$$

where $\{p\}_e$ are the prescribed nodal tractions on e-th interface (Figure 5.4).

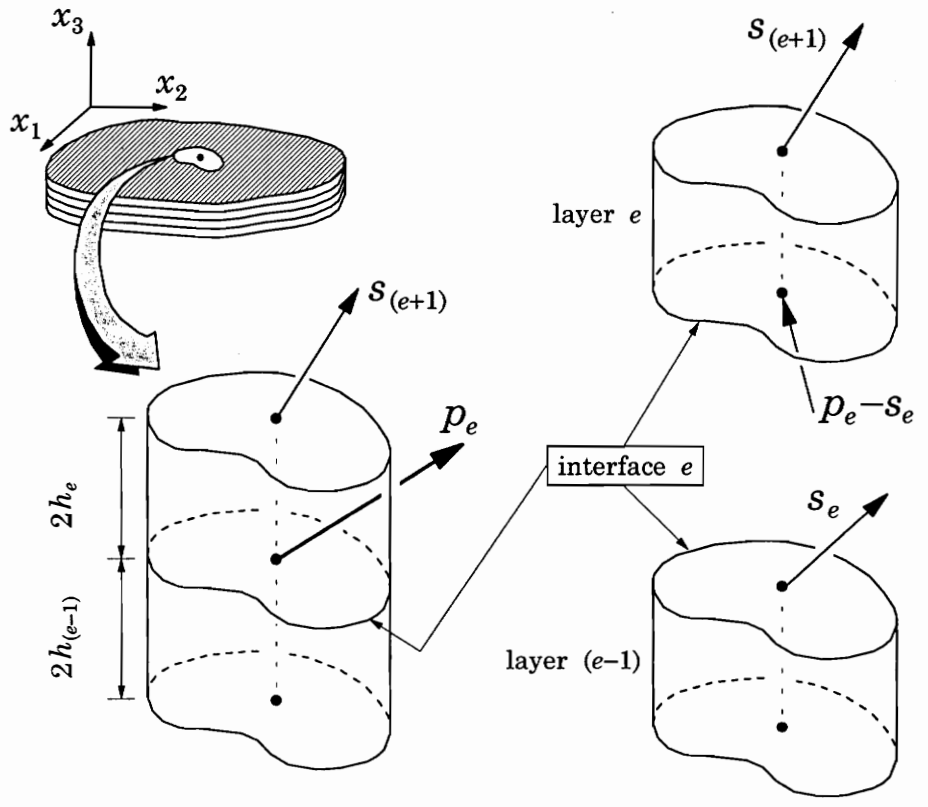

Figure 5.4 Traction equilibrium conditions at *domain* nodal points on the e-th interface of the multilayered system.

The conditions (5.20) are imposed on all nodal points of the domain mesh, and because, the triangular mesh is the same for all the layers and the linear approximation of the surface tractions (equation 5.2) is utilized for all the triangular elements, the traction equilibrium condition holds at any point of the interface. Using the definitions (5.18) into equations (5.19) and (5.20), we derive the following expressions for the surface and boundary tractions at points of the lower surface of each layer ($e = 2, 3, ..., L$)

$$\left\{\hat{t}\right\}_1^e = \{p\}_e - \{s\}_e \tag{5.21a}$$

and

$$\left\{\hat{Q}\right\}_1^e = \{q\}_e - \{t\}_e \ . \tag{5.21b}$$

The generalized nodal tractions at the bottom surface of the multilayered system, which is the first interface ($e = 1$), are

$$\left\{\hat{Q}\right\}_1^1 = \{q\}_1 \quad \text{and} \quad \left\{\hat{t}\right\}_1^1 = \{p\}_1 \ , \tag{5.22a,b}$$

for boundary and domain nodes, respectively. For nodal points on the top surface (interface $e = L + 1$), the tractions are

$$\left\{\hat{Q}\right\}_2^L = \{q\}_{L+1} \quad \text{and} \quad \left\{\hat{t}\right\}_2^L = \{p\}_{L+1} \ . \tag{5.23a,b}$$

The algebraic expressions of the displacement continuity conditions and the revised notation for the generalized displacement vectors are

$$\{v\}_2^{e-1} = \{v\}_1^e = \{u\}_e \tag{5.24a}$$

and

$$\{v^*\}_2^{e-1} = \{v^*\}_1^e = \{u^*\}_e \ , \tag{5.24b}$$

where $e = 2, 3, ..., L$, and the superscript of the v-vectors denotes the layer, while the subscript of the u-vectors denotes the interface. The generalized vectors $\{u\}_e$ and $\{u^*\}_e$ are the boundary and domain nodal displacements at the e-th interface. If the physical layers are not firmly bonded together and

delamination is allowed in the model, then the displacement vectors $\{v\}_2^{e-1}$ and $\{v^*\}_2^{e-1}$ of the $(e-1)$-th layer and the displacement vectors $\{v\}_1^e$ and $\{v^*\}_1^e$ of the e-th layer will not satisfy the continuity conditions, but they are going to be both unknown and, along with the corresponding nodal tractions, they will have to satisfy conditions that describe separation (debonding), slip and friction between the layers at the e-th interface. The displacements at nodal points of the bottom and top surface of the multilayered system are defined as

$$\{v\}_1^1 = \{u\}_1 \ , \quad \{v^*\}_1^1 = \{u^*\}_1 \ , \tag{5.25a,b}$$

and

$$\{v\}_2^L = \{u\}_{L+1} \ , \quad \{v^*\}_2^L = \{u^*\}_{L+1} \ , \tag{5.26a,b}$$

respectively.

At every *boundary nodal point* of the e-th interface $(e = 1, 2, ..., L+1)$ and along each of the three directions x_i, there is, generally, only one prescribed quantity, either the displacement or the traction component, and the other component is unknown. Thus, if an entry of the vector $\{q\}_e$ is prescribed, the corresponding entry of vector $\{u\}_e$ will be unknown, and vice versa. The same conditions also apply for the *domain nodal points* of the top and bottom surface of the multilayered system, *i.e.* interfaces 1 and $(L+1)$, if the surfaces are free and there are no internal supports or elastic foundations. In the case of elastically supported plates, or plates on elastic foundations, both the displacements and the tractions will be unknown on the bottom surface. Even so, they will be related through additional equations which are the constitutive relations of the springs,

$$[\alpha_b]\{u\}_1 + [\beta_b]\{p\}_1 = \{\gamma_b\} \tag{5.27a}$$

and

$$[\alpha_d]\{u^*\}_1 + [\beta_d]\{q\}_1 = \{\gamma_d\}, \tag{5.27b}$$

where the matrices $[\alpha]$, $[\beta]$ and $\{\gamma\}$ represent the properties of the supporting foundation, and the subscripts b and d denote boundary or domain nodal points, respectively. Equations (5.27) are general and they may be applied for any type of support conditions at the bottom face of the plate, and in a similar way, they may also be applied for the top surface, where the subscript of the generalized vectors becomes $L+1$.

5.3–2 Equilibrium Equations for the Numerical Layers

Equation (5.16) is used to express the boundary displacements of each numerical layer of the system in terms of the boundary quantities of this layer (*i.e.* displacements and tractions), the internal tractions at its two faces and the body forces. Equation (5.17) relates the displacements at domain nodal points on the faces of the layer to all the aforementioned quantities. These two equations may also be viewed as equilibrium equations for the e-th numerical layer of the multilayered system. Introducing into (5.16) and (5.17) the new notation and the continuity conditions for the nodal tractions from equations (5.18) and (5.21), and also for the nodal displacements from equations (5.24), the equilibrium equations will be expressed in a matrix form as

$$\begin{bmatrix} [\hat{\mathrm{H}}]^e_{11} & [\hat{\mathrm{H}}]^e_{12} \\ [\hat{\mathrm{H}}]^e_{21} & [\hat{\mathrm{H}}]^e_{22} \end{bmatrix} \begin{Bmatrix} \{u\}_e \\ \{u\}_{e+1} \end{Bmatrix} - \begin{bmatrix} [\mathrm{G}]^e_{11} & [\mathrm{G}]^e_{12} \\ [\mathrm{G}]^e_{21} & [\mathrm{G}]^e_{22} \end{bmatrix} \begin{Bmatrix} \{q\}_e - \{t\}_e \\ \{t\}_{e+1} \end{Bmatrix}$$

$$- \begin{bmatrix} [\mathrm{D}]^e_{11} & [\mathrm{D}]^e_{12} \\ [\mathrm{D}]^e_{21} & [\mathrm{D}]^e_{22} \end{bmatrix} \left(\begin{Bmatrix} \{p\}_e - \{s\}_e \\ \{s\}_{e+1} \end{Bmatrix} + \begin{Bmatrix} \{F\}^e_1 \\ \{F\}^e_2 \end{Bmatrix} \right) = \begin{Bmatrix} \{0\} \\ \{0\} \end{Bmatrix} \tag{5.28}$$

$$\begin{bmatrix} [\mathrm{H}^*]^e_{11} & [\mathrm{H}^*]^e_{12} \\ [\mathrm{H}^*]^e_{21} & [\mathrm{H}^*]^e_{22} \end{bmatrix} \begin{Bmatrix} \{u\}_e \\ \{u\}_{e+1} \end{Bmatrix} - \begin{bmatrix} [\mathrm{G}^*]^e_{11} & [\mathrm{G}^*]^e_{12} \\ [\mathrm{G}^*]^e_{21} & [\mathrm{G}^*]^e_{22} \end{bmatrix} \begin{Bmatrix} \{q\}_e - \{t\}_e \\ \{t\}_{e+1} \end{Bmatrix}$$

$$- \begin{bmatrix} [\mathrm{D}^*]^e_{11} & [\mathrm{D}^*]^e_{12} \\ [\mathrm{D}^*]^e_{21} & [\mathrm{D}^*]^e_{22} \end{bmatrix} \left(\begin{Bmatrix} \{p\}_e - \{s\}_e \\ \{s\}_{e+1} \end{Bmatrix} + \begin{Bmatrix} \{F\}^e_1 \\ \{F\}^e_2 \end{Bmatrix} \right) = - \begin{Bmatrix} \{u^*\}_e \\ \{u^*\}_{e+1} \end{Bmatrix} \tag{5.29}$$

where e refers to the typical numerical layer having values $e = 2, 3, ..., (L-1)$. In equation (5.28) the matrix $\left[\hat{\mathrm{H}}\right]^e$ is defined as

$$\left[\hat{\mathrm{H}}\right]^e = [\mathrm{H}]^e + \tfrac{1}{2}[\mathrm{I}] \tag{5.30a}$$

or

$$\begin{bmatrix} [\hat{\mathrm{H}}]^e_{11} & [\hat{\mathrm{H}}]^e_{12} \\ [\hat{\mathrm{H}}]^e_{21} & [\hat{\mathrm{H}}]^e_{22} \end{bmatrix} = \begin{bmatrix} [\mathrm{H}]^e_{11} & [\mathrm{H}]^e_{12} \\ [\mathrm{H}]^e_{21} & [\mathrm{H}]^e_{22} \end{bmatrix} + \frac{1}{2}\begin{bmatrix} [\mathrm{I}] & [0] \\ [0] & [\mathrm{I}] \end{bmatrix} \tag{5.30b}$$

where [I] is the identity matrix with dimensions $3N_b \times 3N_b$. The equilibrium equations for the first ($e = 1$) and last ($e = L$) layer are going to be slightly different, because the nodal quantities for these layers have separate definitions, which are given in equations (5.22) and (5.23) for the tractions, and (5.25) and (5.26) for the displacements, and also the boundary conditions correspond to a free surface and not to a common interface between layers. Therefore, equation (5.16) may be written for the end layers of the system as

$$\begin{bmatrix} [\hat{\mathrm{H}}]^1_{11} & [\hat{\mathrm{H}}]^1_{12} \\ [\hat{\mathrm{H}}]^1_{21} & [\hat{\mathrm{H}}]^1_{22} \end{bmatrix} \begin{Bmatrix} \{u\}_1 \\ \{u\}_2 \end{Bmatrix} - \begin{bmatrix} [\mathrm{G}]^1_{11} & [\mathrm{G}]^1_{12} \\ [\mathrm{G}]^1_{21} & [\mathrm{G}]^1_{22} \end{bmatrix} \begin{Bmatrix} \{q\}_1 \\ \{t\}_2 \end{Bmatrix}$$
$$- \begin{bmatrix} [\mathrm{D}]^1_{11} & [\mathrm{D}]^1_{12} \\ [\mathrm{D}]^1_{21} & [\mathrm{D}]^1_{22} \end{bmatrix} \left(\begin{Bmatrix} \{p\}_1 \\ \{s\}_2 \end{Bmatrix} + \begin{Bmatrix} \{F\}^1_1 \\ \{F\}^1_2 \end{Bmatrix} \right) = \begin{Bmatrix} \{0\} \\ \{0\} \end{Bmatrix} \tag{5.31a}$$

$$\begin{bmatrix} [\hat{\mathrm{H}}]^L_{11} & [\hat{\mathrm{H}}]^L_{12} \\ [\hat{\mathrm{H}}]^L_{21} & [\hat{\mathrm{H}}]^L_{22} \end{bmatrix} \begin{Bmatrix} \{u\}_L \\ \{u\}_{L+1} \end{Bmatrix} - \begin{bmatrix} [\mathrm{G}]^L_{11} & [\mathrm{G}]^L_{12} \\ [\mathrm{G}]^L_{21} & [\mathrm{G}]^L_{22} \end{bmatrix} \begin{Bmatrix} \{q\}_L - \{t\}_L \\ \{q\}_{L+1} \end{Bmatrix}$$
$$- \begin{bmatrix} [\mathrm{D}]^L_{11} & [\mathrm{D}]^L_{12} \\ [\mathrm{D}]^L_{21} & [\mathrm{D}]^L_{22} \end{bmatrix} \left(\begin{Bmatrix} \{p\}_L - \{s\}_L \\ \{p\}_{L+1} \end{Bmatrix} + \begin{Bmatrix} \{F\}^L_1 \\ \{F\}^L_2 \end{Bmatrix} \right) = \begin{Bmatrix} \{0\} \\ \{0\} \end{Bmatrix} \tag{5.31b}$$

while, for the same layers, equation (5.17) takes the following form

$$\begin{bmatrix} [\mathrm{H}^*]^1_{11} & [\mathrm{H}^*]^1_{12} \\ [\mathrm{H}^*]^1_{21} & [\mathrm{H}^*]^1_{22} \end{bmatrix} \begin{Bmatrix} \{u\}_1 \\ \{u\}_2 \end{Bmatrix} - \begin{bmatrix} [\mathrm{G}^*]^1_{11} & [\mathrm{G}^*]^1_{12} \\ [\mathrm{G}^*]^1_{21} & [\mathrm{G}^*]^1_{22} \end{bmatrix} \begin{Bmatrix} \{q\}_1 \\ \{t\}_2 \end{Bmatrix} -$$

$$-\begin{bmatrix} [D^*]^1_{11} & [D^*]^1_{12} \\ [D^*]^1_{21} & [D^*]^1_{22} \end{bmatrix} \left(\begin{Bmatrix} \{p\}_1 \\ \{s\}_2 \end{Bmatrix} + \begin{Bmatrix} \{F\}^1_1 \\ \{F\}^1_2 \end{Bmatrix} \right) = -\begin{Bmatrix} \{u^*\}_1 \\ \{u^*\}_2 \end{Bmatrix} \tag{5.32a}$$

$$\begin{bmatrix} [H^*]^L_{11} & [H^*]^L_{12} \\ [H^*]^L_{21} & [H^*]^L_{22} \end{bmatrix} \begin{Bmatrix} \{u\}_L \\ \{u\}_{L+1} \end{Bmatrix} - \begin{bmatrix} [G^*]^L_{11} & [G^*]^L_{12} \\ [G^*]^L_{21} & [G^*]^L_{22} \end{bmatrix} \begin{Bmatrix} \{q\}_L - \{t\}_L \\ \{q\}_{L+1} \end{Bmatrix}$$
$$-\begin{bmatrix} [D^*]^L_{11} & [D^*]^L_{12} \\ [D^*]^L_{21} & [D^*]^L_{22} \end{bmatrix} \left(\begin{Bmatrix} \{p\}_L - \{s\}_L \\ \{p\}_{L+1} \end{Bmatrix} + \begin{Bmatrix} \{F\}^L_1 \\ \{F\}^L_2 \end{Bmatrix} \right) = -\begin{Bmatrix} \{u^*\}_L \\ \{u^*\}_{L+1} \end{Bmatrix} \tag{5.32b}$$

Equations (5.28), (5.29), (5.31) and (5.32) are the equilibrium equations for all the numerical layers in the system, and if they are combined with the prescribed conditions at the boundary nodal points of all the interfaces and at the domain nodes of the bottom and top surfaces of the plate, they will form a system of linear algebraic equations which can be solved for the unknown quantities. These quantities are: the nodal tractions and displacements at the interfaces between the numerical layers, and the boundary displacements or tractions depending on the support conditions. However, if there is no interest in finding the displacements at domain nodal points, or if it is required to reduce the dimensions of the system of equations, then the displacements $\{u^*\}_e$ may be eliminated by combining equations (5.29) of two consecutive layers. If this operation is repeated for all the $(L-1)$ common interfaces of the layers, we will obtain equations that involve, from the group of domain quantities, only the tractions at the interfaces, and the displacements at the top and bottom surface of the multilayered system. The resulting reduced system of linear algebraic equations can be solved using either standard methods, if the number of unknowns is relatively small, or by employing special iterative solvers, if the number of unknowns becomes very large. In the next section, we are going to present in detail the formulation of the reduced system of equations and produce the matrix equations that will eventually yield the numerical solution.

5.3–3 Continuity Equations at the Domain Nodal Points

The equilibrium equations of each numerical layer are given, for nodal points in the domain of the layer, in equations (5.29) and (5.32). Equation (5.29) applies for layers $e = 2, 3, ..., (L-1)$, while equation (5.32) applies for the first and last layer in the model ($e = 1, L$). If equation (5.29) is written for the adjacent layers $(e-1)$ and e, then it becomes apparent that the generalized displacement vector $\{u^*\}_e$ is expressed, in one equation in terms of the vectors associated with the $(e-1)$-th layer, and in the other equation in terms of the vectors of the e-th layer. Equating the two expressions of the nodal displacements $\{u^*\}_e$, we obtain the following equation for the domain nodal points on the e-th interface

$$
\begin{aligned}
&\left[\, [\mathrm{H}^*]_{21}^{e-1} \quad \left([\mathrm{H}^*]_{22}^{e-1} - [\mathrm{H}^*]_{11}^{e}\right) \quad -[\mathrm{H}^*]_{12}^{e} \,\right] \begin{Bmatrix} \{u\}_{e-1} \\ \{u\}_e \\ \{u\}_{e+1} \end{Bmatrix} \\
&+\left[\, [\mathrm{G}^*]_{21}^{e-1} \quad -\left([\mathrm{G}^*]_{22}^{e-1} + [\mathrm{G}^*]_{11}^{e}\right) \quad [\mathrm{G}^*]_{12}^{e} \,\right] \begin{Bmatrix} \{t\}_{e-1} \\ \{t\}_e \\ \{t\}_{e+1} \end{Bmatrix} \\
&+\left[\, [\mathrm{D}^*]_{21}^{e-1} \quad -\left([\mathrm{D}^*]_{22}^{e-1} + [\mathrm{D}^*]_{11}^{e}\right) \quad [\mathrm{D}^*]_{12}^{e} \,\right] \begin{Bmatrix} \{s\}_{e-1} \\ \{s\}_e \\ \{s\}_{e+1} \end{Bmatrix} \\
&= \left[\, [\mathrm{G}^*]_{21}^{e-1} \quad -[\mathrm{G}^*]_{11}^{e} \,\right] \begin{Bmatrix} \{q\}_{e-1} \\ \{q\}_e \end{Bmatrix} + \left[\, [\mathrm{D}^*]_{21}^{e-1} \quad -[\mathrm{D}^*]_{11}^{e} \,\right] \begin{Bmatrix} \{p\}_{e-1} \\ \{p\}_e \end{Bmatrix} \\
&+\left[\, [\mathrm{D}^*]_{21}^{e-1} \quad [\mathrm{D}^*]_{22}^{e-1} \quad -[\mathrm{D}^*]_{11}^{e} \quad -[\mathrm{D}^*]_{12}^{e} \,\right] \begin{Bmatrix} \{F\}_1^{e-1} \\ \{F\}_2^{e-1} \\ \{F\}_1^{e} \\ \{F\}_2^{e} \end{Bmatrix}
\end{aligned}
\tag{5.33}
$$

where $e = 3, 4, ..., (L-1)$. Equation (5.33) represents physically, the equilibrium of the layers at points in the domain and, at the same time, ensures the continuity of the displacements at the interface between adjacent layers. The corresponding equations on the 2-nd and L-th interface of the multilayered system are obtained using (5.32a) and (5.32b), and also equation (5.29) for layers $e = 2$ and $e = L-1$. The resulting matrix equation for the interface with number 2 is,

$$\begin{aligned}
&\left[\, [\mathrm{H}^*]^1_{21} \quad \left([\mathrm{H}^*]^1_{22} - [\mathrm{H}^*]^2_{11}\right) \quad -[\mathrm{H}^*]^2_{12} \,\right] \begin{Bmatrix} \{u\}_1 \\ \{u\}_2 \\ \{u\}_3 \end{Bmatrix} \\
&+ \left[\, -\left([\mathrm{G}^*]^1_{22} + [\mathrm{G}^*]^2_{11}\right) \quad [\mathrm{G}^*]^2_{12} \,\right] \begin{Bmatrix} \{t\}_2 \\ \{t\}_3 \end{Bmatrix} \\
&+ \left[\, -\left([\mathrm{D}^*]^1_{22} + [\mathrm{D}^*]^2_{11}\right) \quad [\mathrm{D}^*]^2_{12} \,\right] \begin{Bmatrix} \{s\}_2 \\ \{s\}_3 \end{Bmatrix} \\
&= \left[\, [\mathrm{G}^*]^1_{21} \quad -[\mathrm{G}^*]^2_{11} \,\right] \begin{Bmatrix} \{q\}_1 \\ \{q\}_2 \end{Bmatrix} + \left[\, [\mathrm{D}^*]^1_{21} \quad -[\mathrm{D}^*]^2_{11} \,\right] \begin{Bmatrix} \{p\}_1 \\ \{p\}_2 \end{Bmatrix} \\
&+ \left[\, [\mathrm{D}^*]^1_{21} \quad [\mathrm{D}^*]^1_{22} \quad -[\mathrm{D}^*]^2_{11} \quad -[\mathrm{D}^*]^2_{12} \,\right] \begin{Bmatrix} \{F\}^1_1 \\ \{F\}^1_2 \\ \{F\}^2_1 \\ \{F\}^2_2 \end{Bmatrix}
\end{aligned} \tag{5.34}$$

while the equation for interface L is

$$\begin{aligned}
&\left[\, [\mathrm{H}^*]^{L-1}_{21} \quad \left([\mathrm{H}^*]^{L-1}_{22} - [\mathrm{H}^*]^L_{11}\right) \quad -[\mathrm{H}^*]^L_{12} \,\right] \begin{Bmatrix} \{u\}_{L-1} \\ \{u\}_L \\ \{u\}_{L+1} \end{Bmatrix} \\
&+ \left[\, [\mathrm{G}^*]^{L-1}_{21} \quad -\left([\mathrm{G}^*]^{L-1}_{22} + [\mathrm{G}^*]^L_{11}\right) \,\right] \begin{Bmatrix} \{t\}_{L-1} \\ \{t\}_L \end{Bmatrix} +
\end{aligned}$$

$$+\left[\begin{array}{cc} [D^*]_{21}^{L-1} & -\left([D^*]_{22}^{L-1}+[D^*]_{11}^{L}\right)\end{array}\right]\left\{\begin{array}{c}\{s\}_{L-1}\\ \{s\}_{L}\end{array}\right\}$$

$$=\left[\begin{array}{ccc} [G^*]_{21}^{L-1} & -[G^*]_{11}^{L} & -[D^*]_{12}^{L}\end{array}\right]\left\{\begin{array}{c}\{q\}_{L-1}\\ \{q\}_{L}\\ \{q\}_{L+1}\end{array}\right\}$$

$$+\left[\begin{array}{ccc} [D^*]_{21}^{L-1} & -[D^*]_{11}^{L} & -[G^*]_{12}^{L}\end{array}\right]\left\{\begin{array}{c}\{p\}_{L-1}\\ \{p\}_{L}\\ \{p\}_{L+1}\end{array}\right\}$$

$$+\left[\begin{array}{cccc} [D^*]_{21}^{L-1} & [D^*]_{22}^{L-1} & -[D^*]_{11}^{L} & -[D^*]_{12}^{L}\end{array}\right]\left\{\begin{array}{c}\{F\}_{1}^{L-1}\\ \{F\}_{2}^{L-1}\\ \{F\}_{1}^{L}\\ \{F\}_{2}^{L}\end{array}\right\}. \qquad (5.35)$$

In forming the reduced system of equations, we must retain the two equations for the end interfaces (numbered as 1 and $L+1$), which are included in (5.32) and were not utilized in the construction of equations (5.33), (5.34) and (5.35). These two equations express the generalized displacements at nodal points of the domain mesh for the bottom surface of the first layer and the top surface of the last layer in terms of the other domain quantities and all the boundary nodal quantities of the corresponding layers. These relations may be written again in the following form

$$\left[\begin{array}{cc} [H^*]_{11}^{1} & [H^*]_{12}^{1}\end{array}\right]\left\{\begin{array}{c}\{u\}_1\\ \{u\}_2\end{array}\right\}-[G^*]_{12}^{1}\{t\}_2-[D^*]_{12}^{1}\{s\}_2+\{u^*\}_1$$

$$=[G^*]_{11}^{1}\{q\}_1+[D^*]_{11}^{1}\{p\}_1+\left[\begin{array}{cc} [D^*]_{11}^{1} & [D^*]_{12}^{1}\end{array}\right]\left\{\begin{array}{c}\{F\}_{1}^{1}\\ \{F\}_{2}^{1}\end{array}\right\}, \qquad (5.36)$$

and

$$\left[[H^*]^L_{21} \; [H^*]^L_{22} \right] \left\{ \begin{matrix} \{u\}_L \\ \{u\}_{L+1} \end{matrix} \right\} + [G^*]^L_{21} \{t\}_L + [D^*]^L_{21} \{s\}_L + \{u^*\}_{L+1}$$

$$= \left[[G^*]^L_{21} \; [G^*]^L_{22} \right] \left\{ \begin{matrix} \{q\}_L \\ \{q\}_{L+1} \end{matrix} \right\} + \left[[D^*]^L_{21} \; [D^*]^L_{22} \right] \left\{ \begin{matrix} \{p\}_L \\ \{p\}_{L+1} \end{matrix} \right\}$$

$$+ \left[[D^*]^L_{21} \; [D^*]^L_{22} \right] \left\{ \begin{matrix} \{F\}^L_1 \\ \{F\}^L_2 \end{matrix} \right\} . \qquad (5.37)$$

Any boundary conditions associated with the bottom and top faces of the multilayered system will be introduced into the numerical model through the above two equations, and, particularly, through the displacement vectors $\{u\}_1$, $\{u^*\}_1$, $\{u\}_{L+1}$ and $\{u^*\}_{L+1}$, and the traction vectors $\{q\}_1$, $\{p\}_1$, $\{q\}_{L+1}$ and $\{p\}_{L+1}$ of the boundary and domain nodal points on the faces of the discretized system. In the case of plates resting on elastic supports or foundation and plates which are supported also internally (rigid supports) and not only at their side boundaries, equations (5.36) and (5.37) must be properly combined with the boundary conditions (5.27).

5.4 GLOBAL MATRIX EQUATIONS FOR THE MULTILAYERED SYSTEM AND NUMERICAL IMPLEMENTATION

The matrix equations of equilibrium (5.28) and (5.31) derived in Section 5.3–2, and the continuity equations at the interfaces between the layers, which are equations (5.33–37) developed in Section 5.3–3, will be combined to form the global system of equations for the discretized three-dimensional layered plate. The solution of this system will provide all the unknown nodal displacements and interlaminar tractions.

The generalized vectors that appear in the governing matrix equations of the layers and their interfaces are the nodal displacements $\{u\}_e$ and tractions $\{q\}_e$ at the boundaries of the interfaces, where $e = 1, 2, ..., (L+1)$, the tractions $\{t\}_e$ and $\{s\}_e$ at the boundary and domain nodal points of the interfaces $e = 2, 3, ..., L$, the applied nodal loads $\{p\}_e$ at the domain nodes of all the interfaces ($e = 1, 2, ..., L+1$), and the body forces $\{F\}_I^e$ at the faces ($I = 1, 2$) of every numerical layer ($e = 1, 2, ..., L$). Also, at the bottom and top surface of the plate, *i.e.* at interfaces 1 and $(L+1)$, there are two more vectors involved in the continuity equations, the nodal displacements at domain points $\{u^*\}_1$ and $\{u^*\}_{L+1}$. All these generalized vectors are grouped into the following four vectors:

$$\{\tilde{\mathbf{u}}\} = \Big\{\{u\}_1 \ \{t\}_2 \ \{u\}_2 \ \{t\}_3 \ \{u\}_3 \ \{u\}_4 \ \{t\}_4 \ \cdots \ \{t\}_e \ \{u\}_e \ \{t\}_{e+1} \ \{u\}_{e+1} \ \cdots \ \{t\}_{L-1} \ \{u\}_{L-1} \ \{t\}_L \ \{u\}_L \ \{u\}_{L+1}\Big\}^T \tag{5.38}$$

$$\{\mathbf{s}\} = \Big\{\{s\}_2 \ \{s\}_3 \ \{s\}_4 \ \cdots \ \{s\}_e \ \{s\}_{e+1} \ \cdots \ \{s\}_{L-1} \ \{s\}_L\Big\}^T \tag{5.39}$$

$$\{\mathbf{q}\} = \Big\{\{q\}_1 \ \{q\}_2 \ \{q\}_3 \ \cdots \ \{q\}_e \ \{q\}_{e+1} \ \cdots \ \{q\}_L \ \{q\}_{L+1}\Big\}^T \tag{5.40}$$

$$\{\mathbf{p}\} = \Big\{\{p\}_1 \ \{p\}_2 \ \{p\}_3 \ \cdots \ \{p\}_e \ \{p\}_{e+1} \ \cdots \ \{p\}_L \ \{p\}_{L+1}\Big\}^T \tag{5.41}$$

and

$$\{\mathbf{u}^*\} = \Big\{\{u^*\}_1 \ \{u^*\}_{L+1}\Big\}^T \tag{5.42}$$

The entries of vector $\{\tilde{\mathbf{u}}\}$ are placed in the order shown in the above equation, so that the final system of equations, independently of the prescribed boundary conditions, will never contain zero elements in the diagonal of the coefficient matrix. The dimensions of the above vectors are:

Vector	Dimension
$\{\tilde{\mathbf{u}}\}$	$6N_bL$
$\{\mathbf{s}\}$	$3N_d(L-1)$
$\{\mathbf{q}\}$	$3(L+1)N_b$
$\{\mathbf{p}\}$	$3(L+1)N_d$
$\{\mathbf{u}^*\}$	$6N_d$

where L is the number of numerical layers used to model the plate through its thickness, N_b is the number of boundary elements on the boundary of the typical layer and is the same for all the layers, and N_d is the number of nodal points in the domain mesh which is introduced for the numerical evaluation of domain integrals of the surface tractions.

The prescribed conditions of the problem at the boundaries or on the domains of the interfaces will be introduced into the numerical model through the generalized vectors $\{u\}_e$ in $\{\tilde{\mathbf{u}}\}$, the boundary tractions $\{q\}_e$, the domain tractions $\{p\}_e$ and the displacements at nodal points of the bottom and top surface of the layered system, *i.e.* vectors $\{u^*\}_1$ and $\{u^*\}_{L+1}$, respectively. For all these vectors the subscript e denotes the number of the interface and it is $e = 1, 2, ..., (L+1)$.

All the equilibrium and continuity equations of the previous section can be cast in the following matrix equation (reduced system of equations)

$$\begin{bmatrix} [\mathbf{A}^{11}] & [\mathbf{A}^{12}] & [0] \\ [\mathbf{A}^{21}] & [\mathbf{A}^{22}] & [0] \\ [\mathbf{A}^{31}] & [\mathbf{A}^{32}] & [\mathbf{I}] \end{bmatrix} \begin{Bmatrix} \{\tilde{\mathbf{u}}\} \\ \{\mathbf{s}\} \\ \{\mathbf{u}^*\} \end{Bmatrix} = \begin{bmatrix} [\mathbf{B}^{11}] & [\mathbf{B}^{12}] \\ [\mathbf{B}^{21}] & [\mathbf{B}^{22}] \\ [\mathbf{B}^{31}] & [\mathbf{B}^{32}] \end{bmatrix} \begin{Bmatrix} \{\mathbf{q}\} \\ \{\mathbf{p}\} \end{Bmatrix}. \tag{5.43}$$

where [I] is the identity matrix. The matrix equation of the first row of (5.43) represents the equilibrium equations (5.28), the matrix equation of the second row contains all the continuity conditions (5.33–35) at the interfaces

between the layers, and the last row embodies the support conditions associated with the bottom and top faces of the multilayered system which are given in equations (5.36) and (5.37). In the system (5.43), the body forces have not been included, since it may be assumed that, either they are zero, *i.e.*,

$$\{F\}_1^e = \{F\}_2^e = \{0\} \qquad (e = 1, 2, ..., L), \tag{5.44}$$

which is true for most applications, or they may be combined with the externally applied loads $\{p\}_e$ at the interfaces and the faces of the layered plate. The dimensions of the sub-matrices in equation (5.43) are:

$$\begin{array}{ccc} \underline{6N_b L} & \underline{3N_d (L-1)} & \underline{6N_d} \\ \left[\mathbf{A}^{11}\right] & \left[\mathbf{A}^{12}\right] & [0] \\ \left[\mathbf{A}^{21}\right] & \left[\mathbf{A}^{22}\right] & [0] \\ \left[\mathbf{A}^{31}\right] & \left[\mathbf{A}^{32}\right] & [\mathbf{I}] \end{array} \begin{array}{l} \} \ 6N_b L \\ \} \ 3N_d (L-1) \\ \} \ 6N_d \end{array}$$

and

$$\begin{array}{cc} \underline{3N_b (L+1)} & \underline{3N_d (L+1)} \\ \left[\mathbf{B}^{11}\right] & \left[\mathbf{B}^{12}\right] \\ \left[\mathbf{B}^{21}\right] & \left[\mathbf{B}^{22}\right] \\ \left[\mathbf{B}^{31}\right] & \left[\mathbf{B}^{32}\right] \end{array} \begin{array}{l} \} \ 6N_b L \\ \} \ 3N_d (L-1) \\ \} \ 6N_d \end{array}$$

where the expressions at the top of the matrices denote the number of columns in the subsequent sub-matrices, and the expressions at the right side denote the number of rows in the sub-matrices of the corresponding line. The complete expressions of all the $\left[\mathbf{A}^{ij}\right]$ and $\left[\mathbf{B}^{ij}\right]$ matrices $(i = 1, 2, 3;\ j = 1, 2)$ are presented on the following pages in equations (5.45) through (5.56).

Matrix $\left[\mathbf{A}^{11}\right]$ (Dimensions: $6N_bL \times 6N_bL$)

$$
\left[\mathbf{A}^{11}\right] = \begin{array}{c}
\begin{array}{ccccccccc} \{u\}_1 & & \{t\}_2 & \{u\}_2 & \{t\}_3 & \{u\}_3 & \{t\}_4 & \{u\}_4 & \cdots \end{array} \\
\left[\begin{array}{ccccccccc}
\begin{bmatrix} [\hat{H}]^1_{11} \\ [\hat{H}]^1_{21} \end{bmatrix} & \begin{bmatrix} -[G]^1_{12} \\ -[G]^1_{22} \end{bmatrix} & \begin{bmatrix} [\hat{H}]^1_{12} \\ [\hat{H}]^1_{22} \end{bmatrix} & [0] & [0] & [0] & [0] & & \\
[0] & \begin{bmatrix} [G]^2_{11} \\ [G]^2_{21} \end{bmatrix} & \begin{bmatrix} [\hat{H}]^2_{11} \\ [\hat{H}]^2_{21} \end{bmatrix} & \begin{bmatrix} -[G]^2_{12} \\ -[G]^2_{22} \end{bmatrix} & \begin{bmatrix} [\hat{H}]^2_{12} \\ [\hat{H}]^2_{22} \end{bmatrix} & [0] & [0] & & \\
[0] & [0] & [0] & \begin{bmatrix} [G]^3_{11} \\ [G]^3_{21} \end{bmatrix} & \begin{bmatrix} [\hat{H}]^3_{11} \\ [\hat{H}]^3_{21} \end{bmatrix} & \begin{bmatrix} -[G]^3_{12} \\ -[G]^3_{22} \end{bmatrix} & \begin{bmatrix} [\hat{H}]^3_{12} \\ [\hat{H}]^3_{22} \end{bmatrix} & & \\
 & & & & & \ddots & \ddots & \ddots &
\end{array}\right]
\end{array}
\begin{array}{cc} \text{Layers} & \\ \leftarrow & 1 \\ \leftarrow & 2 \\ \leftarrow & 3 \\ & \vdots \end{array}
\qquad (5.45a)
$$

$$
\left[\mathbf{A}^{11}\right] = \begin{array}{c}
\begin{array}{ccccccccc} \cdots & \{t\}_{(e-1)} & \{u\}_{(e-1)} & \{t\}_e & \{u\}_e & \{t\}_{(e+1)} & \{u\}_{(e+1)} & \cdots & \end{array} \\
\left[\begin{array}{ccccccccc}
\ddots & \ddots & \ddots & \ddots & & & & & \\
 & \begin{bmatrix} [G]^{(e-1)}_{11} \\ [G]^{(e-1)}_{21} \end{bmatrix} & \begin{bmatrix} [\hat{H}]^{(e-1)}_{11} \\ [\hat{H}]^{(e-1)}_{21} \end{bmatrix} & \begin{bmatrix} -[G]^{(e-1)}_{12} \\ -[G]^{(e-1)}_{22} \end{bmatrix} & \begin{bmatrix} [\hat{H}]^{(e-1)}_{12} \\ [\hat{H}]^{(e-1)}_{22} \end{bmatrix} & [0] & [0] & & \\
 & [0] & [0] & \begin{bmatrix} [G]^e_{11} \\ [G]^e_{21} \end{bmatrix} & \begin{bmatrix} [\hat{H}]^e_{11} \\ [\hat{H}]^e_{21} \end{bmatrix} & \begin{bmatrix} -[G]^e_{12} \\ -[G]^e_{22} \end{bmatrix} & \begin{bmatrix} [\hat{H}]^e_{12} \\ [\hat{H}]^e_{22} \end{bmatrix} & & \\
 & & & & & \ddots & \ddots & \ddots &
\end{array}\right]
\end{array}
\begin{array}{cc} \text{Layers} & \\ & \vdots \\ \leftarrow & (e-1) \\ \leftarrow & e \\ & \vdots \end{array}
\qquad (5.45b)
$$

$$
\begin{array}{c}
\qquad\quad \cdots \quad \{t\}_{(L-1)} \qquad \{u\}_{(L-1)} \qquad \{t\}_L \qquad\quad \{u\}_L \qquad\quad \{u\}_{(L+1)} \qquad\quad \text{Layers} \\
\left[\mathbf{A}^{11}\right] = \left[\begin{array}{ccccccc}
\ddots & \ddots & \ddots & \ddots & & & \\
 & \begin{bmatrix}[G]_{11}^{(L-1)} \\ [G]_{21}^{(L-1)}\end{bmatrix} & \begin{bmatrix}[\hat{H}]_{11}^{(L-1)} \\ [\hat{H}]_{21}^{(L-1)}\end{bmatrix} & \begin{bmatrix}-[G]_{12}^{(L-1)} \\ -[G]_{22}^{(L-1)}\end{bmatrix} & \begin{bmatrix}[\hat{H}]_{12}^{(L-1)} \\ [\hat{H}]_{22}^{(L-1)}\end{bmatrix} & [0] & \leftarrow \quad (L-1) \\
[0] & [0] & \begin{bmatrix}[G]_{11}^{L} \\ [G]_{21}^{L}\end{bmatrix} & \begin{bmatrix}[\hat{H}]_{11}^{L} \\ [\hat{H}]_{21}^{L}\end{bmatrix} & \begin{bmatrix}[\hat{H}]_{12}^{L} \\ [\hat{H}]_{22}^{L}\end{bmatrix} & & \leftarrow \quad L
\end{array}\right]
\end{array}
\tag{5.45c}
$$

Matrix $\left[\mathbf{A}^{12}\right]$ (Dimensions: $6N_b L \times 3N_d(L-1)$)

$$
\begin{array}{c}
\qquad\quad \{s\}_2 \qquad \{s\}_3 \qquad \{s\}_4 \qquad \cdots \qquad \{s\}_e \qquad \{s\}_{(e+1)} \qquad \cdots \qquad \{s\}_{(L-1)} \qquad \{s\}_L \qquad\quad \text{Layers} \\
\left[\mathbf{A}^{12}\right] = \left[\begin{array}{ccccccccccc}
\begin{bmatrix}-[D]_{12}^{1} \\ -[D]_{22}^{1}\end{bmatrix} & [0] & [0] & \cdots & [0] & [0] & \cdots & [0] & [0] & \leftarrow & 1 \\
\begin{bmatrix}[D]_{11}^{2} \\ [D]_{21}^{2}\end{bmatrix} & \begin{bmatrix}-[D]_{12}^{2} \\ -[D]_{22}^{2}\end{bmatrix} & [0] & \cdots & [0] & [0] & \cdots & [0] & [0] & \leftarrow & 2 \\
[0] & \begin{bmatrix}[D]_{11}^{3} \\ [D]_{21}^{3}\end{bmatrix} & \begin{bmatrix}-[D]_{12}^{3} \\ -[D]_{22}^{3}\end{bmatrix} & \cdots & [0] & [0] & \cdots & [0] & [0] & \leftarrow & 3 \\
\vdots & \vdots & \vdots & \ddots & \vdots & \vdots & & \vdots & \vdots & & \vdots \\
[0] & [0] & [0] & \cdots & \begin{bmatrix}[D]_{11}^{e} \\ [D]_{21}^{e}\end{bmatrix} & \begin{bmatrix}-[D]_{12}^{e} \\ -[D]_{22}^{e}\end{bmatrix} & \cdots & [0] & [0] & \leftarrow & e \\
\vdots & \vdots & \vdots & & \vdots & \vdots & \ddots & \vdots & \vdots & & \vdots \\
[0] & [0] & [0] & \cdots & [0] & [0] & \cdots & \begin{bmatrix}[D]_{11}^{(L-1)} \\ [D]_{21}^{(L-1)}\end{bmatrix} & \begin{bmatrix}-[D]_{12}^{(L-1)} \\ -[D]_{22}^{(L-1)}\end{bmatrix} & \leftarrow & (L-1) \\
[0] & [0] & [0] & \cdots & [0] & [0] & \cdots & [0] & \begin{bmatrix}[D]_{11}^{L} \\ [D]_{21}^{L}\end{bmatrix} & \leftarrow & L
\end{array}\right]
\end{array}
\tag{5.46}
$$

Matrix $\left[\mathbf{A}^{21}\right]$ (Dimensions: $3N_d(L-1) \times 6N_bL$)

$\left[\mathbf{A}^{21}\right] =$

$$
\begin{array}{c}
\begin{array}{cccccccccc}
\{u\}_1 & \{t\}_2 & \{u\}_2 & \{t\}_3 & \{u\}_3 & \{t\}_4 & \{u\}_4 & \{t\}_5 & \{u\}_5 & \cdots
\end{array} \\
\left[\begin{array}{cccccccccc}
[H^*]^1_{21} & -([G^*]^1_{22}+[G^*]^2_{11}) & ([H^*]^1_{22}-[H^*]^2_{11}) & [G^*]^2_{12} & -[H^*]^2_{12} & [0] & [0] & [0] & [0] & \\
[0] & [G^*]^2_{21} & [H^*]^2_{21} & -([G^*]^2_{22}+[G^*]^3_{11}) & ([H^*]^2_{22}-[H^*]^3_{11}) & [G^*]^3_{12} & -[H^*]^3_{12} & [0] & [0] & \\
[0] & [0] & [0] & [G^*]^3_{21} & [H^*]^3_{21} & -([G^*]^3_{22}+[G^*]^4_{11}) & ([H^*]^3_{22}-[H^*]^4_{11}) & [G^*]^4_{12} & -[H^*]^4_{12} & \\
 & & & & & \ddots & \ddots & \ddots & \ddots & \ddots
\end{array}\right]
\end{array}
\begin{array}{l}
\underline{\text{Interfaces}} \\
\leftarrow 2 \\
\leftarrow 3 \\
\leftarrow 4 \\
\vdots
\end{array}
$$

(5.47a)

$$
\begin{array}{c}
\begin{array}{cccccccccc}
\cdots & \{t\}_{(e-1)} & \{u\}_{(e-1)} & \{t\}_e & \{u\}_e & \{t\}_{(e+1)} & \{u\}_{(e+1)} & \{t\}_{(e+2)} & \{u\}_{(e+2)} & \cdots
\end{array} \\
\left[\begin{array}{cccccccccc}
\ddots & \ddots & \ddots & \ddots & \ddots & & & & & \\
 & [G^*]^{(e-1)}_{21} & [H^*]^{(e-1)}_{21} & -([G^*]^{(e-1)}_{22}+[G^*]^e_{11}) & ([H^*]^{(e-1)}_{22}-[H^*]^e_{11}) & [G^*]^e_{12} & -[H^*]^e_{12} & [0] & [0] & \\
 & [0] & [0] & [G^*]^e_{21} & [H^*]^e_{21} & -([G^*]^e_{22}+[G^*]^{(e+1)}_{11}) & ([H^*]^e_{22}-[H^*]^{(e+1)}_{11}) & [G^*]^{(e+1)}_{12} & -[H^*]^{(e+1)}_{12} & \\
 & & & & & \ddots & \ddots & \ddots & \ddots & \ddots
\end{array}\right]
\end{array}
\begin{array}{l}
\underline{\text{Interfaces}} \\
\vdots \\
\leftarrow e \\
\leftarrow (e+1) \\
\vdots
\end{array}
$$

(5.47b)

$$
\begin{array}{c}
\begin{array}{cccccccc}
\cdots & \{t\}_{(L-2)} & \{u\}_{(L-2)} & \{t\}_{(L-1)} & \{u\}_{(L-1)} & \{t\}_L & \{u\}_L & \{u\}_{(L+1)}
\end{array} \\
\left[\begin{array}{cccccccc}
\ddots & \ddots & \ddots & \ddots & \ddots & & & \\
 & [G^*]^{(L-2)}_{21} & [H^*]^{(L-2)}_{21} & -\left([G^*]^{(L-2)}_{22}+[G^*]^{(L-1)}_{11}\right) & \left([H^*]^{(L-2)}_{22}-[H^*]^{(L-1)}_{11}\right) & [G^*]^{(L-1)}_{12} & -[H^*]^{(L-1)}_{12} & [0] \\
 & [0] & [0] & [G^*]^{(L-1)}_{21} & [H^*]^{(L-1)}_{21} & -\left([G^*]^{(L-1)}_{22}+[G^*]^L_{11}\right) & \left([H^*]^{(L-1)}_{22}-[H^*]^L_{11}\right) & -[H^*]^L_{12}
\end{array}\right]
\end{array}
\begin{array}{l}
\underline{\text{Interfaces}} \\
\vdots \\
\leftarrow (L-1) \\
\leftarrow L
\end{array}
$$

(5.47c)

Matrix $\left[\mathbf{A}^{22}\right]$ (Dimensions: $3N_d(L-1) \times 3N_d(L-1)$)

$$\left[\mathbf{A}^{22}\right] = \begin{array}{c} \begin{array}{cccc} \{s\}_2 & \{s\}_3 & \{s\}_4 & \{s\}_5 \ \cdots \end{array} \\ \left[\begin{array}{cccc} -\left([\mathrm{D}^*]^1_{22}+[\mathrm{D}^*]^2_{11}\right) & [\mathrm{D}^*]^2_{12} & [0] & [0] \\ [\mathrm{D}^*]^2_{21} & -\left([\mathrm{D}^*]^2_{22}+[\mathrm{D}^*]^3_{11}\right) & [\mathrm{D}^*]^3_{12} & [0] \\ [0] & [\mathrm{D}^*]^3_{21} & -\left([\mathrm{D}^*]^3_{22}+[\mathrm{D}^*]^4_{11}\right) & [\mathrm{D}^*]^4_{12} \\ & & \ddots & \ddots \quad \ddots \end{array}\right] \end{array} \begin{array}{c} \underline{\text{Interfaces}} \\ \leftarrow \ 2 \\ \leftarrow \ 3 \\ \leftarrow \ 4 \\ \vdots \end{array} \tag{5.48a}$$

$$\left[\mathbf{A}^{22}\right] = \begin{array}{c} \begin{array}{ccccccc} \cdots \{s\}_{(e-1)} & \{s\}_e & \{s\}_{(e+1)} & \cdots & \{s\}_{(L-2)} & \{s\}_{(L-1)} & \{s\}_L \end{array} \\ \left[\begin{array}{ccccccc} \ddots & \ddots & \ddots & & & & \\ [\mathrm{D}^*]^{(e-1)}_{21} & -\left([\mathrm{D}^*]^{(e-1)}_{22}+[\mathrm{D}^*]^e_{11}\right) & [\mathrm{D}^*]^e_{12} & & & & \\ & \ddots & \ddots & \ddots & \ddots & & \\ & & & [\mathrm{D}^*]^{(L-2)}_{21} & -\left([\mathrm{D}^*]^{(L-2)}_{22}+[\mathrm{D}^*]^{(L-1)}_{11}\right) & [\mathrm{D}^*]^{(L-1)}_{12} & \\ & & & [0] & [\mathrm{D}^*]^{(L-1)}_{21} & -\left([\mathrm{D}^*]^{(L-1)}_{22}+[\mathrm{D}^*]^L_{11}\right) & \end{array}\right] \end{array} \begin{array}{c} \underline{\text{Interfaces}} \\ \vdots \\ \leftarrow \ e \\ \vdots \\ \leftarrow \ (L-1) \\ \leftarrow \ L \end{array} \tag{5.48b}$$

Matrix $\left[\mathbf{B}^{11}\right]$ (Dimensions: $6N_bL \times 3N_b(L+1)$)

$$
\left[\mathbf{B}^{11}\right] = \begin{array}{c}
\begin{array}{ccccccccc}
\{q\}_1 & \{q\}_2 & \{q\}_3 & \cdots & \{q\}_e & \cdots & \{q\}_{(L-1)} & \{q\}_L & \{q\}_{(L+1)}
\end{array} \\
\left[\begin{array}{ccccccccc}
\begin{bmatrix}[G]^1_{11}\\ [G]^1_{21}\end{bmatrix} & \begin{bmatrix}[0]\\ [0]\end{bmatrix} & \begin{bmatrix}[0]\\ [0]\end{bmatrix} & & & & & & \\
\begin{bmatrix}[0]\\ [0]\end{bmatrix} & \begin{bmatrix}[G]^2_{11}\\ [G]^2_{21}\end{bmatrix} & \begin{bmatrix}[0]\\ [0]\end{bmatrix} & & & & & & \\
\begin{bmatrix}[0]\\ [0]\end{bmatrix} & \begin{bmatrix}[0]\\ [0]\end{bmatrix} & \begin{bmatrix}[G]^3_{11}\\ [G]^3_{21}\end{bmatrix} & & & & & & \\
 & & & \ddots & & & & & \\
 & & & & \begin{bmatrix}[G]^e_{11}\\ [G]^e_{21}\end{bmatrix} & & & & \\
 & & & & & \ddots & & & \\
 & & & & & & \begin{bmatrix}[G]^{(L-1)}_{11}\\ [G]^{(L-1)}_{21}\end{bmatrix} & \begin{bmatrix}[0]\\ [0]\end{bmatrix} & \begin{bmatrix}[0]\\ [0]\end{bmatrix} \\
 & & & & & & \begin{bmatrix}[0]\\ [0]\end{bmatrix} & \begin{bmatrix}[G]^L_{11}\\ [G]^L_{21}\end{bmatrix} & \begin{bmatrix}[G]^L_{12}\\ [G]^L_{22}\end{bmatrix}
\end{array}\right]
\end{array}
\begin{array}{ll}
 & \underline{\text{Layers}} \\
\leftarrow & 1 \\
\leftarrow & 2 \\
\leftarrow & 3 \\
 & \vdots \\
\leftarrow & e \\
 & \vdots \\
\leftarrow & (L-1) \\
\leftarrow & L
\end{array}
\tag{5.49}
$$

Matrix $\left[\mathbf{B}^{12}\right]$ (Dimensions: $6N_bL \times 3N_d(L+1)$)

$$\left[\mathbf{B}^{12}\right] = \begin{array}{c} \begin{array}{ccccccccc} \{p\}_1 & \{p\}_2 & \{p\}_3 & \cdots & \{p\}_e & \cdots & \{p\}_{(L-1)} & \{p\}_L & \{p\}_{(L+1)} \end{array} \\ \begin{bmatrix} \begin{bmatrix} [\mathrm{D}]^1_{11} \\ [\mathrm{D}]^1_{21} \end{bmatrix} & \begin{bmatrix} [0] \\ [0] \end{bmatrix} & \begin{bmatrix} [0] \\ [0] \end{bmatrix} & & & & & & \\ \begin{bmatrix} [0] \\ [0] \end{bmatrix} & \begin{bmatrix} [\mathrm{D}]^2_{11} \\ [\mathrm{D}]^2_{21} \end{bmatrix} & \begin{bmatrix} [0] \\ [0] \end{bmatrix} & & & & & & \\ \begin{bmatrix} [0] \\ [0] \end{bmatrix} & \begin{bmatrix} [0] \\ [0] \end{bmatrix} & \begin{bmatrix} [\mathrm{D}]^3_{11} \\ [\mathrm{D}]^3_{21} \end{bmatrix} & & & & & & \\ & & & \ddots & & & & & \\ & & & & \begin{bmatrix} [\mathrm{D}]^e_{11} \\ [\mathrm{D}]^e_{21} \end{bmatrix} & & & & \\ & & & & & \ddots & & & \\ & & & & & & \begin{bmatrix} [\mathrm{D}]^{(L-1)}_{11} \\ [\mathrm{D}]^{(L-1)}_{21} \end{bmatrix} & \begin{bmatrix} [0] \\ [0] \end{bmatrix} & \begin{bmatrix} [0] \\ [0] \end{bmatrix} \\ & & & & & & \begin{bmatrix} [0] \\ [0] \end{bmatrix} & \begin{bmatrix} [\mathrm{D}]^L_{11} \\ [\mathrm{D}]^L_{21} \end{bmatrix} & \begin{bmatrix} [\mathrm{D}]^L_{12} \\ [\mathrm{D}]^L_{22} \end{bmatrix} \end{bmatrix} \end{array} \begin{array}{l} \underline{\text{Layers}} \\ \leftarrow \quad 1 \\ \leftarrow \quad 2 \\ \leftarrow \quad 3 \\ \vdots \\ \leftarrow \quad e \\ \vdots \\ \leftarrow \quad (L-1) \\ \leftarrow \quad L \end{array} \qquad (5.50)$$

Matrix $\left[\mathbf{B}^{21}\right]$ (Dimensions: $3N_d(L-1) \times 3N_b(L+1)$)

$$\left[\mathbf{B}^{21}\right] = \begin{array}{c} \begin{array}{cccccccccccc} \{q\}_1 & \{q\}_2 & \{q\}_3 & \{q\}_4 & \cdots & \{q\}_{(e-1)} & \{q\}_e & \cdots & \{q\}_{(L-2)} & \{q\}_{(L-1)} & \{q\}_L & \{q\}_{(L+1)} \end{array} \\ \begin{bmatrix} [G^*]^1_{21} & -[G^*]^2_{11} & [0] & [0] & & & & & & & & \\ [0] & [G^*]^2_{21} & -[G^*]^3_{11} & [0] & & & & & & & & \\ [0] & [0] & [G^*]^3_{21} & -[G^*]^4_{11} & & & & & & & & \\ & & & \ddots & \ddots & & & & & & & \\ & & & & & [G^*]^{(e-1)}_{21} & -[G^*]^e_{11} & & & & & \\ & & & & & & \ddots & \ddots & & & & \\ & & & & & & & & [G^*]^{(L-2)}_{21} & -[G^*]^{(L-1)}_{11} & [0] & [0] \\ & & & & & & & & [0] & [G^*]^{(L-1)}_{21} & -[G^*]^L_{11} & -[G^*]^L_{12} \end{bmatrix} \end{array} \begin{array}{ll} & \underline{\text{Interfaces}} \\ \leftarrow & 2 \\ \leftarrow & 3 \\ \leftarrow & 4 \\ & \vdots \\ \leftarrow & e \\ & \vdots \\ \leftarrow & (L-1) \\ \leftarrow & L \end{array} \tag{5.51}$$

Matrix $\left[\mathbf{B}^{22}\right]$ (Dimensions: $3N_d(L-1) \times 3N_d(L+1)$)

$$\left[\mathbf{B}^{22}\right] = \begin{array}{c} \begin{array}{cccccccccccc} \{p\}_1 & \{p\}_2 & \{p\}_3 & \{p\}_4 & \cdots & \{p\}_{(e-1)} & \{p\}_e & \cdots & \{p\}_{(L-2)} & \{p\}_{(L-1)} & \{p\}_L & \{p\}_{(L+1)} \end{array} \\ \begin{bmatrix} [D^*]^1_{21} & -[D^*]^2_{11} & [0] & [0] & & & & & & & & \\ [0] & [D^*]^2_{21} & -[D^*]^3_{11} & & & & & & & & & \\ [0] & [0] & [D^*]^3_{21} & -[D^*]^4_{11} & & & & & & & & \\ & & & \ddots & \ddots & & & & & & & \\ & & & & & [D^*]^{(e-1)}_{21} & -[D^*]^e_{11} & & & & & \\ & & & & & & \ddots & \ddots & & & & \\ & & & & & & & & [D^*]^{(L-2)}_{21} & -[D^*]^{(L-1)}_{11} & [0] & [0] \\ & & & & & & & & [0] & [D^*]^{(L-1)}_{21} & -[D^*]^L_{11} & -[D^*]^L_{12} \end{bmatrix} \end{array} \begin{array}{ll} & \underline{\text{Interfaces}} \\ \leftarrow & 2 \\ \leftarrow & 3 \\ \leftarrow & 4 \\ & \vdots \\ \leftarrow & e \\ & \vdots \\ \leftarrow & (L-1) \\ \leftarrow & L \end{array} \tag{5.52}$$

Matrix $\left[\mathbf{A}^{31}\right]$ (Dimensions: $6N_d \times 6N_b L$)

$$\left[\mathbf{A}^{31}\right] = \begin{array}{c} \begin{array}{cccccccccccc} \{u\}_1 & \{t\}_2 & \{u\}_2 & \{t\}_3 & \{u\}_3 & \cdots & \{t\}_{(L-1)} & \{u\}_{(L-1)} & \{t\}_L & \{u\}_L & \{u\}_{(L+1)} & \end{array} \\ \left[\begin{array}{cccccccccccc} [H^*]^1_{11} & -[G^*]^1_{12} & [H^*]^1_{12} & [0] & [0] & \cdots & [0] & [0] & [0] & [0] & [0] \\ [0] & [0] & [0] & [0] & [0] & \cdots & [0] & [0] & [G^*]^L_{21} & [H^*]^L_{21} & [H^*]^L_{22} \end{array}\right] \end{array} \begin{array}{ll} & \underline{\text{Faces}} \\ \leftarrow & 1, \text{ bottom} \\ \leftarrow & (L+1), \text{ top} \end{array} \tag{5.53}$$

Matrix $\left[\mathbf{A}^{32}\right]$ (Dimensions: $6N_d \times 3N_d(L-1)$)

$$\left[\mathbf{A}^{32}\right] = \begin{array}{c} \begin{array}{ccccccc} \{s\}_2 & \{s\}_3 & \{s\}_4 & \cdots & \{s\}_{(L-2)} & \{s\}_{(L-1)} & \{s\}_L \end{array} \\ \left[\begin{array}{ccccccc} -[D^*]^1_{12} & [0] & [0] & \cdots & [0] & [0] & [0] \\ [0] & [0] & [0] & \cdots & [0] & [0] & [D^*]^L_{21} \end{array}\right] \end{array} \begin{array}{ll} & \underline{\text{Faces}} \\ \leftarrow & 1, \text{ bottom} \\ \leftarrow & (L+1), \text{ top} \end{array} \tag{5.54}$$

Matrix $\left[\mathbf{B}^{31}\right]$ (Dimensions: $6N_d \times 3N_b(L+1)$)

$$\left[\mathbf{B}^{31}\right] = \begin{array}{c} \begin{array}{cccccccc} \{q\}_1 & \{q\}_2 & \{q\}_3 & \cdots & \{q\}_{(L-2)} & \{q\}_{(L-1)} & \{q\}_L & \{q\}_{(L+1)} \end{array} \\ \left[\begin{array}{cccccccc} [\mathrm{G}^*]^1_{11} & [0] & [0] & \cdots & [0] & [0] & [0] & [0] \\ [0] & [0] & [0] & \cdots & [0] & [0] & [\mathrm{G}^*]^L_{21} & [\mathrm{G}^*]^L_{22} \end{array}\right] \end{array} \begin{array}{ll} & \underline{\text{Faces}} \\ \leftarrow & 1, \text{ bottom} \\ \leftarrow & (L+1), \text{ top} \end{array} \tag{5.55}$$

Matrix $\left[\mathbf{B}^{32}\right]$ (Dimensions: $6N_d \times 3N_d(L+1)$)

$$\left[\mathbf{B}^{32}\right] = \begin{array}{c} \begin{array}{cccccccc} \{p\}_1 & \{p\}_2 & \{p\}_3 & \cdots & \{p\}_{(L-2)} & \{p\}_{(L-1)} & \{p\}_L & \{p\}_{(L+1)} \end{array} \\ \left[\begin{array}{cccccccc} [\mathrm{D}^*]^1_{11} & [0] & [0] & \cdots & [0] & [0] & [0] & [0] \\ [0] & [0] & [0] & \cdots & [0] & [0] & [\mathrm{D}^*]^L_{21} & [\mathrm{D}^*]^L_{22} \end{array}\right] \end{array} \begin{array}{ll} & \underline{\text{Faces}} \\ \leftarrow & 1, \text{ bottom} \\ \leftarrow & (L+1), \text{ top} \end{array} \tag{5.56}$$

The total number of equations in the system (5.43) is apparently

$$N_{\text{total}} = 6N_b L + 3N_d(L-1) + 6N_d = 6N_b L + 3N_d(L+1). \qquad (5.57)$$

The unknown quantities are: the $3N_b(L-1)$ interlaminar boundary traction components in the vectors $\{t\}_e$ $(e=2,3,...,L)$, the $3N_d(L-1)$ interlaminar traction components at the domain nodes in vector $\{\mathbf{s}\}$, and at each nodal point of the boundaries and each nodal point on the two faces of the plate either the displacement or the corresponding traction component. This indicates that at these nodal points there will be $3N_b(L+1)$ unknown quantities among the displacements $\{u\}_e$ and the tractions $\{q\}_e$ $(e=1,2,...,L+1)$, $3N_d$ unknowns among the domain displacements $\{u^*\}_1$ and tractions $\{p\}_1$ of the bottom face of the plate, and finally, $3N_d$ unknowns among the domain displacements $\{u^*\}_{L+1}$ and tractions $\{p\}_{L+1}$ of the top face. All the other nodal quantities in each of the aforementioned generalized vectors will be prescribed, and the total number of prescribed quantities is equal to the number of the unknown displacement and traction components. Therefore, the total number of unknowns in the system (5.43) comes up to N_{total}, and it is the same as the number of available equations.

After incorporating into (5.43) the prescribed boundary displacements and tractions, the resulting reduced system of N_{total} linear algebraic equations will be solved by employing a special iterative solver which is referred to as *Jacobi bi-conjugate gradient* acceleration method and is described in Section 6.3. Once the system has been solved and the unknown components of the vectors in equations (5.38–42) have been determined, the domain nodal displacements $\{u^*\}_e$ on the interfaces $e=2,3,...,L$ are computed from equations (5.29) and (5.32). Displacements at other than the nodal points, strain and stress components at any point in the three-dimensional layered system are evaluated using the equations of Section 4.6.

Chapter 6

NUMERICAL TECHNIQUES

6.1 NUMERICAL EVALUATION OF BOUNDARY INTEGRALS

6.1–1 Conversion of Line Integrals to Definite Integrals

The boundary integrals that appear in the boundary element model of the problem were presented in Section 5.2 and generally they have the form:

$$\int_{\Gamma_e^n} U_{\beta\alpha}^e\left(\vec{x},\vec{\xi}\right) d\Gamma(\vec{x}) \quad \text{and} \quad \int_{\Gamma_e^n} T_{\beta\alpha}^e\left(\vec{x},\vec{\xi}\right) d\Gamma(\vec{x}) \tag{6.1}$$

where $\alpha,\beta = 1,2,...,6$; $e = 1,2,...,L$ and $n = 1,2,...,N_b$. The point $\vec{\xi}$ is a constant *field* or *reference point*, while $\vec{x}$ is the *source* or *integration point* on the boundary element Γ_e^n. The integrands in the above integrals are the components of the fundamental solution $U_{\alpha\beta}^e(x_1,x_2;\xi_1,\xi_2)$ and the traction matrix $T_{\alpha\beta}^e(x_1,x_2;\xi_1,\xi_2)$, which are given in equations (3.36) and (4.6), respectively. If we evaluate the strain or stress components, these integrands become the

derivatives with respect to the coordinates of point $\vec{\xi}$ of the corresponding components (Section 3.7). For the sake of mathematical convenience, in the rest of this analysis both integrals of equation (6.1) will be referred to as

$$I\left(\vec{\xi}\right) = \int_{\Gamma_e^n} f\left(\vec{x}, \vec{\xi}\right) ds(\vec{x}) \tag{6.2}$$

where the function $f(\vec{x}, \vec{\xi})$ may represent any component of the matrices $U_{\beta\alpha}^e$ and $T_{\beta\alpha}^e$, or their derivatives.

The elements on the boundary are numbered consecutively counterclockwise (Section 5.2) and the direction of integration over the boundary element is defined to be also in the counterclockwise direction, *i.e.*, from the end-point of the element with local number 1 to the end-point with number 2 (see Figure 6.1). The distance between the points $\vec{x}$ and $\vec{\xi}$ is denoted by R, and it is

$$R = \sqrt{(x_1 - \xi_1)^2 + (x_2 - \xi_2)^2} = \sqrt{x^2 + y^2} \tag{6.3}$$

where Pxy is a Cartesian coordinate system with origin at $\vec{\xi}$ and with axes x and y parallel to the axes x_1 and x_2, respectively.

The line integral $I(\xi_1, \xi_2)$ will be evaluated in a coordinate system $\bar{x}\bar{y}$, which is obtained by rotating the xy-system through an angle θ in the counterclockwise direction, which is the same as the direction of the integration. This is the angle of rotation that will make the new $\bar{y}$-axis parallel to the chord and with its positive direction from point 1 to point 2. The $\bar{x}$ axis will then be perpendicular to the chord of the boundary element, as it is shown in Figure 6.1. The equations of the coordinate transformation may be written in the following way

$$\left\{ \begin{array}{l} \bar{x} = x\ \cos\theta + y\ \sin\theta \\ \bar{y} = -x\ \sin\theta + y\ \cos\theta \end{array} \right\} \quad \text{and} \quad \left\{ \begin{array}{l} x = \bar{x}\ \cos\theta - \bar{y}\ \sin\theta \\ y = \bar{x}\ \sin\theta + \bar{y}\ \cos\theta \end{array} \right\}. \tag{6.4}$$

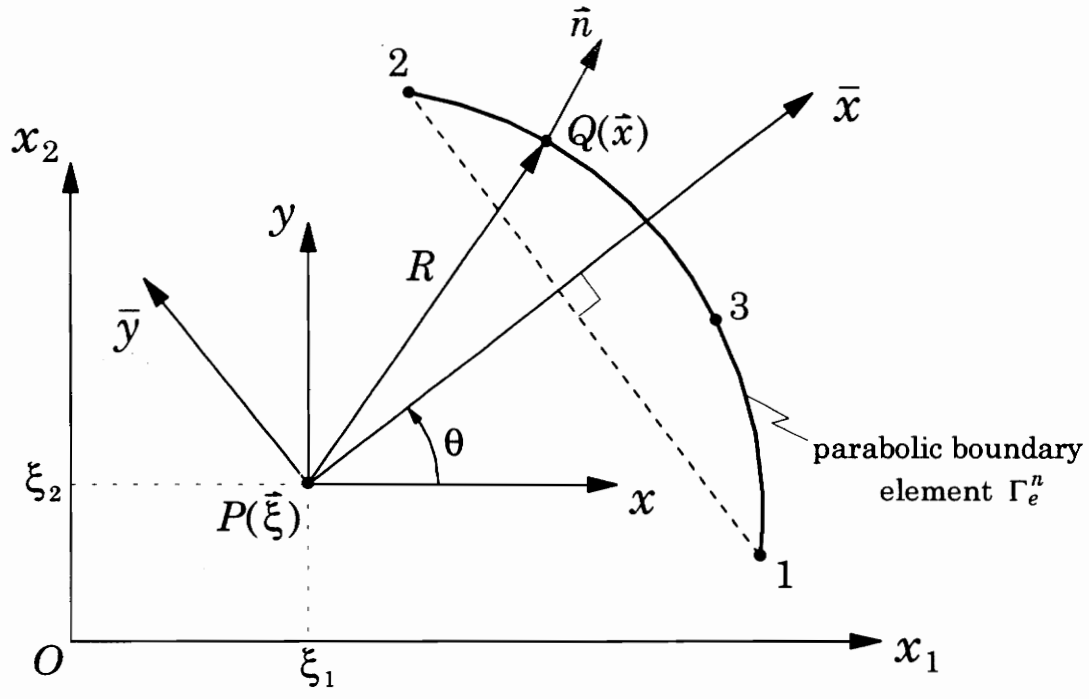

Figure 6.1 Typical boundary element and coordinate systems used in the numerical evaluation of the boundary integrals.

As it was discussed in Section 5.2, the geometry of each element in the boundary element model of the layer is approximated by a parabolic arc. The equation of this arc in the $\bar{x}\bar{y}$-system is defined as

$$\bar{x} = g(\bar{y}) = a_1 \bar{y}^2 + a_2 \bar{y} + a_3 \tag{6.5}$$

where the coefficients a_i $(i = 1, 2, 3)$ are computed from the coordinates of the two end-points and the nodal point of the element. These points are represented in Figure 6.1 by the numbers 1, 2 and 3, respectively. Denoting by $\bar{x}_i$ and $\bar{y}_i$, the coordinates of these three points in the $\bar{x}\bar{y}$ coordinate system, the coefficients of the polynomial (6.5) are found to be

$$a_1 = -\frac{(\bar{x}_3 - \bar{x}_1)}{\Delta}\,, \tag{6.6a}$$

$$a_2 = \frac{(\bar{x}_3 - \bar{x}_1)\,(\bar{y}_1 + \bar{y}_2)}{\Delta}\,, \tag{6.6b}$$

and

$$a_3 = \frac{\bar{x}_1\,\bar{y}_3\,(\bar{y}_1 + \bar{y}_2 - \bar{y}_3) - \bar{x}_3\,\bar{y}_1\,\bar{y}_2}{\Delta}\,. \tag{6.6c}$$

where $\Delta = (\bar{y}_2 - \bar{y}_3)\,(\bar{y}_3 - \bar{y}_1)$, and $\bar{x}_2 = \bar{x}_1$ since the axis $\bar{x}$ is perpendicular to the chord of the element.

The line integral can be reduced to a definite integral in terms of $\bar{y}$ by incorporating into equation (6.2) the transformations (6.4) and the equation (6.5) of the parabolic arc. The infinitesimal element *ds* may be expressed in terms of $\bar{y}$ as,

$$ds = \sqrt{d\bar{x}^2 + d\bar{y}^2} = \sqrt{\left(\frac{dg}{d\bar{y}}\right)^2 + 1}\;\; d\bar{y} = \sqrt{(2a_1\bar{y} + a_2)^2 + 1}\;\; d\bar{y}\,, \tag{6.7}$$

and the definite integral of equation (6.2) takes then the form

$$I = \int_{\bar{y}_1}^{\bar{y}_2} f(\bar{y}, \theta)\,\sqrt{(2a_1\bar{y} + a_2)^2 + 1}\;\; d\bar{y}\,. \tag{6.8}$$

Equation (6.8) can be used to evaluate the line integrals with kernels the components of the displacement matrix $U^e_{\beta\alpha}$ and the traction matrix $T^e_{\beta\alpha}$, or even their derivatives with respect to the coordinates ξ_1 and ξ_2, where in all cases the components must be expressed first in the bar coordinate system.

It must be noted that, the components of the traction matrix, or their derivatives, depend also on the unit normal vector $\vec{n}$, which varies along the boundary of the element Γ^n_e. The direction of this unit vector is dictated always by the direction in which we have numbered the elements on the boundary. Since, on the exterior boundary of a layer the numbering direction is counterclockwise, according to the right-hand rule, the unit vector will

have an outward direction. On the interior boundaries of the layer, which are the boundaries of holes or inclusions, the numbering direction is clockwise, and thus, according to the right-hand rule, the unit vector will point again away from the domain of the matrix material. On the boundaries of the inclusions, whose boundaries coincide with those of the matrix, one can use for each element the corresponding components of the unit vector for the matrix but with opposite sign. The components n_1 and n_2 of the normal vector may be expressed at any point of the boundary element as continuous functions of the $\bar{y}$ coordinate by using the quadratic polynomial (6.5) which approximates the geometry of the element. These expressions are,

$$n_1 = \frac{1}{\| \nabla(\bar{x} - g(\bar{y})) \|} \frac{\partial(\bar{x} - g(\bar{y}))}{\partial \bar{x}} = \left[\sqrt{(2a_1 \bar{y} + a_2)^2 + 1} \right]^{-1} \tag{6.9a}$$

and

$$n_2 = \frac{1}{\| \nabla(\bar{x} - g(\bar{y})) \|} \frac{\partial(\bar{x} - g(\bar{y}))}{\partial \bar{y}} = -(2a_1 \bar{y} + a_2) \left[\sqrt{(2a_1 \bar{y} + a_2)^2 + 1} \right]^{-1} . \tag{6.9b}$$

6.1–2 Singular Integrals

The definite integral of equation (6.8) behaves differently according to the position of the field point $P(\vec{\xi})$. If $\vec{\xi} \notin \Gamma_e^n$, the integrals are regular and they can be computed using a standard Gaussian quadrature rule (Stroud and Secrest, 1966). For all cases the eight-point rule gives very accurate results. However, if $\vec{\xi} \in \Gamma_e^n$ (*i.e.*, the field point belongs in the interval of integration), the integrals become singular, because the integrands tend to infinity when the integration point $\vec{x}$ approaches the point $\vec{\xi}$, and therefore a special approach must be adopted. The behavior of the integrands can be studied through the functions of equations (3.51) and (3.63) which are used in the expressions of the fundamental solution and the traction matrix. The two

different cases for the behavior of integral (6.8) are shown graphically in Figure 6.2.

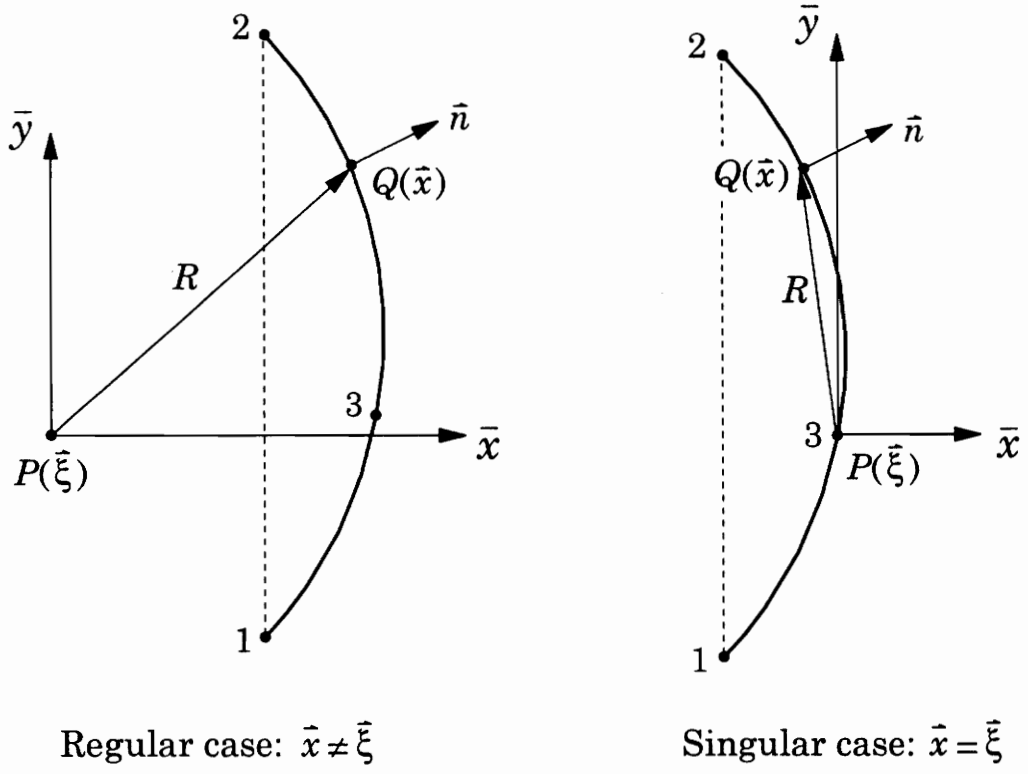

Figure 6.2 Relative position of field point $P(\vec{\xi})$ and integration point $Q(\vec{x})$ for regular and singular integrals.

The singularities that appear in the kernels of (6.8) are generally of logarithmic type, weak singularities or singularities that exist only in the Cauchy principal value sense. Various integration schemes have been proposed in the literature for these types of singularities and many of them have been reviewed by Telles (1987), Alarcón *et al.* (1989), Cerrolaza and Alarcón (1989), and Lutz (1992). In the case of a Cauchy-type singularity most of the techniques remove the singularity in the following way

$$\int_a^b \frac{f(x)}{x-\lambda}dx = \int_a^b \frac{f(x)-f(\lambda)}{x-\lambda}\,dx + f(\lambda)\int_a^b \frac{1}{x-\lambda}\,dx \tag{6.10a}$$

or

$$\int_a^b \frac{f(x)}{x-\lambda}dx = \int_a^b \frac{f(x)-f(\lambda)}{x-\lambda}dx + f(\lambda)\,\ln\left|\frac{b-\lambda}{\lambda-a}\right| \tag{6.10b}$$

where $f(x)$ is a regular function in the interval $[a, b]$ and $\lambda \in (a, b)$. The integral on the right-hand side of (6.10b) is now regular, so it is possible to integrate it by means of standard Gaussian quadratures, provided that no sampling point coincides with the singular point λ. Other techniques involve exact integration over straight elements, or subdivision of the original interval at the regions close to the singularity, and application of standard Gaussian quadrature over each subinterval. Nevertheless, these techniques have the disadvantage of not being applicable in the presence of logarithmic singularities or weak singularities of the type x^{-a} with $a > 1$. Many of these approaches are also unstable when the number of subdivisions is increased, and their accuracy is highly dependent upon the number of subdivisions.

In the case of a logarithmic singularity the integration can be performed by splitting the kernel, as it is shown below

$$\int_a^b f(x)\,\ln|x-\lambda|\,dx = \int_a^b [f(x)-f(\lambda)]\,\ln|x-\lambda|\,dx + f(\lambda)\int_a^b \ln|x-\lambda|\,dx, \tag{6.11}$$

and evaluating the two integrals using special quadratures with logarithmic weighting functions (Stroud and Secrest, 1966). A similar approach has also been suggested by Katsikadelis and Armenàkas (1985) for the case of elements whose geometry is described by a quadratic polynomial. It is clear that the aforementioned procedures imply a certain number of added numerical

and computational complications and are not general enough to handle other types of singularities.

In order to overcome these problems and develop an approach that can deal with all types of singularities, different authors have recently suggested the use of nonlinear coordinate transformations of the integrands, which smooth out the singularity near the singular point (Telles, 1987; Cerrolaza and Alarcón, 1989).

6.1–3 Numerical Evaluation of Singular Integrals

In the present work, a fully numerical procedure is developed for the evaluation of all types of singular kernels (*i.e.*, Cauchy-type singularities, logarithmic and weak singularities), using a bi-cubic transformation proposed by Cerrolaza and Alarcón (1989), in conjunction with a subdivision of the original interval at the region close to the singularity. Let the integral

$$I_0 = \int_{\bar{y}_1}^{\bar{y}_2} F(\bar{y},\theta)\, d\bar{y} = \lim_{\varepsilon\to 0}\left[\int_{\bar{y}_1}^{-\varepsilon} F(\bar{y},\theta)\, d\bar{y} + \int_{\varepsilon}^{\bar{y}_2} F(\bar{y},\theta)\, d\bar{y}\right] \tag{6.12}$$

represent the integral in equation (6.8) for the singular case, where $\bar{y}=0$ is the point of singularity, and $\bar{y}_1 < 0 < \bar{y}_2$. Depending on the component which is being integrated in equation (6.1), the integrand in the above equation will generally have one of the following forms,

$$F(\bar{y},\theta) = f\left(\vec{x},\vec{\xi}\right) \Rightarrow F(\bar{y},\theta) = f(\bar{y},\theta)\,\sqrt{(2a_1\bar{y}+a_2)^2+1}\,, \tag{6.13a}$$

$$F(\bar{y},\theta) = n_1\left(\vec{\xi}\right) f\left(\vec{x},\vec{\xi}\right) \Rightarrow F(\bar{y},\theta) = f(\bar{y},\theta), \tag{6.13b}$$

and

$$F(\bar{y},\theta) = n_2\left(\vec{\xi}\right) f\left(\vec{x},\vec{\xi}\right) \Rightarrow F(\bar{y},\theta) = -(2a_1\bar{y}+a_2)\, f(\bar{y},\theta), \tag{6.13c}$$

in which we have used the transformed expressions (6.9) for the unit vector. Equation (6.13a) refers to terms of the fundamental solution or the traction matrix which do not involve the components of the unit vector, while equations (6.13b,c) represent terms of the traction components which contain the unit vector.

The central idea of the numerical procedure proposed here is based on the following two requirements :

(a) gather the sampling points near the singularity to improve the numerical representation of the high gradients, and

(b) obtain a sampling point distribution which essentially respects the demands of equation (6.12), *i.e.*, the quantity ε must be the same at both sides of the singular point.

Although, the bi-cubic transformation may be applied directly to the integrands of (6.12) for the whole interval $[\bar{y}_1, \bar{y}_2]$, it was observed that better results can be obtained if the original interval $[\bar{y}_1, \bar{y}_2]$ is divided into smaller intervals, and especially if the subintervals right before and after the singular point are of equal length $\bar{y}_c$, which is relatively small compared to the length of the element chord. Controlling these subintervals we can enforce the above two requirements more effectively and especially the second one. A good choice for the length $\bar{y}_c$ is found to be:

$$\bar{y}_c = \tfrac{1}{4} \min(\bar{y}_1, \bar{y}_2). \tag{6.14}$$

The suggested method of subdivision is shown graphically in Figure 6.3, where also the intervals $[\bar{y}_1, -\bar{y}_c]$ and $[\bar{y}_c, \bar{y}_2]$ have been bisected, although it is not necessary for most applications. If this approach is applied to the integrals of equation (6.12), it yields the following expression for the evaluation of the singular integral I_0,

$$I_0 = \int_{\bar{y}_1}^{\bar{y}_2} F(\bar{y},\theta)\, d\bar{y} = \int_{\bar{y}_1}^{-\bar{y}_c} F(\bar{y},\theta)\, d\bar{y}$$

$$+ \lim_{\varepsilon\to 0}\left[\int_{-\bar{y}_c}^{-\varepsilon} F(\bar{y},\theta)\, d\bar{y} + \int_{\varepsilon}^{\bar{y}_c} F(\bar{y},\theta)\, d\bar{y}\right] + \int_{\bar{y}_c}^{\bar{y}_2} F(\bar{y},\theta)\, d\bar{y} \ . \qquad (6.15)$$

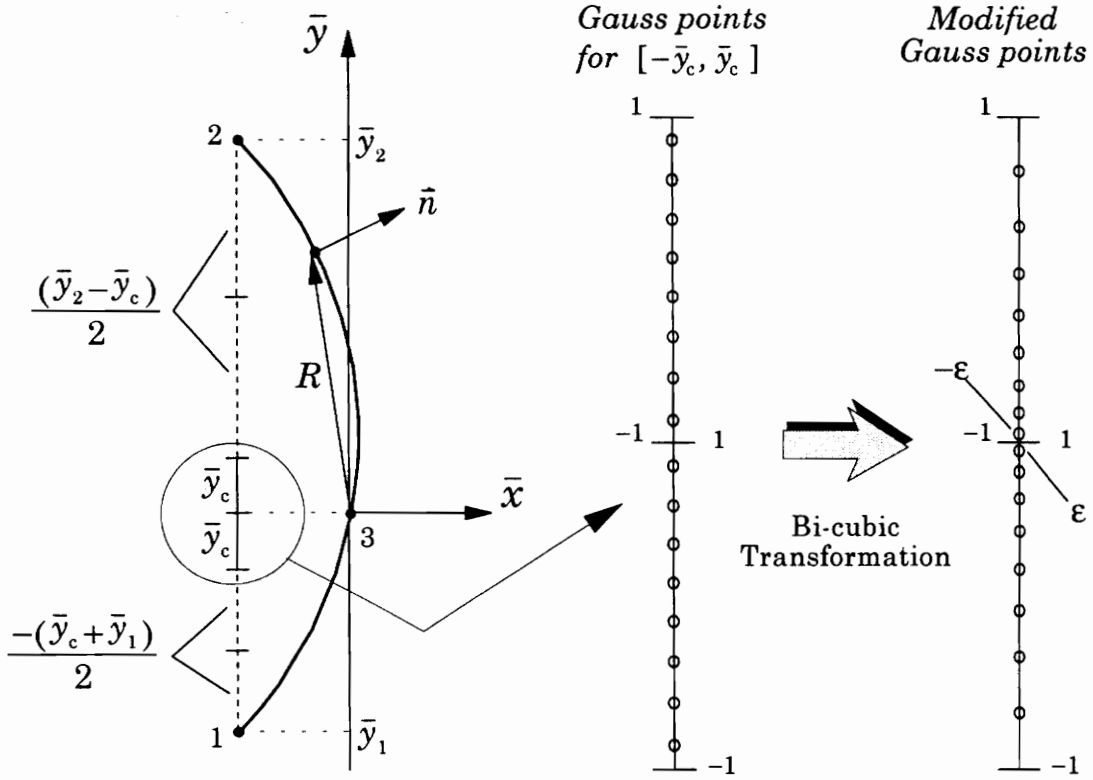

Figure 6.3 Element subdivisions and bi-cubic transformation for the evaluation of the singular integrals.

Each of the two integrals in brackets of equation (6.15) must be mapped into a domain $\eta[-1, 1]$ in order to evaluate them numerically by means of standard Gaussian quadratures. This mapping is performed using two cubic functions (hence the name *bi-cubic transformation*) which are defined over both sides of the singularity, and they have the following general form:

$$Y_i(\eta) = A_i\,\eta^3 + B_i\,\eta^2 + C_i\,\eta + D_i \qquad (i = 1, 2) \tag{6.16}$$

where $i = 1$ and $i = 2$ denote, respectively, the regions before and after the singularity. The following conditions must be satisfied by the two functions:

$$Y_1(-1) = -\bar{y}_c\,, \qquad Y_1(1) = 0 \tag{6.17a,b}$$

$$Y_1(\eta_l) = -\varepsilon \tag{6.18}$$

$$\left.\frac{dY_1}{d\eta}\right|_{\eta=1} = 0 \tag{6.19}$$

and

$$Y_2(-1) = 0\,, \qquad Y_2(1) = \bar{y}_c \tag{6.20a,b}$$

$$Y_2(\eta_f) = \varepsilon \tag{6.21}$$

$$\left.\frac{dY_2}{d\eta}\right|_{\eta=-1} = 0 \tag{6.22}$$

where $\eta_l = -\eta_f$ is the last point in the Gaussian quadrature. Restraints (6.17) and (6.20) impose, respectively, the new integration bounds for the intervals before and after the singular point. The conditions (6.18) and (6.21) force the images of the last Gauss point (*i.e.*, η_l) in the interval $[-\bar{y}_c, 0]$, and the first Gauss point (*i.e.*, η_f) in the interval $[0, \bar{y}_c]$ to be placed at distances $-\varepsilon$ and ε, respectively, from the singular point (see Figure 6.3). Finally, restraints (6.19) and (6.22) smooth out the singularity near the singular point and, therefore, an even better accuracy can be achieved.

The application of the previous conditions to equations (6.16) yields the following polynomial coefficients,

$$\left.\begin{aligned} A_1 &= \frac{-1}{1+\eta_l}\left[\tfrac{1}{4}\bar{y}_A + \frac{\varepsilon}{(1-\eta_l)^2}\right], & B_1 &= -A_1 + \tfrac{1}{4}\bar{y}_A \\ C_1 &= -A_1 - \tfrac{1}{2}\bar{y}_A\,, & D_1 &= A_1 + \tfrac{1}{4}\bar{y}_A \end{aligned}\right\} \tag{6.23}$$

$$A_2 = \frac{1}{1-\eta_f}\left[\tfrac{1}{4}\,\bar{y}_B - \frac{\varepsilon}{(1+\eta_f)^2}\right], \qquad B_2 = A_2 + \tfrac{1}{4}\,\bar{y}_B$$

$$C_2 = -A_2 + \tfrac{1}{2}\,\bar{y}_B\,, \qquad D_2 = -A_2 + \tfrac{1}{4}\,\bar{y}_B \qquad (6.24)$$

for the first and second cubic polynomials, respectively. In the above expressions (6.23) and (6.24) it is $\bar{y}_A = -\bar{y}_c$ and $\bar{y}_B = \bar{y}_c$ (Figure 6.3).

According to the previous analysis, the numerical evaluation of the integrals in equation (6.15) by means of the bi-cubic transformation is going to be as follows

$$I_0 \approx \int_{\bar{y}_1}^{-\bar{y}_c} F(\bar{y},\theta)\; d\bar{y} + \sum_{k=1}^{NGP} w_k \left\{ F\Big(Y_1(\eta_k),\theta\Big)\, \mathrm{J}_1(\eta_k) + F\Big(Y_2(\eta_k),\theta\Big)\, \mathrm{J}_2(\eta_k)\right\} + \int_{\bar{y}_c}^{\bar{y}_2} F(\bar{y},\theta)\; d\bar{y} \qquad (6.25)$$

where

$$\mathrm{J}_i(\eta) = 3A_i\,\eta^2 + 2B_i\,\eta + C_i \qquad (6.26)$$

are the Jacobians of the two transformations, and η_k and w_k are the abscissas and the weights of the Gaussian quadrature of order *NGP*. The use of the same order of quadrature in both intervals of integration is implicit in equation (6.25). The intervals $[\bar{y}_1, -\bar{y}_c\,]$ and $[\bar{y}_c, \bar{y}_2\,]$ do not have any singular points and thus the integration can be performed using standard Gaussian quadrature rules.

This approach was tested for various types of singular functions found in equations (3.51) and (3.63) of the present work and also other found in the literature (Jun *et al.*, 1985; Telles, 1987; Katsikadelis and Kokkinos, 1987), and

the results were always in excellent agreement with the exact values. For example, if each of the outer intervals $[\bar{y}_1, -\bar{y}_c]$ and $[\bar{y}_c, \bar{y}_2]$, is subdivided into two equal intervals (Figure 6.3), and if a 24-point quadrature rule is used for all numerical integrations in (6.25), with a value of $\varepsilon = 2 \times 10^{-6}\ \bar{y}_c(1-\eta_l)$, which for $NGP = 24$ becomes almost $\varepsilon = 10^{-8}\ \bar{y}_c$, then the error is consistently less than 10^{-5} %. When the element is symmetric about the $\bar{x}$ axis and the nodal point is located at the center of the element, subdivision of the outer intervals is not required. In this case, the 8-point quadrature rule applied for all numerical integrations in (6.25) and a value of $\varepsilon = 2 \times 10^{-5}\ \bar{y}_c(1-\eta_l)$, produce excellent results and the error is less than 3×10^{-4} %. For the numerical evaluation of line integrals involved in the present work, we adopt a subdivision into four intervals: $[\bar{y}_1, -\bar{y}_c]$, $[-\bar{y}_c, 0]$, $[0, \bar{y}_c]$ and $[\bar{y}_c, \bar{y}_2]$, as it is demonstrated in equation (6.25). The $\bar{y}_c$ is computed according to (6.14) and, for all four intervals, the number of Gauss points in the quadrature is $NGP = 8$. It should also be noted that for both regular and singular integrals, the Bessel functions involved in the expressions of the fundamental solution are evaluated numerically, according to the equations provided in Appendix D.

6.2 NUMERICAL EVALUATION OF DOMAIN INTEGRALS

6.2–1 Introduction

The formulation of the multilayered plate problem using integral equations produces, except from the boundary integrals (contour integrals) which were studied in the previous section, domain integrals. The domain integrals appear in the integral representation of the solution in equation (5.4) as influence or coefficient matrices. In the case of a single numerical layer, these

integrals introduce into the model the effect of the prescribed surface tractions and body forces on the displacement components at a point $\vec{\xi}$ of the layer's domain Ω_e (equations 5.16 and 5.17), while in the case of a multilayered system, they introduce the effect of the unknown interlaminar tractions and prescribed body forces (equations 5.28 and 5.29). The numerical evaluation of domain integrals is facilitated by discretizing the domain Ω_e into a number of elements, creating in this way a finite element mesh as it is shown in Figure 5.1. The mesh used in the present analysis consists of triangular three-node linear isoparametric elements (Cruse, 1969) and the surface tractions are approximated over each triangular region with the corresponding linear interpolation functions (Reddy, 1993).

The general form of the domain integrals may be written as

$$I_k\left(\vec{\xi}\right) = \int_{\Omega_e^m} f\left(\vec{x}, \vec{\xi}\right) \phi_k(\vec{x}) \; d\Omega(\vec{x}), \tag{6.27}$$

where the two-point function $f(\vec{x}, \vec{\xi})$ represents the components of the fundamental solution $U^e_{\alpha\beta}(\vec{x}, \vec{\xi})$ or the components of its derivatives with respect to the coordinates ξ_1 and ξ_2. The functions $\phi_k(\vec{x})$ $(k = 1, 2, 3)$ are the linear two-dimensional interpolation functions used in equation (5.2) for the approximation of the surface tractions, and Ω_e^m is the m-th triangular element of the e-th layer. The reference point $\vec{\xi}\,(\xi_1, \xi_2)$ may be a point on the boundary or in the domain of the numerical layer, and it may coincide with boundary or domain nodal points. When the reference point coincides with the p-th boundary nodal point, the domain integral has the form given in equation (5.6).

The domain integral in equation (6.27) behaves differently depending on the position of the reference point relative to the triangular element of integration. The integral is characterized as *regular* for $\vec{\xi} \notin \Omega_e^m$, *singular* for $\vec{\xi} \in \Omega_e^m$, and *near-singular* or *quasi-singular* when the point $\vec{\xi}$ is very close to

the boundaries of the domain Ω_e^m. Numerical evaluation of all three types of domain integrals has been studied extensively in the literature and many of the proposed techniques produce accurate results. The regular integrals are usually evaluated using standard Gaussian quadratures over each domain element. This approach is used by the finite element method (Reddy, 1993) and the boundary element method (Brebbia *et al.*, 1984), and extensive research work has been published on quadrature formulas over triangular elements and their applications (Cowper, 1973).

The singular and quasi-singular integrals are a major concern for the BEM, since they also contribute to the main diagonal of the influence (coefficient) matrices of the numerical model (see, equation 5.33). A common technique to overcome the singularity is subdivision of the target element (to which the field point is internal) into sub-elements with the field point as a vertex to each of them (Lachat and Watson, 1976; Crook and Smith, 1992). In this case the reference point is on the boundary of the sub-element, and since the Gauss points are in the domain of the sub-element, the singularity technically is weakened. Another approach is to formulate the problem in a way that eliminates the singularity of all the integrands through analytical integration (Takhteyev and Brebbia, 1990) or Taylor expansion of the critical terms (Cruse and Aithal, 1993). This technique, although it is very effective, it is greatly dependent on the functions that construct the fundamental solution of the problem. Zhang and Xu (1989) used the triangle polar coordinate mapping for the Cauchy principal value integral in three-dimensional problems, and Liao and Xu (1992) suggested a method which expresses the singular integral as the sum of a weakly singular integral, which is computed by means of the standard Gaussian quadrature, and an integrable Cauchy principal value integral, which is calculated by direct integration in the Cauchy principal value sense.

For near-singular integration, the usual Gauss integration procedure with simple elemental subdivision has been considered by Jun *et al.* (1985). Lutz (1992) used the fundamental definition of Gaussian integration to derive for specific integrands new quadrature points and weights that apply at particular normalized distances from the element. A method by Telles (1987) based on a cubic transformation of the variables in each local coordinate direction has proved to be reliable for many applications. This technique is self-adaptive, it produces a variable lumping of the Gauss stations toward the singularity, and it can also be applied for the case of singular integrals if it is combined with a subdivision of the element.

However, the various techniques found in the literature have limitations, many of them require subdivision into sub-elements and also employ many Gauss points for a successful computation of the domain integrals. Here, the compromise between accuracy and computer time is the key factor when choosing the most appropriate scheme. Since, for the problem at hand, there is a wide variety of singular, near-singular and regular integrals that must be evaluated numerically, and the number of numerical integrations which need to be performed in order to construct all the influence matrices is enormous, we have to consider an approach that requires a small number of Gauss points, does not incorporate subdivision, it is accurate and fast, and can deal effectively with regular, singular and near-singular domain integrals. A technique with all these characteristics has been developed and is presented in the following sections. The technique is semi-analytical in nature, it is developed primarily for the singular cases and it is applied in the same way to regular and near-singular domain integrals. The proposed method converts, through an analytic integration, the singular integral over the triangular domain to a definite and regular integral along the three sides of the element. The regular and definite integrals may then be evaluated

numerically using a standard Gaussian quadrature (for all cases, an 8-point quadrature gives excellent results). The regular or quasi-singular integrals are treated as a special case of the singular, by superimposing the results of a singular integration over three new triangular domains which are defined by the field point $\vec{\xi} \notin \Omega_e^m$ and each side of the original triangle Ω_e^m.

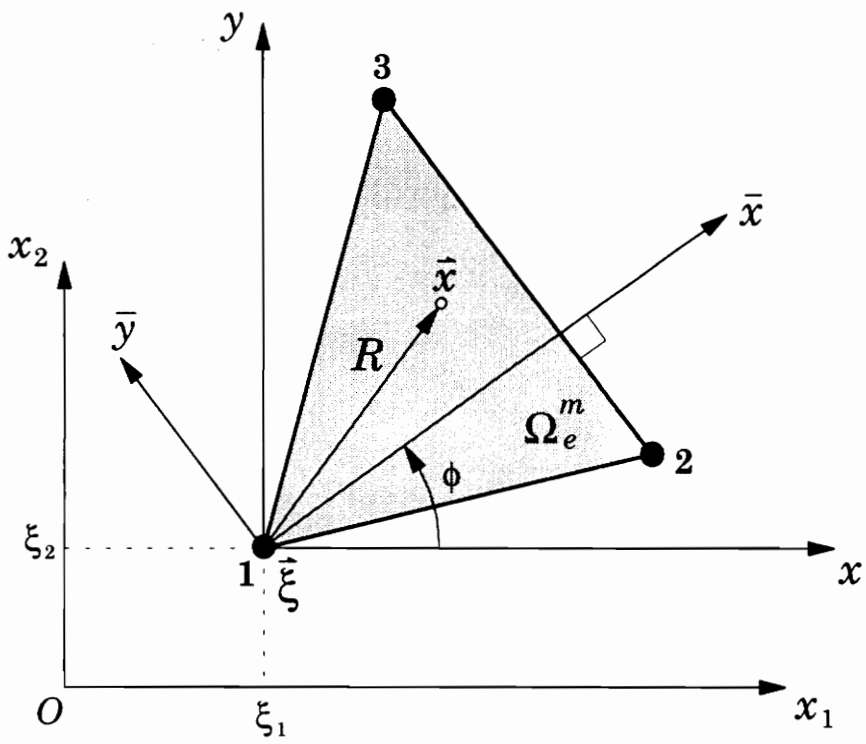

Figure 6.4 Typical triangular element and coordinate systems for the numerical evaluation of singular domain integrals.

6.2–2 Conversion of Singular Domain Integrals to Definite Integrals

Consider the typical triangular element occupying the domain Ω_e^m, as it is shown in Figure 6.4, and assume that the field point $\vec{\xi}(\xi_1, \xi_2)$ coincides with the local node-1 of the domain element. Since all the functions $f(\vec{x}, \vec{\xi})$ in the integrand of equation (6.27) depend on the relative position $(\vec{x} - \vec{\xi})$ of the field

point $\vec{\xi}$ and the integration point $\vec{x}$, the domain integral may be evaluated in a Cartesian coordinate system having its origin at $\vec{\xi}$ and axes x and y parallel to the x_1 and x_2 axes, respectively. The coordinates of point $\vec{x}$ in the xy-system are

$$x = x_1 - \xi_1 , \qquad y = x_2 - \xi_2 \tag{6.28}$$

and the distance R between the points $\vec{x}$ and $\vec{\xi}$ is

$$R = \sqrt{(x_1 - \xi_1)^2 + (x_2 - \xi_2)^2} = \sqrt{x^2 + y^2} . \tag{6.29}$$

The domain integral in the new Cartesian system may now be written as

$$I_k\left(\vec{\xi}\right) = \int_{\Omega_e^m} f(x,y)\, \phi_k(x,y)\; dx\, dy. \tag{6.30}$$

The domain integral of equation (6.30) is transformed to a new coordinate system which is obtained by rotating the xy-system through an angle ϕ in the counterclockwise direction, which is also the direction from node-2 to node-3, so that the new $\bar{x}$-axis is perpendicular to the side 2-3 of the triangle and $\bar{y}$ has the same orientation as the line segment from point 2 to point 3. This transformation is similar to the one used for the evaluation of the line integrals in the previous section, and is the key point in reducing the domain integrals to line integrals. In the new system the linear interpolation functions associated with the triangular element are

$$\phi_1(\bar{x},\bar{y}) = 1 - \frac{\bar{x}}{\bar{x}_2}, \tag{6.31a}$$

$$\phi_2(\bar{x},\bar{y}) = \frac{\bar{y}_3}{\bar{y}_3 - \bar{y}_2}\,\frac{\bar{x}}{\bar{x}_2} - \frac{\bar{y}}{\bar{y}_3 - \bar{y}_2}, \tag{6.31b}$$

and

$$\phi_3(\bar{x},\bar{y}) = \frac{-\bar{y}_2}{\bar{y}_3 - \bar{y}_2}\,\frac{\bar{x}}{\bar{x}_2} + \frac{\bar{y}}{\bar{y}_3 - \bar{y}_2}, \tag{6.31c}$$

where $\bar{x}_i$ and $\bar{y}_i$ are the transformed coordinates of the nodes $i = 2, 3$, and which can be computed from the coordinate transformation of equation (6.4) by setting $\theta = \phi$. It is apparent that for node-1 it is: $\bar{x}_1 = \bar{y}_1 = 0$, since this point is the origin for both systems, xy and $\bar{x}\bar{y}$. The expressions (6.31) are derived by assuming linear interpolation functions over the triangular element of the form

$$\phi_i(\bar{x}, \bar{y}) = a_i\, \bar{x} + b_i\, \bar{y} + c_i \qquad (i = 1, 2, 3), \tag{6.32}$$

then imposing the conditions that must be satisfied by these functions at the three nodes:

$$\phi_1(\bar{x}_1, \bar{y}_1) = 1, \quad \phi_1(\bar{x}_2, \bar{y}_2) = 0, \quad \phi_1(\bar{x}_3, \bar{y}_3) = 0 \tag{6.33}$$

$$\phi_2(\bar{x}_1, \bar{y}_1) = 0, \quad \phi_2(\bar{x}_2, \bar{y}_2) = 1, \quad \phi_2(\bar{x}_3, \bar{y}_3) = 0 \tag{6.34}$$

$$\phi_3(\bar{x}_1, \bar{y}_1) = 0, \quad \phi_3(\bar{x}_2, \bar{y}_2) = 0, \quad \phi_3(\bar{x}_3, \bar{y}_3) = 1 \tag{6.35}$$

and finally, solving the three systems of equations.

The last in these series of transformations will be one from the Cartesian bar-coordinates to triangle polar coordinates, as it is depicted in Figure 6.5. The bar-coordinates will be expressed in terms of the polar coordinates as

$$\bar{x} = R\, \cos\theta \quad \text{and} \quad \bar{y} = R\, \sin\theta\,, \tag{6.36}$$

or

$$\bar{y} = \bar{x}\, \tan\theta\,, \tag{6.37}$$

where θ is the angle between the $\bar{x}$-axis and the position vector to point $\vec{x}$, and R has been defined in (6.29). Using equation (6.37) into the polynomials (6.31) for the linear interpolation functions, we obtain:

$$\phi_1(\bar{x}, \theta) = 1 - \psi_1\, \bar{x}\,, \quad \phi_2(\bar{x}, \theta) = \psi_2(\theta)\, \bar{x}\,, \quad \text{and} \quad \phi_3(\bar{x}, \theta) = \psi_3(\theta)\, \bar{x} \tag{6.38}$$

in which the functions ψ_i are defined as

$$\psi_1 = \frac{1}{\bar{x}_2} = \psi_2(\theta) + \psi_3(\theta) \tag{6.39a}$$

$$\psi_2(\theta) = \frac{1}{\bar{y}_3 - \bar{y}_2}\left(\frac{\bar{y}_3}{\bar{x}_2} - \tan\theta\right) \tag{6.39b}$$

$$\psi_3(\theta) = \frac{1}{\bar{y}_3 - \bar{y}_2}\left(-\frac{\bar{y}_2}{\bar{x}_2} + \tan\theta\right) \tag{6.39c}$$

where ψ_1 is constant and $\bar{x}_3 = \bar{x}_2$ (Figure 6.5).

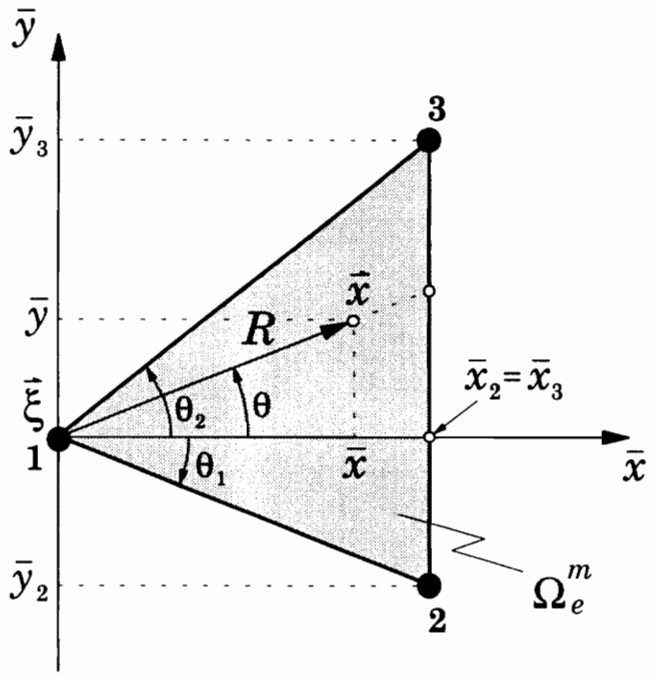

Figure 6.5 Typical triangular element in the $\bar{x}\bar{y}$-coordinate system and triangle polar coordinates.

Substituting equation (6.37) into (6.4), we derive the relations for the direct transformation from the xy-coordinates to the triangle polar coordinates $\bar{x}$ and θ,

$$x = \frac{\cos(\phi + \theta)}{\cos\theta}\,\bar{x} \quad \text{and} \quad y = \frac{\sin(\phi + \theta)}{\cos\theta}\,\bar{x}\,. \tag{6.40}$$

This transformation applied to the domain integrals of (6.30) yields the following double integral in the final coordinate system

$$I_k\left(\vec{\xi}\right) = \int_{\theta_1}^{\theta_2} \int_0^{\bar{x}_2} f(\bar{x},\theta)\, \phi_k(\bar{x},\theta)\, J(\bar{x},\theta)\, d\bar{x}\, d\theta \tag{6.41}$$

where $J(\bar{x},\theta)$ is the Jacobian for the transformation from xy to polar coordinates, and is given as

$$J(\bar{x},\theta) = \det \begin{bmatrix} \dfrac{\partial x}{\partial \bar{x}} & \dfrac{\partial y}{\partial \bar{x}} \\ \dfrac{\partial x}{\partial \theta} & \dfrac{\partial y}{\partial \theta} \end{bmatrix} = \frac{\bar{x}}{\cos^2\theta}. \tag{6.42}$$

The limits θ_1 and θ_2 of the integration in (6.41) may be expressed in terms of the coordinates of the nodal points 2 and 3, as

$$\theta_1 = \tan^{-1}\left(\frac{\bar{y}_2}{\bar{x}_2}\right) \quad \text{and} \quad \theta_2 = \tan^{-1}\left(\frac{\bar{y}_3}{\bar{x}_2}\right). \tag{6.43}$$

It is interesting to note that, at the beginning of this analysis the geometry and orientation of the element in the bar-system was described by the coordinates of the nodal points 2 and 3, while now the element is described by another set of four quantities which are: the angle ϕ for the orientation of triangle, and the polar coordinates $\bar{x}_2$, θ_1 and θ_2 for its geometry.

Introducing equations (6.38) and (6.42) in the domain integral of equation (6.41), we find

$$I_1\left(\vec{\xi}\right) = \int_{\theta_1}^{\theta_2} \frac{L_1(\theta) - \psi_1 L_2(\theta)}{\cos^2\theta}\, d\theta = \int_{\theta_1}^{\theta_2} \frac{L_1(\theta)}{\cos^2\theta}\, d\theta - I_2\left(\vec{\xi}\right) - I_3\left(\vec{\xi}\right), \tag{6.44a}$$

$$I_2\left(\vec{\xi}\right) = \int_{\theta_1}^{\theta_2} L_2(\theta)\, \frac{\psi_2(\theta)}{\cos^2\theta}\, d\theta, \tag{6.44b}$$

and

$$I_3\left(\vec{\xi}\right) = \int_{\theta_1}^{\theta_2} L_2(\theta)\, \frac{\psi_3(\theta)}{\cos^2\theta}\, d\theta \tag{6.44c}$$

where

$$L_1(\theta) = \int_0^{\bar{x}_2} \bar{x}\, f(\bar{x}, \theta)\ d\bar{x}\ , \tag{6.45a}$$

and

$$L_2(\theta) = \int_0^{\bar{x}_2} \bar{x}^2\, f(\bar{x}, \theta)\ d\bar{x}\ . \tag{6.45b}$$

The kernel functions $f(\vec{x}, \vec{\xi})$, which in triangle polar coordinates are expressed as $f(\bar{x}, \theta)$, are either the components of the fundamental solution or its derivatives with respect to the coordinates ξ_1 and ξ_2, as it was also mentioned in the introductory part of this chapter. However, all these quantities are related to the functions $f_{\alpha\beta}(x, y)$ of equations (3.51), (3.63) and (3.80), and thus the integrals in equation (6.45) may be evaluated analytically for all these functions. This task can always be accomplished easily and effortlessly through symbolic algebra on a computer (Wolfram, 1991). The expressions for the integrals $L_1(\theta)$ and $L_2(\theta)$ have been obtained for all the functions $f_{\alpha\beta}$ of Chapter 3, using symbolic algebra and properties of the modified Bessel functions of the second kind and properties of their integrals (Wheelon, 1968; Luke, 1962; McLachlan, 1941). These expressions have been implemented directly into a computer code for the numerical evaluation of domain integrals. The only integral, which is not evaluated analytically, is that of the Bessel function $K_0(\bar{x})$ from zero to $\bar{x}_2$, but for this integral one may find expressions for its numerical evaluation in Appendix D.

Substituting equations (6.39) for the interpolation functions and (6.43) for the ordinates of nodes 2 and 3 in the polar coordinate system in the integrals of equation (6.44), we obtain the final expressions for the evaluation of the singular domain integrals (6.27):

$$I_1\left(\vec{\xi}\right) = R_1(\theta_1, \theta_2) - \frac{1}{\bar{x}_2} R_2(\theta_1, \theta_2) \tag{6.46a}$$

$$I_2\left(\vec{\xi}\right) = \frac{\tan\theta_2\ R_2(\theta_1,\theta_2) - R_3(\theta_1,\theta_2)}{\bar{x}_2\ (\tan\theta_2 - \tan\theta_1)} \tag{6.46b}$$

$$I_3\left(\vec{\xi}\right) = \frac{-\tan\theta_1\ R_2(\theta_1,\theta_2) + R_3(\theta_1,\theta_2)}{\bar{x}_2\ (\tan\theta_2 - \tan\theta_1)} \tag{6.46c}$$

where $R_i(\theta_1,\theta_2)$ $(i=1,2,3)$ denote regular and definite integrals over the angle θ and they are given as

$$R_1(\theta_1,\theta_2) = \int_{\theta_1}^{\theta_2} \frac{L_1(\theta)}{\cos^2\theta}\, d\theta, \tag{6.47a}$$

$$R_2(\theta_1,\theta_2) = \int_{\theta_1}^{\theta_2} \frac{L_2(\theta)}{\cos^2\theta}\, d\theta, \tag{6.47b}$$

and

$$R_3(\theta_1,\theta_2) = \int_{\theta_1}^{\theta_2} \frac{\tan\theta}{\cos^2\theta}\, L_2(\theta)\, d\theta. \tag{6.47c}$$

The above three integrals are evaluated numerically using a standard quadrature rule. The Bessel functions involved in some of the integrands are computed numerically using the formulae in Appendix D.

The procedure for computing the integrals $I_k(\xi_1,\xi_2)$ of equation (6.27) over the triangular element Ω_e^m can be summarized for the singular case where the reference point $\vec{\xi}(\xi_1,\xi_2)$ coincides with the local node-1 of the triangular element in the following five steps:

(1) Express the kernel functions $f(\vec{x},\vec{\xi}) = f(x,y)$ in terms of the triangle polar coordinates $\bar{x}$ and θ using the transformation (6.40).

(2) Determine the geometry and orientation of the triangular element in the polar coordinate system by calculating the ϕ, $\bar{x}_2$, θ_1 and θ_2 from the coordinates of nodes 2 and 3 (equations 6.4 and 6.43).

(3) Derive analytic expressions for the integrals $L_1(\theta)$ and $L_2(\theta)$ of equations (6.45).

(4) Compute numerically the definite integrals $R_1(\theta_1, \theta_2)$, $R_2(\theta_1, \theta_2)$ and $R_3(\theta_1, \theta_2)$ of equation (6.47), by employing a 8-point Gaussian quadrature rule.

(5) Finally, obtain the values for the integrals $I_k(\xi_1, \xi_2)$ by substituting the results of the previous four steps into equations (6.46).

6.2–3 Evaluation of Singular Domain Integrals

The methodology developed in Section 6.2–2 applies to the special case where the reference point $\vec{\xi}$ is located at one of the nodal points of the triangular element Ω_e^m, and in particular at node 1. Generally, the reference point can be anywhere on the plane Ω_e of the numerical layer, and if it is in the triangular element or on one of its three sides, the domain integrals of equation (6.27) become singular.

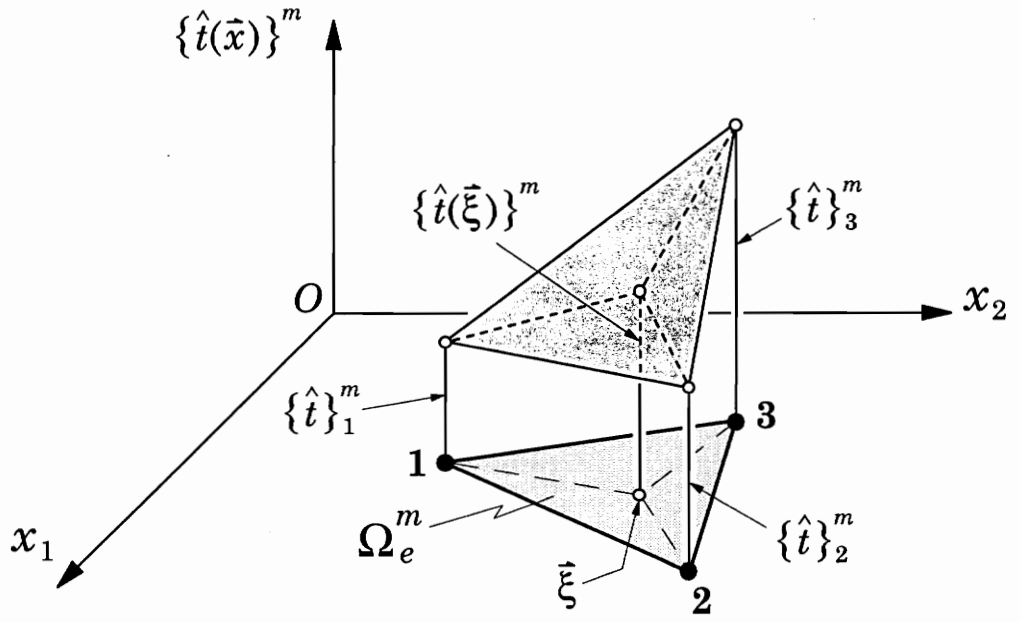

Figure 6.6 Linear distribution of the surface tractions over a triangular element which contains the reference point.

In order to evaluate the singular integrals for these two cases, let us assume that $\vec{\xi} \in \Omega_e^m$ as it is shown in Figures 6.6 or 6.7, and denote the vector of the surface tractions associated with this point by $\left\{\hat{t}(\vec{\xi})\right\}$ and the corresponding vectors at the three nodes of the m-th element by $\left\{\hat{t}\right\}_k^m$ (Figure 6.6). Since the tractions are approximated over the element using the linear interpolation functions (equation 5.2), the traction vector at point $\vec{\xi}$ may be expressed in terms of the nodal values as

$$\left\{\hat{t}\left(\vec{\xi}\right)\right\} = \left\{\hat{t}\right\}_\xi^m = \sum_{k=1}^{3} \phi_k\left(\vec{\xi}\right) \left\{\hat{t}\right\}_k^m$$

$$= \phi_1(\xi_1, \xi_2) \left\{\hat{t}\right\}_1^m + \phi_2(\xi_1, \xi_2) \left\{\hat{t}\right\}_2^m + \phi_3(\xi_1, \xi_2) \left\{\hat{t}\right\}_3^m . \quad (6.48)$$

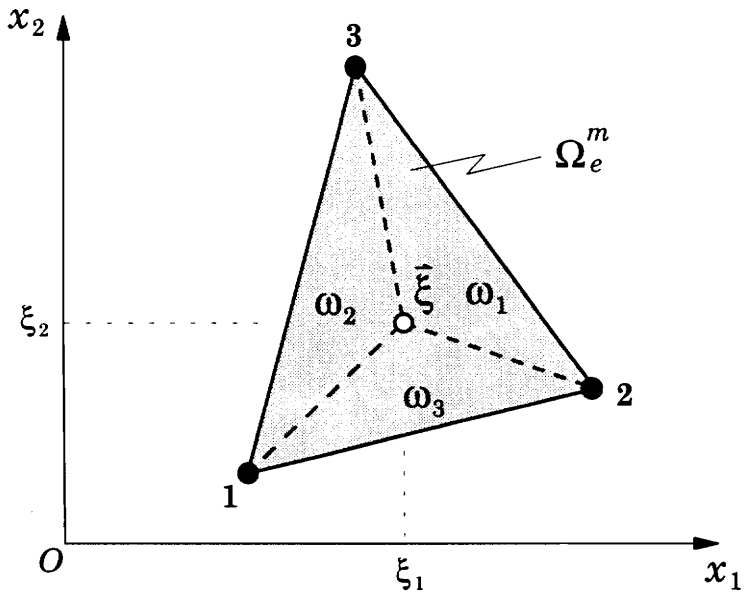

Figure 6.7 Subdivision of a triangular element for reference point located in the domain of the element.

Having the reference point inside the triangular domain, the element is subdivided into three sub-elements with a common vertex at this point $\vec{\xi}$. These new triangular elements are denoted by ω_1, ω_2 and ω_3 as it is shown in Figure 6.7, and it is $\Omega_e^m = \omega_1 \cup \omega_2 \cup \omega_3$. The first sub-domain has vertices $\xi - 2 - 3$, the second $\xi - 3 - 1$ and the third $\xi - 1 - 2$, where the order in which the vertices are referred to indicates the way they are numbered locally within each sub-domain.

The domain integral which must be evaluated for all the different positions of the reference point has the general form (see equations 5.6 and 6.27)

$$\int_{\Omega_e^m} f\left(\vec{x},\vec{\xi}\right)\left\{\hat{t}(\vec{x})\right\}\, d\Omega(\vec{x}) = \left\{\hat{t}\right\}_k^m \int_{\Omega_e^m} f\left(\vec{x},\vec{\xi}\right)\phi_k(\vec{x})\, d\Omega(\vec{x}), \tag{6.49}$$

and for a reference point $\vec{\xi}$ located in the element Ω_e^m, it becomes

$$\begin{aligned}\int_{\Omega_e^m} f\left(\vec{x},\vec{\xi}\right)\left\{\hat{t}(\vec{x})\right\}\, d\Omega(\vec{x}) &= \int_{\omega_1} f\left(\vec{x},\vec{\xi}\right)\left\{\hat{t}(\vec{x})\right\}\, d\omega(\vec{x}) \\ &+ \int_{\omega_2} f\left(\vec{x},\vec{\xi}\right)\left\{\hat{t}(\vec{x})\right\}\, d\omega(\vec{x}) + \int_{\omega_3} f\left(\vec{x},\vec{\xi}\right)\left\{\hat{t}(\vec{x})\right\}\, d\omega(\vec{x})\end{aligned} \tag{6.50}$$

where $\vec{\xi}$ coincides always with the *first* local node of each sub-domain (*local* for the sub-element). All three integrals of the right-hand side of equation (6.50) are singular and they have the same form as the singular integral studied in the previous sub-section. Therefore, the proposed semi-analytical methodology can be applied for every integral in equation (6.50). Denoting the results over each sub-element ω_i $(i = 1, 2, 3)$ by $I_1^{(i)}$, $I_2^{(i)}$ and $I_3^{(i)}$, the nine integrals associated with the m-th triangular element may be evaluated using equations (6.46) and (6.47), and the singular integral of (6.50) takes the following form,

$$\int_{\Omega_e^m} f\left(\vec{x},\vec{\xi}\right)\left\{\hat{t}(\vec{x})\right\}\, d\Omega(\vec{x}) = \left\{\hat{t}\right\}_{\xi}^{m} I_1^{(1)} + \left\{\hat{t}\right\}_{2}^{m} I_2^{(1)} + \left\{\hat{t}\right\}_{3}^{m} I_3^{(1)}$$
$$+\left\{\hat{t}\right\}_{\xi}^{m} I_1^{(2)} + \left\{\hat{t}\right\}_{3}^{m} I_2^{(2)} + \left\{\hat{t}\right\}_{1}^{m} I_3^{(2)}$$
$$+\left\{\hat{t}\right\}_{\xi}^{m} I_1^{(3)} + \left\{\hat{t}\right\}_{1}^{m} I_2^{(3)} + \left\{\hat{t}\right\}_{2}^{m} I_3^{(3)} \qquad (6.51)$$

where $\left\{\hat{t}\right\}_{k}^{m}$ with $k = 1, 2, 3$ are the traction vectors at the three nodes of the m-th element, and $\left\{\hat{t}\right\}_{\xi}^{m}$ is the vector at the reference point $\vec{\xi}$.

Substitution of the linear interpolation equations of (6.48) into (6.51), yields the expression for the evaluation of the singular domain integral for a reference point $\vec{\xi}$ in the triangular element Ω_e^m:

$$\int_{\Omega_e^m} f\left(\vec{x},\vec{\xi}\right)\left\{\hat{t}(\vec{x})\right\}\, d\Omega(\vec{x}) = \left[\phi_1(\vec{\xi})\left(I_1^{(1)} + I_1^{(2)} + I_1^{(3)}\right) + I_2^{(3)} + I_3^{(2)}\right]\left\{\hat{t}\right\}_{1}^{m}$$
$$+\left[\phi_2(\vec{\xi})\left(I_1^{(1)} + I_1^{(2)} + I_1^{(3)}\right) + I_2^{(1)} + I_3^{(3)}\right]\left\{\hat{t}\right\}_{2}^{m}$$
$$+\left[\phi_3(\vec{\xi})\left(I_1^{(1)} + I_1^{(2)} + I_1^{(3)}\right) + I_2^{(2)} + I_3^{(1)}\right]\left\{\hat{t}\right\}_{3}^{m} \qquad (6.52)$$

where the values of the interpolation functions at the reference point are computed from the following expressions

$$\phi_1\left(\vec{\xi}\right) = \phi_1(\xi_1,\xi_2) = \frac{x_{(2)}\, y_{(3)} - x_{(3)}\, y_{(2)}}{A}, \qquad (6.53a)$$

$$\phi_2\left(\vec{\xi}\right) = \phi_2(\xi_1,\xi_2) = \frac{x_{(3)}\, y_{(1)} - x_{(1)}\, y_{(3)}}{A}, \qquad (6.53b)$$

and

$$\phi_3\left(\vec{\xi}\right) = \phi_3(\xi_1,\xi_2) = \frac{x_{(1)}\, y_{(2)} - x_{(2)}\, y_{(1)}}{A}, \qquad (6.53c)$$

in which the denominator A is

$$A = (x_{(2)} - x_{(1)})\,(y_{(3)} - y_{(1)}) - (x_{(3)} - x_{(1)})\,(y_{(2)} - y_{(1)})\ . \qquad (6.54)$$

In equation (6.54), $x_{(k)}$ and $y_{(k)}$ $(k = 1, 2, 3)$ denote the coordinates of the local nodal points of the triangular element Ω_e^m in the xy-Cartesian system (Figure 6.4).

Equations (6.52) can also be used to evaluate numerically domain integrals in the case where the reference point is located on one of the sides of the triangular element Ω_e^m. This case is shown in Figure 6.8 where the point $\vec{\xi}$ is placed on the side 3-1 of the element. The triangular domain is divided now into two sub-elements, namely ω_1 and ω_3, which correspond to the same sub-elements of Figure 6.7. The only difference from the previous case is that the sub-domain ω_2 has now vanished, and thus, the values of all the integrals $I_k^{(2)}$ in equation (6.52) become zero.

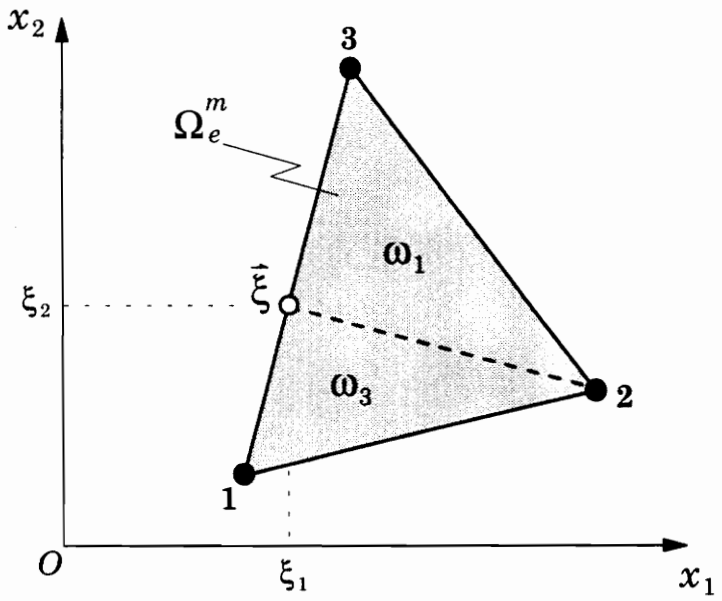

Figure 6.8 Subdivision of a triangular element for reference point located on the side 3-1 of the element.

6.2–4 Evaluation of Regular and Near-Singular Domain Integrals

Consider the triangular element Ω_e^m of Figure 6.9 and a reference point such that $\vec{\xi} \notin \Omega_e^m$. In this case the integrals of equation (6.27) are regular, or near-singular if the point is very close to the boundary of the element. These two types of domain integrals will be evaluated using the methodology developed for the singular cases and equations (6.52). This approach, when applied to regular integrals, is the most *accurate*, because the expressions developed in Section 6.2–3 can treat all the singularities analytically, and therefore the numerical scheme is not affected by the near-singular integrals. It is also the most *economical*, since it reduces the domain integrals to definite integrals, which can be evaluated very accurately by employing eight Gauss points on each side of the triangular element.

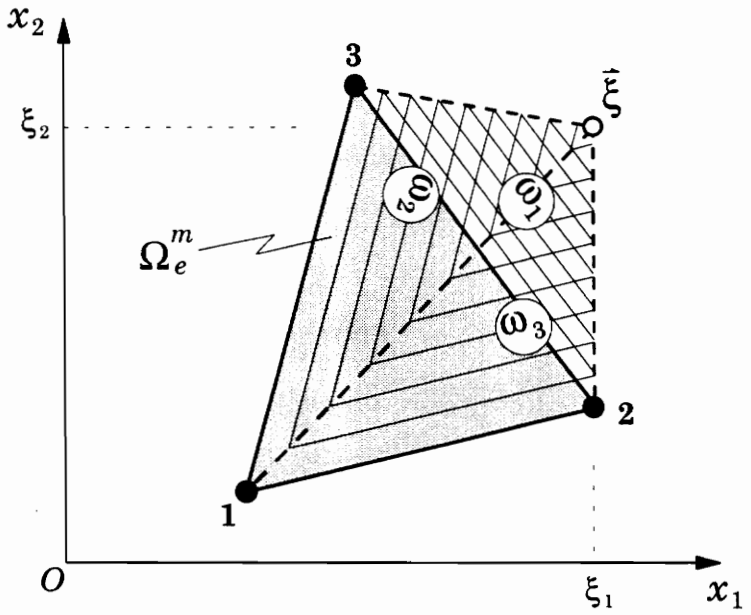

Figure 6.9 Subdivision of an element for reference point located out of the triangular domain.

The three domains of integration, ω_1, ω_2 and ω_3, are depicted in Figure 6.9 by the cross-hatched areas and the domain Ω_e^m is composed from the three sub-domains as $\Omega_e^m = \omega_2 \cup \omega_3 \cup (-\omega_1)$. The fact that the domain ω_1, along with the corresponding integrals over this region, must be subtracted from the other two domains and the integrals associated with them, is due to the specific position of $\vec{\xi}$ with respect to the element. For another position of the reference point, the domains will be combined differently, in order to produce the element Ω_e^m. Nevertheless, this situation is automatically recognized and treated by the developed procedure. That is true because, the method as it was presented for singular integrals with $\vec{\xi}$ at node-1 in Section 6.2–2, requires that the local nodes are numbered counterclockwise, and the general approach for all types of singular integrals in Section 6.2–3 was developed by considering the reference point as the first vertex for all three triangular sub-domains and for ω_1, ω_2 and ω_3 the local nodes were numbered in the order $\xi-2-3$, $\xi-3-1$ and $\xi-1-2$, respectively. So in the numerical analysis of singular integrals, the nodes are always numbered counterclockwise as it is shown in Figure 6.7. Referring now to the regular integrals, the local nodes of the triangle ω_1 will be considered in the order $\xi-2-3$ (clockwise) for the evaluation of the coefficients $I_k^{(i)}$ by the numerical scheme (equation 6.52). This order, however, for a point out of the domain Ω_e^m (Figure 6.9), is clockwise and, thus, all the integrals over the sub-domain ω_1 will have opposite sign compared to those for counterclockwise numbering of the nodes. This is exactly what we expected, according to our original observations based on Figure 6.9.

It is therefore evident that the proposed technique of Section 6.2–3 is general, and it can be used to evaluate numerically regular, near singular and all types of singular domain integrals. The method does not have any

limitations and for all the tests that were performed produced excellent results. Its salient features are the accuracy, the speed and the generality. The approach, in its present form, may also be applied to linear four-node quadrilateral elements, if each domain is subdivided into triangular sub-elements. Using the same concept and the triangle polar coordinate transformation, one can derive integration schemes for higher order elements.

6.2–5 Constant Traction Distribution over a Triangular Element

The numerical evaluation of the domain integrals, which is described by equations (6.52), is developed assuming a linear distribution of the surface tractions over the triangular element. If the surface tractions (or the body forces) are considered to be constant over each triangular element, then the expressions for the numerical evaluation of the domain integrals are simplified and the work involved in the calculations is considerably reduced.

For constant traction vector over the m-th element, the nodal values are equal and they are represented by the value at the center of the element. Denoting by $\{\hat{t}\}^m$ the value at the centroid of the triangular element, it is

$$\{\hat{t}\}_1^m = \{\hat{t}\}_2^m = \{\hat{t}\}_3^m = \{\hat{t}\}^m. \tag{6.55}$$

Incorporating equation (6.55) into (6.52) and using also the property of the interpolation functions,

$$\phi_1(\vec{\xi}) + \phi_2(\vec{\xi}) + \phi_3(\vec{\xi}) = 1, \tag{6.56}$$

the domain integral is written as follows

$$\int_{\Omega_e^m} f\left(\vec{x}, \vec{\xi}\right) \{\hat{t}(\vec{x})\}\, d\Omega(\vec{x}) = \left[I_1^{(1)} + I_2^{(1)} + I_3^{(1)} + I_1^{(2)} + I_2^{(2)} + I_3^{(2)} + I_1^{(3)} + I_2^{(3)} + I_3^{(3)}\right] \{\hat{t}\}^m \tag{6.57}$$

Moreover, it is known from equation (6.44a) that the sum of the integrals $I_k\left(\vec{\xi}\right)$ is equal to the integral of equation (6.47a), *i.e.*,

$$I_1\left(\vec{\xi}\right) + I_2\left(\vec{\xi}\right) + I_3\left(\vec{\xi}\right) = R_1(\theta_1, \theta_2)\,, \tag{6.58}$$

for reference point $\vec{\xi}$ located at node-1 of a triangular element. Combining the above relation with equation (6.57), we arrive at the following expression

$$\int_{\Omega_e^m} f\left(\vec{x}, \vec{\xi}\right) \left\{\hat{t}(\vec{x})\right\}\, d\Omega(\vec{x}) = \left[R_1^{(1)} + R_1^{(2)} + R_1^{(3)}\right] \left\{\hat{t}\right\}^m, \tag{6.59}$$

which is the general formula for the numerical evaluation of any type of domain integral for a constant traction distribution over the element. The position of the reference point is the one indicated in Figure 6.7, and from which according to the developed scheme any other configuration can be reproduced. In equation (6.59), $R_1^{(1)}$, $R_1^{(2)}$ and $R_1^{(3)}$ denote, respectively, the integral in equation (6.47a) for each of the three sub-domains ω_1 $(\xi-2-3)$, ω_2 $(\xi-3-1)$ and ω_3 $(\xi-1-2)$ of Figure 6.7. It is important to note that for constant traction components over the element, one needs only to evaluate analytically the integral $L_1(\theta)$ of equation (6.45a) and numerically the integral $R_1^{(i)}(\theta_1, \theta_2)$ of (6.47) for each of the three sub-domains ω_i.

6.3 ITERATIVE SOLUTION OF BEM EQUATIONS BY THE BI-CONJUGATE GRADIENT METHOD

The major costs of large scale finite element or boundary element calculations, particularly in three dimensions, arise from computing solutions to systems of linear equations. Direct methods, *i.e.*, those based upon Gaussian elimination, can easily require prohibitively large amounts of both CPU and

storage. Iterative procedures avoiding the formation and factorization of a global system of equations can circumvent these difficulties. Iterative techniques employed for solving FEM systems of equations (Hughes *et al.*, 1987) take advantage of the fact that the system matrix is symmetric and positive-definite. Unfortunately BEM matrices do not have any of these two favorable characteristics. This fact rules out a great number of iterative methods and makes the solution of BEM systems of equations essentially more difficult. A thorough presentation of the different iterative techniques available in the literature for BEM systems of equations can be found in the papers by Mansur *et al.* (1992), Barra *et al.* (1992), and Araújo and Mansur (1989).

For the problem of the multilayered system, the number of equations, or equivalently the number of unknown quantities, depends on the number of boundary and domain elements used to model each layer, but foremost on the number of numerical layers. Each numerical layer is represented by a set of matrices which are constructed from the equilibrium equations associated with this layer. The global matrix, which describes the whole layered system, is assembled from the matrices of the individual numerical layers (equation 5.43) through compatibility conditions, and in most of the cases it is a very large matrix. It is therefore preferable, and some times it becomes necessary, to adopt an iterative scheme for the solution of the system of equations. The technique used in the present work is the *bi-conjugate gradient method* (bi-CG) with Jacobi preconditioning matrix. This iterative solver is available in the literature (Mansur *et al.*, 1992), and it is considered to be one of the most efficient schemes and one that leads to large computer savings, especially for large systems (for applications with 522 equations the time is about four times smaller than that with the direct Gauss elimination method).

The final matrix of equations for the three-dimensional analysis of a multilayered system has been derived in Chapter 5, and it is given in equation (5.43). The system of equations, however, cannot be rendered to the iterative solver unless the coefficient matrices of the traction vectors are scaled. As it is recommended by many researchers and also checked with specific examples in the present work (two-dimensional elasticity problems), a coefficient scaling is required in order to achieve substantial reductions in the number of iterations (usually 50–60%). For the elasticity problem at hand the scale factor is chosen to be

$$C_s = \max\left[\frac{E_e}{1-\nu_e^2}\right] \tag{6.60}$$

where E_e is the modulus of elasticity and ν_e is the Poisson's ratio for the e-th numerical layer. This scaling coefficient is used to factor the coefficient matrices of all the traction vectors $\{t\}_e$ in the generalized vector $\{\tilde{\mathbf{u}}\}$, the vector $\{\mathbf{s}\}$, and those components of the vectors $\{\mathbf{q}\}$ and $\{\mathbf{p}\}$ which are not prescribed. For example, the coefficient matrix of $\{\mathbf{s}\}$ will be scaled as follows

$$\left[\mathbf{A}^{12}\right]\{\mathbf{s}\} = \left(C_s\left[\mathbf{A}^{12}\right]\right)\left(\frac{1}{C_s}\{\mathbf{s}\}\right) = \left[\mathbf{A}_s^{12}\right]\{\mathbf{s}_s\} \tag{6.61}$$

where the scaled matrices $[\mathbf{A}_s^{12}]$ and $\{\mathbf{s}_s\}$ will replace the $[\mathbf{A}^{12}]$ and $\{\mathbf{s}\}$ in the system of equations (5.43). At the end of the iterative procedure, when the solution has been obtained, the actual vectors may be computed from the scaled ones by multiplying the latter by C_s.

Once the matrices have been factored and the prescribed boundary quantities have been introduced into equation (5.43), the final form of the system of equations will become

$$[\mathbf{A}]\{\mathbf{X}\} = [\mathbf{b}] \tag{6.62}$$

where [A] is the system matrix and {X} is the vector of all the unknown quantities. It should be emphasized that [A] and {b} must not be assembled from the individual matrices of each numerical layer (see equations 5.28 and 5.29), since this will produce a very large matrix and will increase dramatically the storage requirements. In the present work, for each of the six matrices associated with a numerical layer (element), a three-dimensional matrix is created. The first two dimensions of this matrix are the same as the dimensions of the element matrix and the third is L (number of numerical layers). The entries of each element matrix are stored directly into the corresponding 3-D matrix and, along the third dimension, at the same position where the numerical layer appears in the model of the multilayered system (Figure 5.2). For the evaluation of products required by the iterative scheme and involving either [A] or {b}, subroutines have been designed especially for this purpose, which control the assembly process and evaluate these products at the element level.

The matrix [A] is preconditioned employing the splitting matrix $[Q]$, whose components are defined for the Jacobi method as

$$Q_{ij} = \begin{cases} A_{ij} & \text{if } i = j \\ 0 & \text{if } i \neq j \end{cases} \tag{6.63}$$

The algorithm for the computational implementation of the bi-conjugate gradient method with Jacobi preconditioning matrix $\{Q\}$, is given below:

$\text{TOL} = 10^{-7}$ (initial tolerance)

$\{\mathbf{X}\} = \{\mathbf{X}_0\}$ (initial solution vector)

$\{b^*\} = [Q]^{-1} \{\mathbf{b}\}$

$\text{TOL} = \text{TOL} * \sqrt{\{b^*\}^{\mathrm{T}} \{b^*\}}$ (working tolerance)

$\{r^*\} = [Q]^{-1}(\{\mathbf{b}\} - [\mathbf{A}]\{\mathbf{X}\})$

DEL0 $= \{r^*\}^{\mathrm{T}}\{r^*\} \quad \Rightarrow \quad$ SDEL0 $= \sqrt{\text{DEL0}}$

if SDEL0 $\leq$ TOL then STOP

$\{p\} = \{r^*\}$; $\{\bar{p}\} = \{r^*\}$; $\{\bar{r}^*\} = \{r^*\}$ (initialize the vectors)

R : $\{h\} = [\mathbf{A}]\{p\}$ (iterative scheme begins)

$\{h^*\} = [Q]^{-1}\{h\}$

$$\lambda = \frac{\text{DEL0}}{\{\bar{p}\}^{\mathrm{T}}\{h^*\}}$$

$\{\mathbf{X}\} = \{\mathbf{X}\} + \lambda\{p\}$

$\{r^*\} = \{r^*\} - \lambda\{h^*\}$

DEL1 $= \{r^*\}^{T}\{r^*\} \quad \Rightarrow \quad$ SDEL1$= \sqrt{\text{DEL1}}$

if SDEL1 $\leq$ TOL then STOP

$\{h\} = [Q]^{-1}\{\bar{p}\}$

$\{h^*\} = [\mathbf{A}]^{\mathrm{T}}\{h\}$

$\{\bar{r}^*\} = \{\bar{r}^*\} - \lambda\{h^*\}$

DEL1 $= \{\bar{r}^*\}^{\mathrm{T}}\{r^*\}$

$\alpha = \dfrac{\text{DEL1}}{\text{DEL0}}$, DEL0 = DEL1

$\{p\} = \{r^*\} + \alpha\{p\}$ (the new vectors $\{p\}$ and $\{\bar{p}\}$)

$\{\bar{p}\} = \{\bar{r}^*\} + \alpha\{\bar{p}\}$

GOTO R (next iteration)

In the above iterative scheme the superscript T denotes transpose and the initial solution vector is usually chosen to be $\{\mathbf{X}_0\} = \{0\}$. The matrix $[Q]^{-1}$ is the inverse of the preconditioning matrix, and it is given as

$$[Q]^{-1} = \begin{bmatrix} \frac{1}{A_{11}} & 0 & 0 & \\ 0 & \frac{1}{A_{22}} & 0 & \\ 0 & 0 & \frac{1}{A_{33}} & \\ & & & \ddots \end{bmatrix} \tag{6.64}$$

where A_{ij} denote the entries of the system matrix [A]. These entries are extracted from the three-dimensional matrices, in which we have stored the matrices of each numerical layer.

Chapter 7

CONCLUSIONS AND RECOMMENDATIONS

7.1 SUMMARY AND CONCLUSIONS

A hybrid methodology has been developed for the analysis of layers, plates, and multilayered systems consisting of isotropic linear elastic materials. The multilayered system can have irregular shapes and can contain inclusions and holes. It can be subjected to body forces distributed over the entire volume or over a subregion, line loads and/or point loads either on the boundary or in the domain, and distributed boundary tractions. Regarding the support conditions, the boundary of the multilayered system may be free, clamped, or subjected to prescribed displacements along parts of it and/or at discrete points. It may also be elastically supported over a part or at discrete points on the boundary, and simply supported in a prescribed direction at a point.

The system may be resting on elastic foundation or be rigidly supported at specific areas or points of its bottom and top surfaces (internal supports).

The method decomposes the three-dimensional elasticity problem in a one-dimensional problem through the thickness, and a two-dimensional problem in the plane. A one-dimensional finite element model is constructed for the analysis of the first problem and an exact solution is derived for the second problem. This exact solution is represented by integral equations along the boundaries of the layers. The multilayered system is modeled by discretizing its thickness into numerical layers, and its boundaries into boundary elements. The proposed method models this complicated elasticity problem, which has many interesting physical applications, and provides continuous solutions for the displacement and stress fields over the entire domain of the problem, the strains in each layer, the interlaminar stresses and other localized effects. One of the most fascinating features of this hybrid methodology is that, a thorough three-dimensional analysis is performed by using only contour integrals (boundary integrals).

This innovative method is based on an energy formulation which involves only the displacement components. The total potential energy produces, first, the weak form of the problem, which is used to introduce the layerwise approximation of the displacement field, and then, it produces the governing equations for an infinite layer subjected to a concentrated load. Furthermore, it serves as the foundation for the development of the integral equation model. Through this energy formulation, we not only model the thickness problem and derive the equations of the fundamental problem, but we also manage to couple a finite element formulation through the thickness of the plate, with a boundary integral equation formulation for the plane problem. The usual way of coupling the two methods is to discretize the structure into

elements and to apply appropriate compatibility conditions at the common nodal points of the two models. This approach is not so accurate, because it does weigh evenly the residual (error) over the domain of the problem.

The boundary integral equations can produce the integral representation of the solution, only if the fundamental solution of the problem is available. Since, for the problem at hand, such a solution is not available in the literature, we have proposed a systematic approach for deriving semi-analytical fundamental solutions for the typical infinite numerical layer. This approach incorporates the method of integral Fourier transforms and has been demonstrated for the case of a linear displacement approximation through the thickness of the layer. The fundamental solution has been used to derive expressions for the traction components and the stresses in the infinite layer, and also to produce a Somigliana-type identity for the typical numerical layer. Boundary integral equations have been obtained for the displacement components at points on the boundary of the layer, and the stress and strain components at any point of the layer.

The boundary integral equations have been discretized using the boundary element method and a numerical model has been developed for the single layer. In this model the nodal displacements and tractions at the boundary of the layer are related to any prescribed quantities at the boundary or in the domain through matrix equations. The model of the typical numerical layer (element) has been extended to the case of a multilayered system by introducing appropriate continuity conditions at the interfaces between the layers. These conditions are described in detail for the case of firmly bonded layers, and also for the case of separation (debonding), slip and friction between the layers. Assembly of the element matrices has been used in order to form the global system of equations, and an iterative solver has been suggested for its

solution. This iterative solver is the bi-conjugate gradient method with Jacobi preconditioning matrix.

Numerical techniques have been developed for the evaluation of the boundary and domain integrals involved in the construction of the element matrices. The singular boundary integrals are computed using a special coordinate transformation, along with a subdivision of the boundary element and a bi-cubic transformation of the Gauss points. The domain integrals, either regular, singular or near-singular, are transformed to regular integrals along the boundary of the domain element using triangle polar coordinates and an analytical integration in the radial direction which removes the singularities. The domain integrals that appear in some of the matrices of the typical numerical layer are required, either to introduce the prescribed surface tractions for the case of a single layer, or to introduce the interface equilibrium conditions for the case of a multilayered system.

The novel formulation presented in this work, begins with the total potential energy, and then by incorporating the layerwise theory, the finite element method, fundamental solutions (Green's functions), integral Fourier transforms, boundary integral equations, and finally, the boundary element method, it produces a powerful, efficient and elegant model for the three-dimensional analysis of multilayered systems.

7.2 RECOMMENDATIONS

The proposed model for the analysis of multilayered systems must be tested numerically by analyzing several multilayered systems with irregular shapes subjected to various types of loads. The numerical results must be compared with those from existing numerical solutions in order to demonstrate the

efficiency and accuracy of the proposed method. The layerwise boundary element model with its generality and its powerful features, that were developed in the present work, must be used to study difficult problems associated with laminated plates, for which other methods have failed to produce accurate results.

The same methodology can be applied in an obvious manner to anisotropic materials. The approach is going to be exactly the same and it will only be required to derive a new fundamental solution. However, the methodology for deriving such a solution has already been presented and all the mathematical and computational tools have been developed and applied to the case of the isotropic layers. In a similar way, we may obtain fundamental solutions and develop numerical models for mixed formulations, for layers resting on elastic foundation (Pasternak or Winkler-type foundations), or for higher order approximations of the displacement field through the thickness of a numerical layer. The problem of thermal stresses, vibrations or stability may be treated in an analogous manner.

APPENDICES

APPENDIX A

Properties of Bessel Functions

Inversion of the functions $\bar{f}_{\alpha\beta}$, which compose the transformed fundamental solution $\bar{U}_{ij}(\alpha_1, \alpha_2; \xi_1, \xi_2)$ and transformed stresses $\bar{S}_{ij}(\alpha_1, \alpha_2; \xi_1, \xi_2)$, is performed using the integral expressions (3.50) and incorporating recurrence formulae and analytical evaluation of infinite integrals of Bessel functions. All these properties are listed below (Wheelon, 1968; Abramowitz and Segun, 1968) :

$$J_{k+1}\left(\bar{\rho}\,\frac{R}{h}\right) + J_{k-1}\left(\bar{\rho}\,\frac{R}{h}\right) = \frac{2kh}{\bar{\rho}R}\,J_k\left(\bar{\rho}\,\frac{R}{h}\right) \tag{A.1}$$

$$\int_0^\infty \frac{\bar{\rho}}{b^2+\bar{\rho}^2}\,J_0\left(\bar{\rho}\,\frac{R}{h}\right)d\bar{\rho} = K_0\left(b\,\frac{R}{h}\right) \tag{A.2}$$

$$\int_0^\infty \frac{\bar{\rho}^2}{c^2+\bar{\rho}^2} J_1\left(\bar{\rho}\frac{R}{h}\right) d\bar{\rho} = c K_1\left(c\frac{R}{h}\right) \tag{A.3}$$

$$\int_0^\infty \frac{1}{b^2+\bar{\rho}^2} J_1\left(\bar{\rho}\frac{R}{h}\right) d\bar{\rho} = \frac{h}{b^2 R} - \frac{1}{b} K_1\left(b\frac{R}{h}\right) \tag{A.4}$$

$$\int_0^\infty \frac{1}{\bar{\rho}} J_2\left(\bar{\rho}\frac{R}{h}\right) d\bar{\rho} = \frac{1}{2} \tag{A.5}$$

$$\int_0^\infty J_k\left(\bar{\rho}\frac{R}{h}\right) d\bar{\rho} = \frac{h}{R} \tag{A.6}$$

where K_0 and K_1 are the modified Bessel functions of the second kind of zero and first order, respectively, and J_k are the Bessel functions of the first kind of order k. In the above expressions c is a constant which is given in (3.40) and b is a constant, which in some of the functions $\bar{f}_{\alpha\beta}$ takes the value $b = 3$, while in other functions takes the value $b = c$.

In order to prove that the fundamental solution U_{ij} satisfies the governing equations in the physical space and that the stress matrix S_{ij} is related to the displacements U_{ij} through the constitutive relations (3.64), we use the recurrence formulae for the modified Bessel functions and their derivatives, which are

$$K_{n+1}(z) - K_{n-1}(z) = \frac{2n}{z} K_n(z), \tag{A.7}$$

and

$$\frac{dK_n(z)}{dz} = -K_{n+1}(z) + \frac{n}{z} K_n(z). \tag{A.8}$$

APPENDIX B

Convergent Integrals of the Fundamental Solution

In the construction of the final fundamental solution and the corresponding stress components it is required to evaluate the following two convergent integrals

$$G_1 - G_1^* = \int_0^\infty \frac{1}{\bar{\rho}} J_0\left(\bar{\rho}\,\frac{R}{h}\right) d\bar{\rho} - \int_0^\infty \frac{e^{-\bar{\rho}}}{\bar{\rho}}\, d\bar{\rho} \tag{B.1}$$

$$G_2 - G_2^* = \int_0^\infty \frac{1}{\bar{\rho}^3} J_0\left(\bar{\rho}\,\frac{R}{h}\right) d\bar{\rho} - \int_0^\infty \left(\frac{1}{\bar{\rho}^3} - \frac{R^2}{4h^2}\,\frac{e^{-\bar{\rho}}}{\bar{\rho}}\right) d\bar{\rho}\ . \tag{B.2}$$

(i) *Evaluation of the integral* (B.1)

The integral of equation (B.1) can be re-written in the form

$$G_1 - G_1^* = \int_0^\infty \left\{ \frac{[1 - e^{-\bar{\rho}}]}{\bar{\rho}} J_0\left(\bar{\rho}\,\frac{R}{h}\right) - \frac{e^{-\bar{\rho}}}{\bar{\rho}} \left[1 - J_0\left(\bar{\rho}\,\frac{R}{h}\right)\right] \right\} d\bar{\rho} \tag{B.3}$$

and using the following integral properties of the Bessel functions (Wheelon, 1968; Gray and Mathews, 1931),

$$\int_0^\infty [1 - e^{-px}] \frac{J_0(qx)}{x}\, dx = \ln\left(\frac{p + \sqrt{q^2 + p^2}}{q}\right), \quad \mathrm{R}(p) > \mathrm{R}(iq) \tag{B.4}$$

$$\int_0^\infty \frac{e^{-px}}{x} [1 - J_0(x)]\, dx = -\ln\left(\frac{2p}{p + \sqrt{1 + p^2}}\right), \quad \mathrm{R}(p) > 0 \tag{B.5}$$

equation (B.3) becomes

$$G_1 - G_1^* = \ln\left(\frac{1+\sqrt{(R/h)^2+1}}{R/h}\right) + \ln\left(\frac{2}{1+\sqrt{1+(R/h)^2}}\right) = \ln\left(\frac{2h}{R}\right). \qquad \text{(B.6)}$$

(ii) *Evaluation of the integral* (B.2)

The integrals of equation (B.2) can be re-written in the form

$$G_2 - G_2^* = \int_0^\infty \left\{\frac{1}{\bar{\rho}^3}\left[J_0\left(\bar{\rho}\,\frac{R}{h}\right) - 1\right] + \frac{R^2}{4h^2}\,\frac{e^{-\bar{\rho}}}{\bar{\rho}}\right\} d\bar{\rho} \qquad \text{(B.7)}$$

and after integrating by parts the first term of the integral in the above equation, and using the property $J_0'(x) = -J_1(x)$, we obtain

$$G_2 - G_2^* = -\frac{1}{2}\left[\frac{J_0(\bar{\rho}\,R/h) - 1}{\bar{\rho}^2}\right]_0^\infty + \int_0^\infty \left\{-\frac{R}{2h}\,\frac{J_1(\bar{\rho}\,R/h)}{\bar{\rho}^2} + \frac{R^2}{4h^2}\,\frac{e^{-\bar{\rho}}}{\bar{\rho}}\right\} d\bar{\rho}\,. \qquad \text{(B.8)}$$

The limit of the term in brackets for $\bar{\rho} \to \infty$ can be found using the Hansen series (Watson, 1945),

$$J_0^2(x) + 2\sum_{k=0}^{\infty} J_k^2(x) = 1\,, \qquad \text{(B.9)}$$

from which it is deduced that $|J_0(x)| \le 1$ for any real value of x. This yields

$$\lim_{\bar{\rho}\to\infty} \frac{J_0(\bar{\rho}\,R/h) - 1}{\bar{\rho}^2} = 0\,. \qquad \text{(B.10)}$$

The limit of the term in brackets in (B.8) for $\bar{\rho} \to 0$ is obtained in the following way,

$$\lim_{\bar{\rho}\to 0} \frac{J_0(\bar{\rho}\,R/h) - 1}{\bar{\rho}^2} = \frac{R}{2h} \lim_{\bar{\rho}\to 0} \frac{-J_1(\bar{\rho}\,R/h)}{\bar{\rho}} = -\frac{R^2}{2h^2} \lim_{\bar{\rho}\to 0} J_1'(\bar{\rho}\,R/h)$$

$$= -\frac{R^2}{2h^2} \lim_{\bar{\rho}\to 0} \tfrac{1}{2}\left[J_0(\bar{\rho}\,R/h) - J_2(\bar{\rho}\,R/h)\right] = -\frac{R^2}{4h^2} \qquad \text{(B.11)}$$

in which, we have applied L' Hospital's rule and used the values, $J_0(0) = 1$, $J_1(0) = 0$, and $J_2(0) = 0$, of the Bessel functions of the first kind.

Incorporating the results of equations (B.10) and (B.11) into (B.8), and utilizing the recurrence formula (A.1), equation (B.8) becomes

$$G_2 - G_2^* = -\frac{R^2}{8h^2} + \int_0^\infty \left\{ -\frac{R^2}{4h^2} \frac{J_0(\bar{\rho}\, R/h) + J_2(\bar{\rho}\, R/h)}{\bar{\rho}} + \frac{R^2}{4h^2} \frac{e^{-\bar{\rho}}}{\bar{\rho}} \right\} d\bar{\rho}$$

$$= -\frac{R^2}{8h^2} - \frac{R^2}{4h^2} \left\{ \int_0^\infty \frac{J_2(\bar{\rho}\, R/h)}{\bar{\rho}}\, d\bar{\rho} + \int_0^\infty \left[\frac{J_0(\bar{\rho}\, R/h)}{\bar{\rho}} - \frac{e^{-\bar{\rho}}}{\bar{\rho}} \right] d\bar{\rho} \right\} \tag{B.12}$$

The first integral in the above equation is given by (A.5) and the second by (B.6). Finally, the integral of equation (B.2) takes the form

$$G_2 - G_2^* = -\frac{R^2}{8h^2} - \frac{R^2}{4h^2} \left[\frac{1}{2} + \ln\left(\frac{2h}{R}\right) \right] = -\frac{R^2}{4h^2} \left[1 + \ln\left(\frac{2h}{R}\right) \right]. \tag{B.13}$$

APPENDIX C

Properties of the Fundamental Solution

The final form of the fundamental solution for the single infinite numerical layer is given by equation (3.36) and has the matrix structure of (3.35). This solution possesses some very useful properties, which are listed below.

(i) The 6×6 matrix in equation (3.35) can be described in terms of the following twelve components,

$$U_{11},\ U_{22},\ U_{12},\ U_{14},\ U_{15},\ U_{25},\ U_{13},\ U_{16},\ U_{23},\ U_{26},\ U_{33},\ U_{36}\ .$$

All the other displacement components can be expressed in terms of these twelve components, and the matrix may be written as

$$
[\mathbf{U}(x_1,x_2;\xi_1,\xi_2)] = \begin{array}{c}
\overbrace{}^{\text{node 1}} \quad \overbrace{}^{\text{node 2}} \\
\begin{matrix} P_1^1 & P_2^1 & P_3^1 & P_1^2 & P_2^2 & P_3^2 \end{matrix} \\
\begin{bmatrix}
U_{11} & U_{12} & U_{13} & U_{14} & U_{15} & U_{16} \\
U_{12} & U_{22} & U_{23} & U_{15} & U_{25} & U_{26} \\
-U_{13} & -U_{23} & U_{33} & U_{16} & U_{26} & U_{36} \\
U_{14} & U_{15} & -U_{16} & U_{11} & U_{12} & -U_{13} \\
U_{15} & U_{25} & -U_{26} & U_{12} & U_{22} & -U_{23} \\
-U_{16} & -U_{26} & U_{36} & U_{13} & U_{23} & U_{33}
\end{bmatrix}
\end{array}
\begin{array}{l}
\leftarrow \\ \leftarrow \\ \leftarrow \\ \leftarrow \\ \leftarrow \\ \leftarrow
\end{array}
\begin{array}{l}
\left.\begin{matrix} V_1^1 \\ V_2^1 \\ V_3^1 \end{matrix}\right\} \text{node 1} \\
\left.\begin{matrix} V_1^2 \\ V_2^2 \\ V_3^2 \end{matrix}\right\} \text{node 2}
\end{array}
\tag{C.1}
$$

(ii) The fundamental matrix in (3.35) may also be written in a form which yields a symmetric matrix. Inspection of equation (C.1) reveals that if we multiply the third and sixth column by (–1), and set the unit loads that correspond to these columns in the opposite direction, *i.e.*, $-P_3^1$ and $-P_3^2$, respectively, the fundamental matrix becomes symmetric. Another way to produce a symmetric matrix is to define the displacement components in the x_3 direction as,

$$-V_3^1 = U_{3j} \quad \text{and} \quad -V_3^2 = U_{6j} \qquad (j = 1, 2, ..., 6), \tag{C.2}$$

i.e., change the sign of all components in the third and sixth row.

(iii) In the expressions (3.36) for $U_{ks}(x_1,x_2;\xi_1,\xi_2)$ and expressions (3.51) and (3.63) for the functions $f_{\alpha\beta}(x_1,x_2;\xi_1,\xi_2)$, there exist some properties with respect to the relative position of points (x_1,x_2) and (ξ_1,ξ_2). More specifically, by interchanging (x_1,x_2) and (ξ_1,ξ_2), some components of the fundamental solution are not altered, while the rest change sign. More specifically, it is

$$f_{\alpha\beta}(x_1, x_2; \xi_1, \xi_2) = f_{\alpha\beta}(\xi_1, \xi_2; x_1, x_2) \quad \text{for} \quad \begin{cases} f_{10}, f_{20}, f_{30}, f_{73}, f_{74}, f_{75}, \\ f_{81}, f_{82}, f_{83}, f_{91}, f_{92}, f_{93} \end{cases} \tag{C.3}$$

and

$$f_{\alpha\beta}(x_1, x_2; \xi_1, \xi_2) = -f_{\alpha\beta}(\xi_1, \xi_2; x_1, x_2) \quad \text{for} \quad \begin{cases} f_{41}, f_{42}, f_{51}, f_{52}, f_{61}, f_{62}, f_{71}, f_{72}, \\ f_{76}, f_{77}, f_{84}, f_{85}, f_{94}, f_{95} \end{cases} \tag{C.4}$$

Using the properties (C.3) and (C.4), we can establish similar relations for the components of the fundamental solution,

$$U_{ij}(x_1, x_2; \xi_1, \xi_2) = U_{ij}(\xi_1, \xi_2; x_1, x_2) \text{ for } U_{11}, U_{22}, U_{12}, U_{14}, U_{15}, U_{25}, U_{33}, U_{36} \tag{C.5}$$

and

$$U_{ij}(x_1, x_2; \xi_1, \xi_2) = -U_{ij}(\xi_1, \xi_2; x_1, x_2) \text{ for } U_{13}, U_{16}, U_{23}, U_{26}\,. \tag{C.6}$$

APPENDIX D

Numerical Evaluation of Bessel Functions

The fundamental solution and its derivatives are expressed in terms of the functions $f_{\alpha\beta}(x, y)$, which are given in equations (3.51) and (3.63). Many of these functions involve the modified Bessel functions of the second kind of zero and first order. In the numerical evaluation of the boundary and domain integrals, using the methods developed in Chapter 6, the functions $f_{\alpha\beta}(x, y)$ need to be calculated at the Gauss points for every element and for all the

different positions of the reference point $\vec{\xi}$. Also, the arguments of the Bessel functions will vary from very small values close to zero, in the case of the singular integrals, to large values, in the case of regular integrals. This implies that the approximation pattern which will be adopted for the calculation of the Bessel functions $K_0(x)$ must be fast and also accurate. In the present work, polynomial approximations have been employed, and their expressions are given below along with ranges of the arguments in which they are valid and the associated errors.

Modified Bessel functions of the second kind of zero order:

$$\begin{aligned} K_0(x) = & -\ln(x/2)\ I_0(x) - 0.57721566 + 0.42278420\ (x/2)^2 + 0.23069756\ (x/2)^4 \\ & + 0.03488590\ (x/2)^6 + 0.00262698\ (x/2)^8 + 0.00010750\ (x/2)^{10} \\ & + 0.00000740\ (x/2)^{12} + \varepsilon \\ & \qquad\qquad 0 < x \leq 2\,, \quad |\varepsilon| < 10^{-8} \end{aligned} \tag{D.1}$$

$$\begin{aligned} K_0(x) = & \frac{1}{e^x \sqrt{x}} \Big[1.25331414 - 0.07832358\ (2/x) + 0.02189568\ (2/x)^2 \\ & - 0.01062446\ (2/x)^3 + 0.00587872\ (2/x)^4 - 0.00251540\ (2/x)^5 \\ & + (2/x)^6\ 0.00053208 + \varepsilon \Big] \\ & \qquad\qquad 2 \leq x < \infty\,, \quad |\varepsilon| < 1.9 \times 10^{-7} \end{aligned} \tag{D.2}$$

Modified Bessel functions of the second kind of first order:

$$\begin{aligned} K_1(x) = & \ln(x/2)\ I_1(x) + 1/x \Big[1 + 0.15443144\ (x/2)^2 - 0.67278579\ (x/2)^4 \\ & - 0.18156897\ (x/2)^6 - 0.01919402\ (x/2)^8 - 0.00110404\ (x/2)^{10} \\ & - 0.00004686\ (x/2)^{12} + \varepsilon \Big] \\ & \qquad\qquad 0 < x \leq 2\,, \quad |\varepsilon| < 8 \times 10^{-9} \end{aligned} \tag{D.3}$$

$$K_1(x) = \frac{1}{e^x\sqrt{x}}\left[1.25331414 + 0.23498619\,(2/x) - 0.03655620\,(2/x)^2 + 0.01504268\,(2/x)^3 - 0.00780353\,(2/x)^4 + 0.00325614\,(2/x)^5 - (2/x)^6\,0.00068245 + \varepsilon\right]$$

$$2 \le x < \infty, \quad |\varepsilon| < 2.2 \times 10^{-7} \tag{D.4}$$

where $I_0(x)$ and $I_1(x)$ are the modified Bessel functions of the first kind of zero and first order, and they are computed using ascending series:

$$I_0(x) = \sum_{k=0}^{\infty} \frac{(x^2/4)^k}{(k!)^2} \tag{D.5}$$

and

$$I_1(x) = \frac{x}{2} \sum_{k=0}^{\infty} \frac{(x^2/4)^k}{k!\,(k+1)!} \tag{D.6}$$

In the evaluation of the domain integrals, where all types of integrals are evaluated using the basic singular case with reference point at one of the nodes of the triangular domain, it is required to evaluate integrals of the modified Bessel function of the second kind of zero order, in the interval 0 to a value x. The upper limit x is actually the $\bar{x}_2$ polar coordinate, used in Section 6.2, and this integral is the only one which is not possible to be evaluated analytically. This integral may be approximated using ascending series, for $x < 7.5$, and a polynomial for $7.5 \le x < \infty$. The ascending series are

$$\int_0^x K_0(t)\,dt = -\left(\gamma + \ln\frac{x}{2}\right) x \sum_{k=0}^{\infty} \frac{(x/2)^{2k}}{(k!)^2\,(2k+1)} + x \sum_{k=0}^{\infty} \frac{(x/2)^{2k}}{(k!)^2\,(2k+1)^2} + x \sum_{k=1}^{\infty} \frac{(x/2)^{2k}}{(k!)^2\,(2k+1)} \left(1 + \frac{1}{2} + \frac{1}{3} + \ldots + \frac{1}{k}\right)$$

$$x < 7.5 \tag{D.7}$$

where $\gamma = 0.5772\ 15664\ 90153\ 28606$ is the Euler's constant, while the polynomial approximation is:

$$\int_0^x K_0(t)\,dt = \frac{\pi}{2} - \frac{1}{e^x\sqrt{x}}\Big[1.25331414 - 0.11190289\,(7/x) + 0.02576646\,(7/x)^2 - 0.00933994\,(7/x)^3 + 0.00417454\,(7/x)^4 - 0.00163271\,(7/x)^5 + (7/x)^6\,0.00033934 + \varepsilon(x)\Big]$$

$$7.5 \le x < \infty\,, \quad |\varepsilon(x)| \le 2\times 10^{-7} \tag{D.8}$$

REFERENCES

Abramowitz, M., and Segun, I. A., 1968, *Handbook of Mathematical Functions*, Dover, New York.

Alarcón, E., Doblare, M., and Sanz-Serna, J., 1989, "An Efficient Nonlinear Transformation for the Numerical Computation of the Singular Integrals Appearing in 2-D BEM," in *BEMs in Engineering*, (Eds. Annigeri, B. S., and Tseng, K.), Proc. of the Inter. Symp. on BEMs: Advances in Solid and Fluid Mech., East Hartford, Connecticut, Oct. 2–4, 1989, pp. 472–479.

Araújo, F. C. and Mansur, W. J., 1989, "Iterative Solvers for BEM Systems of Equations," in *Advances in Boundary Elements*, (Eds. Brebbia, C. A., and Connor, J. J.), Vol. 1 (*Computations and Fundamentals*), Proc. of the 11th Inter. Conf. on BEMs, Cambridge, USA, Aug. 1989, Springer-Verlag, pp. 263–274.

Banerjee, P. K., and Butterfield, R., 1981, *Boundary Element Methods in Engineering Science*, McGraw-Hill, London.

Barbero, E. J., Reddy, J. N., and Teply, J. L., 1990, "An Accurate Determination of Stresses in Thick Laminates Using a Generalized Plate Theory," *Int. J. Num. Meth. Eng.*, Vol. 29, pp. 1–14.

Barra, L. P. S., Coutinho, A. L. G. A., Mansur, W. J., and Telles, J. C. F., 1992, "Iterative Solution of BEM Equations by GMRES Algorithm," *Computers and Structures*, Vol. 44 (6), pp. 1249–1253.

Benitez, F. G., and Rosakis, A. J., 1987, "Three-Dimensional Elastostatics of a Layer and a Layered Medium," *J. Elasticity*, Vol. 18, pp. 3–50.

Beskos, D. E., ed., 1991, *Boundary Element Analysis of Plates and Shells*, Springer-Verlag, Berlin.

Brebbia, C. A., Telles, J. C. F., and Wrobel, L. C., 1984, *Boundary Element Techniques*, Springer-Verlag, Berlin.

Brebbia, C. A., and Niku, S. M., 1987, A Comparison Between Continuous Versus Discontinuous Elements in Boundary Elements, in *Boundary Element Techniques: Applications in Stress Analysis and Heat Transfer* (Eds. Brebbia, C.A. and Venturini, W. S.), pp. 193–207, Computational Mechanics Publications, Southampton.

Boussinesq, J., 1885, *Applications des Potentiels á l' Etude de l' Equilibre et du Mouvement des Solides Elastiques*, Gauthier-Villars, Paris.

Bufler, H., 1971, "Theory of Elasticity of a Multilayered Medium," *J. Elasticity*, Vol. 1, pp. 125–143.

Burmister, D. M., 1945, "The General Theory of Stresses and Displacements in Layered Systems I, II, III," *J. Appl. Phys.*, Vol. 16, pp. 89–94, 126–127, 296–302.

Cerrolaza, M., and Alarcón, E., 1989, "A Bi-Cubic Transformation for the Numerical Evaluation of the Cauchy Principal Value Integrals in Boundary Methods," *Int. J. Num. Meth. Eng.*, Vol. 28, pp. 987–999.

Chatterjee, S. N., 1987, "Three- and Two-Dimensional Stress Fields Near Delaminations in Laminated Composite Plates," *Int. J. Solids Structures*, Vol. 23, No. 11, pp. 1535–1549.

Cowper, G. R., 1973, "Gaussian Quadrature Formulas for Triangles," *Int. J. Num. Meth. Eng.*, Vol. 7, pp. 405–408.

Crook, S. H., and Smith, R. N. L., 1992, "Numerical Residual Calculation and Error Estimation for Boundary Element Methods," *Engineering Analysis*, Vol. 9, pp. 159–164.

Cruse, T. A., 1967, *The Transient Problem in Classical Elastodynamics Solved by Integral Equations*, Ph.D. Dissertation, Univ. of Washington.

Cruse, T. A., 1969, "Numerical Solutions in Three Dimensional Elastostatics," *Int. J. Solids Strucrures*, Vol. 5, pp. 1259–1274.

Cruse, T. A., 1973, "Application of the Boundary-Integral Equation Method to Three-Dimensional Stress Analysis," *Computers and Structures*, Vol. 3, pp. 509–527.

Cruse, T. A., and Aithal, R., 1993, "Non-Singular Boundary Integral Equation Implementation," *Int. J. Num. Meth. Eng.*, Vol. 36, pp. 237–254.

Dougall, J., 1904, "An Analytical Theory of the Equilibrium of an Isotropic Elastic Plate," *Trans. Roy. Soc. Edinburgh*, Vol. 41, pp. 129–228.

Gray, A., and Mathews, G. B., 1931, *A Treatise on Bessel Functions and Their Applications to Physics,* 2nd edn., MacMillan and Co., London.

Green, A. E., and Zerna, W., 1960, *Theoretical Elasticity*, Oxford University Press, London.

Harding, J. W., and Sneddon, I. N., 1945, "The Elastic Stresses Produced by the Indentation of the Plane Surface of a Semi-Infinite Elastic Solid by a Rigid Punch," *Proc. Cambridge Phil. Soc.*, Vol. 41, pp. 16–26.

Hartmann, F., 1980, "Computing the C Matrix in Non-smooth Boundary Points," in *New Developments in Boundary Element Methods*, (Brebbia, C. A., ed.), pp. 367–379, CML Publications, Southampton.

Hartmann, F., 1989, *Introduction to Boundary Elements*, Springer-Verlag, Berlin.

Hughes, T. J. R., Ferencz, R. M., and Hallquist, J. O., 1987, "Large-Scale Vectorized Implicit Calculations in Solid Mechanics on a Cray X-MP/48 Utilizing EBE Preconditioned Conjugate Gradients," *Computer Methods in Applied Mechanics and Engineering*, Vol. 61, pp. 215–248.

Jun, L., Beer, G., and Meek, J. L., 1985, "Efficient Evaluation of Integrals of Order $1/r$, $1/r^2$, $1/r^3$ Using Gauss Quadrature," *Engineering Analysis*, Vol. 2 (3), pp. 118–123.

Kellogg, O. D., 1929, *Foundations of Potential Theory*, Springer-Verlag, Berlin.

Katsikadelis, J. T., and Armenàkas, A. E., 1985, "Numerical Evaluation of Line Integrals with a Logarithmic Singularity," *AIAA Journal*, Vol. 23, pp. 1135–1137.

Katsikadelis, J. T., and Kokkinos, F. T., 1987, "Static and Dynamic Analysis of Composite Shear Walls by the Boundary Element Method," *Acta Mechanica*, Vol. 68, pp. 231–250.

Kupradze, V. D., (ed.), 1979, *Three-Dimensional Problems of the Mathematical Theory of Elasticity and Thermoelasticity*, North-Holland, Amsterdam.

Lachat, J. C., and Watson, J. O., 1976, "Effective Numerical Treatment of Boundary Integral Equations: A Formulation for Three-Dimensional Elastostatics," *Int. J. Num. Meth. Eng.*, Vol. 10, pp. 991–1005.

Liao, H., and Xu, Z., 1992, "A method for Direct Evaluation of Singular Integral in Direct Boundary Element Method," *Int. J. Num. Meth. Eng.*, Vol. 35, pp. 1473–1485.

Love, A. E., 1944, *A Treatise on the Mathematical Theory of Elasticity*, 4th edn., Dover Publications, New York.

Luke, Y. L., 1962, *Integrals of Bessel Functions*, McGraw-Hill, New York.

Luré, A. I., 1964, *Three-Dimensional Problems of the Theory of Elasticity*, Interscience Publishers, John Wiley & Sons, New York.

Lutz, E., 1992, "Exact Gaussian Quadrature Methods for Near-Singular Integrals in the Boundary Element Method," *Engineering Analysis*, Vol. 9, pp. 233–245.

Madenci, E., and Westmann, R. A., 1993, "Local Delamination Growth in Layered Systems Under Compressive Load," *ASME Journal of Applied Mechanics*, Vol. 60, pp. 895–902.

Mansur, W. J., Araújo, F. C., and Malaghini, J. E. B., 1992, "Solution of BEM Systems of Equations via Iterative Techniques," *Int. J. Num. Meth. Eng.*, Vol. 33, pp. 1823–1841.

McLachlan, N. W., 1941, *Bessel Functions for Engineers*, 2nd edn., Oxford University Press, London.

Melan, E., 1932, "Der Spannungszustand der durch eine Einzelkraft in innenn Beanspruchten Halbscheibe," *Z. angw Math. Mech.*, Vol. 12, pp. 343–346.

Michell, J. H., 1899a, "On the Direct Determination of Stress in an Elastic Solid, with Application to the Theory of Plates," *Proc. Lond. Math. Soc.*, Vol. 31, pp. 100–124.

Michell, J. H., 1899b, "The Transmission of the Stress across a Plane of Discontinuity in an Isotropic Elastic Solid, and the Potential Solutions for a Plane Boundary," *Proc. Lond. Math. Soc.*, Vol. 31, pp. 182–192.

Michell, J. H., 1900a, "Some Elementary Distributions of Stress in Three Dimensions," *Proc. Lond. Math. Soc.*, Vol. 32, pp. 23–35.

Michell, J. H., 1900b, "Elementary Distributions of Plane Stress," *Proc. Lond. Math. Soc.*, Vol. 32, pp. 35–61.

Mindlin, R. D., 1936, "Force at a Point in the Interior of a Semi-Infinite Solid," *Physics*, Vol. 7, pp. 195–202.

Partridge, P. W. and Brebbia, C. A., 1990, On Derivatives of the Problem Unknowns in BEM Analysis, *Engineering Analysis*, Vol. 7 (1), pp. 50–52.

Pindera, M.-J., and Lane, M. S., 1993, "Frictionless Contact of Layered Half-Planes, Part I: Analysis, Part II: Numerical Results," *ASME Journal of Applied Mechanics*, Vol. 60, pp. 633–639, 640–645.

Reddy, J. N., 1984, *Energy and Variational Methods in Applied Mechanics*, John Wiley & Sons, New York.

Reddy, J. N., 1987, "A Generalization of Two-Dimensional Theories of Laminated Composite Plates," *Communications in Applied Numerical Methods*, Vol. 3, pp. 173–180.

Reddy, J. N., Barbero, E.J., and Teply, J. L., 1989, "A Plate Bending Element Based on a Generalized Laminate Theory," *Int. J. Num. Meth. Eng.*, Vol. 28, pp. 2275–2292.

Reddy, J. N., 1990, "On Refined Theories of Composite Laminates," *Meccanica*, Vol. 25, pp. 230–238.

Reddy, J. N., 1993, *An Introduction to the Finite Element Method*, 2nd edn., McGraw-Hill, New York.

Rizzo, F. J., 1967, "An Integral Equation Approach to Boundary Value Problems of Classical Elastostatics," *Quart. J. Applied Mathematics*, Vol. 25, No. 1, pp. 83–95.

Robbins, D. H., and Reddy, J. N., 1993, "Modelling of Thick Composites Using a Layerwise Laminate Theory," *Int. J. Num. Meth. Eng.*, Vol. 36, pp. 655–677.

Shekhter, O. Y., and Prikhodchenko, O. E., 1964, "Stress and Displacement Distributions in an Elastic Layer Acted on by Internal Point Forces," *Osnovaniya, Fundametry i Mekhanika Gruntov, English Translation*, No. 5, pp. 2–4.

Shekhter, O. Y., 1965, "A Horizontal Force in a Three-Dimensional Layer on a Rigid Base," *Osnovaniya, Fundametry i Mekhanika Gruntov, English Translation*, No. 1, pp. 7–8.

Sneddon, I. N., 1946, "The Elastic Stresses Produced in a Thick Plate by the Application of Pressure to its Free Surfaces," *Proc. Cambridge Phil. Soc.*, Vol. 42, pp. 260–271.

Sneddon, I. N., 1951, *Fourier Transforms*, McGraw-Hill, New York.

Sneddon, I. N., 1975, *Application of Integral Transforms in the Theory of Elasticity*, Springer-Verlag, New York.

Stern, M., 1985, "Formulating Nonsingular Boundary Integral Equations in Linear Elasticity," in *Advanced Topics in Boundary Element Analysis*, ASME, AMD-Vol. 72, pp. 213–223.

Stroud, A. H., and Secrest, D., 1966, *Gaussian Quadrature Formulas*, Prentice-Hall, New Jersey.

Takhteyev, V., and Brebbia, C. A., 1990, "Analytical Integrations in Boundary Elements," *Engineering Analysis*, Vol. 7 (2), pp. 95–100.

Telles, J. C. F., and Brebbia, C. A., 1981, "Boundary Element Solution for Half-Plane Problems," *Int. J. Solids Structures*, Vol. 17, No. 12, pp. 1149–1158.

Telles, J. C. F., 1987, "A Self-Adaptive Co-ordinate Transformation for the Efficient Numerical Evaluation of General Boundary Element Integrals," *Int. J. Num. Meth. Eng.*, Vol. 24, pp. 959–973.

Thompson, W., Sir (Lord Kelvin), 1848, "Note on the Integration of the Equations of Equilibrium of an Elastic Solid," *The Cambridge and Doublin Mathematical Journal*, Vol. III, pp. 87–89.

Watson, G. N., 1945, *A Treatise on the Theory of Bessel Functions*, 2nd edn., Cambridge University Press, London.

Westergaard, H. M., 1952, *Theory of Elasticity and Plasticity*, John Wiley & Sons, New York.

Wheelon, A. D., 1968, *Tables of Summable Series and Integrals Involving Bessel Functions*, Holden-Day, San Francisco.

Wolfram, S., 1991, *Mathematica: A System for Doing Mathematics by Computer*, 2nd edn., Addison-Wesley Publishing Co., Redwood City, CA.

Wu, T. W., and Stern, M., 1991, Boundary Integral Equations in Three-Dimensional Elastostatics Using the Boussinesq-Cerruti Fundamental Solution. *Engineering Analysis*, Vol. 8 (2), pp. 94–102.

Zhang, W., and Xu, H. R., 1989, "A General and Effective Way for Evaluating the Integrals with Various Orders of Singularity in the Direct Boundary Element Method," *Int. J. Num. Meth. Eng.*, Vol. 28, pp. 2059–2064.

VITA

Filis-Triantaphyllos T. Kokkinos was born on July 29, 1961 in Geneva, Switzerland. He was raised in Athens, Greece and attended high school at the Athens College. He obtained his Diploma in Civil Engineering in July 1995 from the National Technical University of Athens. He came to the United States in January 1986 and in 1988 he obtained his Master of Science Degree in Civil Engineering from the University of West Virginia at Morgantown. Although, he had already started working towards the Ph.D. in Civil Engineering at W.V.U., in September of 1988 he was called to go back to Greece and serve the Greek Navy. From October of 1989 until July of 1990, being on secondment from the Greek Navy, he served as an instructor at the Military Technical School for Engineer Officers, and also, as a research and teaching assistant at the Institute of Structural and Aseismic Research (Civil Engineering Department) of the National Technical University of Athens. In September of 1990, he joined the Ph.D. program in Engineering Mechanics of Virginia Polytechnic Institute and State University, and since January of 1995 he has been working as an Assistant Lecturer at the Mechanical Engineering Department of Texas A&M University.

Filis-Triantaphyllos T. Kokkinos